UAB
Universitat Autònoma de Barcelona

Approaches to study the pig nasal microbiota in the context of the host

Laura Bonillo López

Approaches to study the pig nasal microbiota in the context of the host

Laura Bonillo López

PhD Thesis

Bellaterra, 2025

Approaches to study the pig nasal microbiota in the context of the host

Tesis doctoral presentada por Laura Bonillo López para acceder al grado de Doctora en el marco del programa de Doctorado en *Microbiologia de la Facultat de Biociències de la Universitat Autònoma* de Barcelona, bajo la dirección de Virginia Aragón Fernández, Marina Sibila Vidal y Florencia Correa Fiz.

Bellaterra, 2025

La Dra. **Virginia Aragón Fernández**, la Dra. **Marina Sibila Vidal**, y la Dra. **Florencia Correa Fiz** investigadoras del *Institut de Recerca i Tecnologia Agroalimentàries – Centre de Recerca en Sanitat Animal* (IRTA-CReSA) y la Dra. **Esther Julián Gómez**, investigadora del Departament de Genètica i de Microbiologia.

Informan:

Que los trabajos de investigación desarrollados en la memoria de tesis doctoral "*Approaches to study the pig nasal microbiota in the context of the host*" presentados por Laura Bonillo López para la obtención del Grado de Doctora en *Microbiologia* se ha realizado bajo su dirección y tutoría, y autorizan su presentación a fin de ser evaluada por la comisión correspondiente.

Y para que así conste y tenga los efectos que correspondan, firman la presente declaración.

Directora	Directora	Directora	Tutora	Doctoranda

Bellaterra, julio 2025

Este trabajo, para la realización del doctorado, ha sido financiado por el Ministerio de Ciencia e Innovación a través de los proyectos PID2019-388106233RB-I00 y PID2022-138657OB-I00/AEI/10.13039/501100011033, así como el contrato de investigador en formación de Laura Bonillo López PRE2020-096048 /AEI/10.13039/501100011033.

Agradecimientos

Table of contents

Abbreviations

A

ALI: air-liquid interface
AMR: antimicrobial resistance
ASV: amplicon sequence variant
AUC: area under the growth curve

E

ECM: extracellular matrix

I

IFA: immunofluorescent assay
IFN: interferon
IHC: immunohistochemistry assay
IL: interleukin

L

LRT: lower respiratory tract

M

MUC5AC: mucin-5AC

N

NAD^+: nicotinamide adenine dinucleotide
NF-κβ: nuclear factor kappa-light-chain-enhancer of activated B cells
NGS: next-generation sequencing

O

ODM: organoid differentiation medium
OGM: organoid growth medium
OMM12: oligo-mouse-microbiota 12
o/n: overnight
OOC: organ-on-a-chip
OrgOC: organoid-on-a-chip

P

PCV-2: porcine circovirus 2
PCR: polymerase chain reaction
PNC8: porcine nasal consortium
PNO: porcine nasal organoid
PRRSV: porcine reproductive and respiratory syndrome virus

Q

qPCR: quantitative polymerase chain reaction

R

RT-PCR: reverse transcription polymerase chain reaction

S

SCFA: short-chain fatty acids
SIV: swine influenza virus

T

T6SS: type VI secretion system
Th 17: T helper 17
TLR: toll-like receptors
TNFα: tumour necrosis alpha

U

URT: upper respiratory tract

Abstract

The animal microbiota is the ecological community of microorganisms living in multiple body sites. In particular, the nasal microbiota plays an important role in host health as it constitutes a barrier for respiratory pathogens. Interactions among the pig nasal commensal bacteria and with the nasal epithelium are determinant for pathogen exclusion, but no systematic approach was available to elucidate such interactions. This thesis provides new tools for exploring the pig nasal microbiota within its host context.

First, we studied whether an intensive antibiotic treatment to sows could prevent the transfer of nasal microbiota to piglets, as previous work highlighted that sows are the main source of piglet microbiota. The treatment of sows with ceftiofur alone or in combination with tulathromycin diminished the bacterial load in the nasal cavity of sows and piglets, causing dysbiosis in the piglets' nasal microbiota, which showed unusual taxa. However, the transmission of the microbiota was not entirely prevented, which limits the use of this piglet model for microbiota studies. Additional strategies are needed to develop germ-free pigs, while ensuring that the conditions remain easy to implement.

Next, we aimed to establish *in vitro* models to study the network of the piglet nasal microbiota. For this, we developed the Porcine Nasal Consortium (PNC8), a rationally designed synthetic community of 8 strains representing the most prevalent and/or abundant genera found in the nasal microbiota of healthy piglets. We found that PNC8 members varied in their ability to grow across 23 different *in vitro* conditions, which suggests that they harbour distinct metabolic functions. In addition, we confirmed the existence of interactions, such as the cooperation among *Rothia nasimurium* and *Staphylococcus aureus* with *Glaesserella parasuis* (virulent and non-virulent strains). In conclusion, PNC8 represents a valuable tool for examining the interaction network in the piglet nasal microbiota under *in vitro* defined conditions, as well as to elucidate its role in respiratory pathogen exclusion.

To explore the nasal microbiota-host interplay in a controlled *in vitro* system, we developed for the first time Porcine Nasal Organoids (PNOs), which showed similar structure and cell types than the *in vivo* pig nasal mucosa. We confirmed that some PNC8 members (*Moraxella pluranimalium*, *R. nasimurium* and *G. parasuis*) as well as a virulent *G. parasuis* strain adhered and colonized the PNOs, although at different levels. We also examined microbial-microbial and microbial-host interactions in this system by co-culturing *R. nasimurium* with the remaining 3 strains. Besides, PNOs reacted to the bacteria secreting different cytokines. *M. pluranimalium* and *G. parasuis* stimulated the production of proinflammatory cytokines, while *R. nasimurium* induced the secretion of INFγ and diminished the proinflammatory effect produced by the other bacteria. We conclude that PNOs recapitulate the *in vivo* nasal mucosa and can be useful to study host-microbe interactions in an *in vivo*-like system, contributing to the 3Rs principles.

In summary, this thesis provides new approaches to explore the nasal microbiota network under controlled conditions that mimic the *in vivo* environment of the piglet's nose. This work will contribute to understand the role of microbiota in pathogen exclusion.

Resumen

La microbiota animal es la comunidad ecológica de microorganismos que viven en múltiples partes del cuerpo. En particular, la microbiota nasal desempeña un papel importante en la salud del huésped, ya que constituye una barrera contra los patógenos respiratorios. A pesar de que las interacciones entre las bacterias comensales de la cavidad nasal de los lechones y el epitelio nasal son determinantes para la exclusión de patógenos, no existe ninguna metodología para estudiar estas interacciones de una forma sistemática. La presente tesis proporciona nuevas herramientas para explorar la microbiota nasal del cerdo en el contexto del huésped.

Inicialmente, se estudió si el efecto de un tratamiento intensivo de antibióticos en cerdas podía evitar la transferencia de microbiota nasal a sus lechones, dado que en previos estudios se ha visto que las cerdas son la principal fuente de microbiota para los lechones. Se observó que un tratamiento con ceftiofur solo o en combinación con tulatromicina reducía la carga bacteriana en la cavidad nasal de cerdas y lechones, causando disbiosis en la microbiota nasal de los lechones, que mostraba taxones inusuales. Sin embargo, la transmisión de la microbiota no se evitó por completo, lo que limita el uso de este modelo para estudios de microbiota. Por ello, se necesitan estrategias adicionales para desarrollar lechones *germ-free*, asegurando a la vez que las condiciones sean fáciles de implementar.

A continuación, nos propusimos establecer modelos *in vitro* para estudiar la red de interacciones de la microbiota nasal de los lechones. Para ello, se desarrolló el consorcio nasal porcino PNC8 (*Porcine Nasal Consortium*), una comunidad sintética diseñada racionalmente con 8 cepas que representan los géneros más prevalentes y/o abundantes de la microbiota nasal de lechones sanos. Se observó que los miembros del PNC8 variaban en su capacidad de crecer en 23 condiciones *in vitro* distintas, sugiriendo que poseen funciones metabólicas diferentes. Además, confirmamos la existencia de interacciones, como la cooperación entre *Rothia nasimurium* y *Staphylococcus aureus* con *Glaesserella parasuis* (tanto cepas virulentas como no virulentas). En conclusión, el PNC8 es una herramienta valiosa

para examinar la red de interacciones en la microbiota nasal de los lechones bajo condiciones *in vitro* definidas, así como para entender su papel en la exclusión de patógenos respiratorios.

Para explorar la interacción entre la microbiota nasal y el huésped en un sistema *in vitro* controlado, se desarrollaron por primera vez organoides nasales porcinos (*Porcine Nasal Organoids*, PNOs), que mostraron una estructura y tipos celulares similares a los encontrados en la mucosa nasal del cerdo. Confirmamos que algunos miembros de PNC8 (*Moraxella pluranimalium*, *R. nasimurium* y *G. parasuis*), así como una cepa virulenta de *G. parasuis*, se adherían y colonizaban los PNOs, aunque en distinto grado. También examinamos las interacciones microbio-microbio y microbio-huésped en este sistema, co-cultivando *R. nasimurium* con las otras 3 cepas. Además, los PNOs reaccionaron a la presencia de bacterias secretando diferentes citocinas. *M. pluranimalium* y *G. parasuis* estimularon la producción de citocinas proinflamatorias, mientras que *R. nasimurium* indujo la secreción de INFγ, reduciendo así el efecto proinflamatorio causado por las otras bacterias. Concluimos que los PNOs representan la mucosa nasal y pueden ser útiles para estudiar interacciones huésped-microbio en un sistema similar al *in vivo*, contribuyendo a los principios de las 3Rs.

En resumen, esta tesis proporciona nuevas herramientas para explorar la microbiota nasal bajo condiciones controladas que imitan el ambiente *in vivo* de la nariz del lechón. Este trabajo contribuirá a comprender el papel de la microbiota en la exclusión de patógenos.

Resum

La microbiota animal és la comunitat ecològica de microorganismes que viuen en múltiples llocs del cos. En particular, la microbiota nasal té un paper important en la salut de l'hoste, ja que constitueix una barrera en front els patògens respiratoris. Les interaccions entre els bacteris comensals de la cavitat nasal dels garrins i amb l'epiteli nasal són determinants per a l'exclusió dels patògens. Tanmateix, no hi ha cap metodologia disponible per estudiar aquestes interaccions de manera sistemàtica. La present tesi proporciona noves eines per explorar la microbiota nasal del porc en el context del seu hoste.

Inicialment, es va estudiar si l'efecte d'un tractament intensiu amb antibiòtics a les truges podia evitar la transferència de la microbiota nasal als seus garrins, ja que estudis previs han demostrat que les truges són la principal font de microbiota pels garrins. El tractament de les truges amb ceftiofur sol o en combinació amb tulatromicina va reduir la càrrega bacteriana a la cavitat nasal de les truges i dels garrins, causant una disbiosi en la microbiota nasal dels garrins la qual presentava taxons inusuals. No obstant això, la transmissió de la microbiota no es va evitar completament, fet que limita l'ús d'aquest model per a estudis de microbiota. Per això, calen estratègies addicionals per desenvolupar garrins *germ-free*, assegurant alhora que les condicions siguin fàcils d'implementar.

A continuació, ens vam proposar establir models *in vitro* per estudiar la xarxa de la microbiota nasal dels garrins. Per això, es va desenvolupar el consorci nasal porcí PNC8 (*Porcine Nasal Consortium*), una comunitat sintètica dissenyada racionalment amb 8 soques que representen els gèneres més prevalents i/o abundants de la microbiota nasal de garrins sans. Vam observar que els membres de PNC8 diferien en la seva capacitat per créixer en 23 condicions *in vitro* diferents, cosa que suggereix que tenen funcions metabòliques diferents. A més, vam confirmar l'existència d'interaccions, com la cooperació entre *Rothia nasimurium* i *Staphylococcus aureus* amb *Glaesserella parasuis* (tant soques virulentes com no virulentes). En conclusió, el PNC8 és una eina valuosa per examinar la xarxa

d'interaccions en la microbiota nasal dels garrins sota condicions *in vitro* definides, així com per entendre el seu paper en l'exclusió de patògens respiratoris.

Per tal d'explorar la interacció entre la microbiota nasal i l'hoste en un sistema *in vitro* controlat, vam desenvolupar per primera vegada organoides nasals porcins (*Porcine Nasal Organoids,* PNOs), els quals van mostrar una estructura i tipus cel·lulars similars als de la mucosa nasal del porc. Vam confirmar que alguns membres de PNC8 (*Moraxella pluranimalium*, *R. nasimurium* i *G. parasuis*), així com una soca virulenta de *G. parasuis*, s'adherien i colonitzaven els PNOs, encara que a diferents nivells. També vam examinar les interaccions microbi-microbi i microbi-hoste en aquest sistema co-cultivant *R. nasimurium* amb els altres 3 bacteris. A més, els PNOs van reaccionar a la presència de bacteris secretant diferents citocines. *M. pluranimalium* i *G. parasuis* van estimular la producció de citocines proinflamatòries, mentre que *R. nasimurium* va induir la secreció d'INFγ, reduint així l'efecte proinflamatori causat pels altres bacteris. Concloem que els PNOs reprodueixen la mucosa nasal i poden ser útils per estudiar les interaccions hoste-microbi en un sistema semblant al *in vivo*, contribuint als principis de les 3Rs.

En resum, aquesta tesi proporciona noves eines per explorar la microbiota nasal sota condicions controlades que imiten l'ambient *in vivo* del nas del garrí. Aquest treball contribuirà a entendre el paper de la microbiota en l'exclusió de patògens.

General introduction

1. The microbiota

1.1. Functions of the microbiota

The animal microbiota is defined as the ecological community of microorganisms that inhabit several body sites, which are considered their niches (1–3). The acquisition and preservation of a proper microbiota are determinant for the host well-being (4), as these communities exert distinct functions through interactions with the host, such as metabolic, immunologic and defensive against external agents (1,5–7). In fact, many health problems have been associated with a disturbed microbiota, a condition called dysbiosis (**Figure 1)**. In contrast, eubiosis is considered when the microbiota is quantitative and qualitative balanced in healthy state (6,8–11).

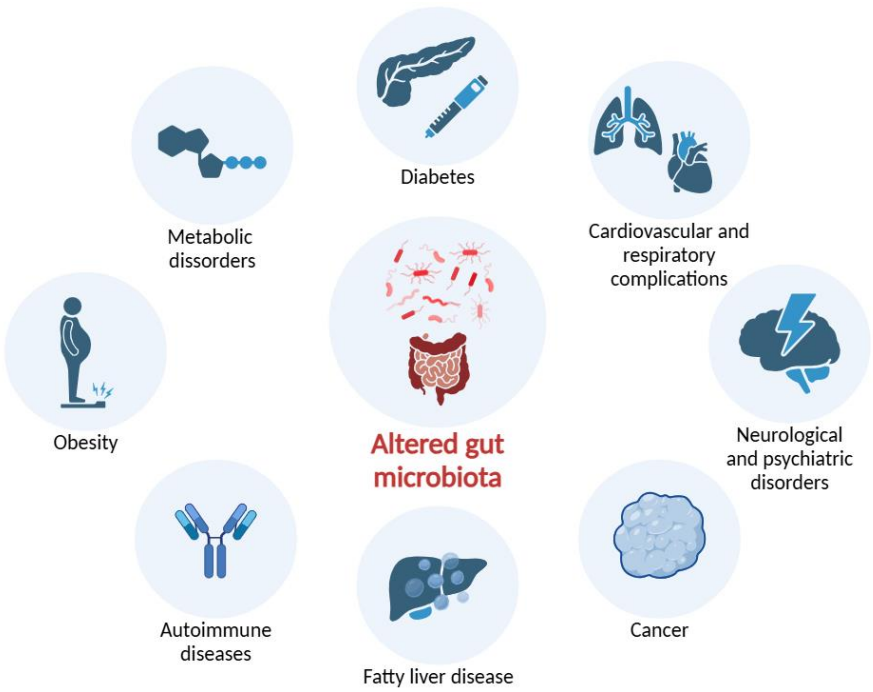

Figure 1. Diseases associated with an altered composition of the human gut microbiota.

Members of the gut microbiota are responsible for the metabolism of dietary elements and nutrient utilization, such as amino acids, proteins and indigestible carbohydrates, including cellulose, pectin, and lignin. These indigestible carbohydrates can be metabolized into short-chain fatty acids (SCFAs), which are important to gut-brain signalling pathways that mediate immune, endocrine, neural and humoral responses (12–14). SCFAs are metabolites mainly produced by *Bacillota* (*Firmicutes*) and *Bacteriodota* (*Bacteroidetes*) that are significant for the integrity of the mucosal barrier and have anti-inflammatory and anti-carcinogenic properties (13). Besides the SCFA production, gut microbiota members also contribute to other vital functions, such as the metabolism of bile salts and the elimination of some toxins (14). Furthermore, microbial communities are actively involved in the biosynthesis of vitamins, hormones, cholesterol, conjugated fatty acids, neurotransmitters and other indispensable compounds, highlighting their multifaceted role in maintaining the host health (13,14).

The microbiota has also an essential role in immune system homeostasis and maturation. The immune system is shaped by the microbiota, since it contributes to the stimulation of the proliferation of neutrophils, eosinophils and macrophages, and modulates the production of cytokines and other molecules of the immune system. Moreover, it is well known that the microbiota controls some specific lymphocyte response. Commensal members can regulate the T cell response, especially the T helper 17 (Th17) cells, which are a specific lineage of $CD4^+$ cells responsible of the production of interleukin 17, interleukin 22 and interleukin 1β (IL-1 β) (4,9). Several studies have shown how interventions on the microbiota can modulate and improve the action of Th17 cells conferring protection against metabolic syndrome among others (15,16). Indeed, in antibiotic treated or germ-free mice, Th17 cells are significantly diminished supporting these findings. Regulatory T cells are also influenced by the microbiota, as they are reduced in gut lamina propria in germ-free mice (17). The microbiota is also involved in the B cell response due to its role in the primary B-cell development and immunoglobulin diversification and production (4). Immunoglobulins are crucial to maintain a well-

balanced relationship between the host and the microbiota. For instance, immunoglobulin A, one of the most important immunoglobulins produced in the gut and the nasal mucosa, regulates the microbiota abundance, upholding the host-commensal mutualism and at the same time supporting a crosstalk communication (4,9,18). In agreement, a dysbiotic microbiota in the inferior turbinate mucosa was related to a high level of immunoglobulin E, and thus, with allergic rhinitis and asthma, suggesting that the microbiota plays a role in allergic responses (19,20).

Toll-like receptors (TLRs) are pattern recognition receptors (PRRs) that recognize the bacterial and viral pathogen-associated molecular patterns (PAMPs) such as lipoproteins, lipopolysaccharide (LPS), flagellin among others (21,22). Moreover, TLRs found in epithelial and lymphoid cells have been associated with the differential recognition between commensal and pathogenic bacteria, promoting the immunological tolerance to the members of the microbiota (9). After TLRs stimulation, a signalling cascade is triggered, resulting in the releasing of the nuclear factor kappa-light-chain-enhancer of activated B cells (NF-κβ), which activates the secretion of cytokines and other mediators of the humoral immune response (9,22). Microbial communities shape a stable network that prevents the invasion of pathogenic microorganisms, conferring a determinant protective role to the host (4). This phenomenon is known as colonization resistance or pathogen exclusion, and it contributes to the maintenance and reinforcement of the mucosal barriers (4,13,23). Microbial symbionts have a myriad of mechanisms to fight pathogen invasion and infection (**Figure 2**):

a. **Direct killing of bacteria**, using the type VI secretion system (T6SS), found in most Gram-negative bacteria (4). For example, commensal *Bacteroides fragilis* use the T6SS to antagonize pathogenic enterotoxigenic *B. fragilis* in the mice gut (24).

b. **Secretion of inhibitory metabolites**, such as SCFAs, which have shown antibacterial effects in the gut (25). For example, butyrate and propionate can supress virulence factors of *Salmonella* ser. *thyphimurium* and pathogenic

Escherichia coli (4). SCFAs can also promote the proliferation of *Bifidobacterium* and in consequence, inhibit pathogenic *Clostridium* and *Klebsiella* proliferation (26). Bacteria can also secret small polypeptides called bacteriocins (4), such as *Lactobacillus salivarus,* that can protect mice from *Listeria monocytogenes* infection by secreting these molecules (27).

c. **Competition for nutrients and space**, such as the competition for mucosal adhesion sites (often glycan structures) (4). For example, *Bacteroidetes* can avoid *Klebsiella pneumoniae* colonization and transmission by using their conserved commensal colonization factor (CCF) polysaccharide locus (28).

d. **Stimulation of the host mucus production**. Mucin-5AC (MUC5AC) is the predominant mucin in the mammal airways and its gene expression and production is normally induced in response to bacteria, viruses, chemicals, etc., which facilitate the expulsion of pathogens (4,29).

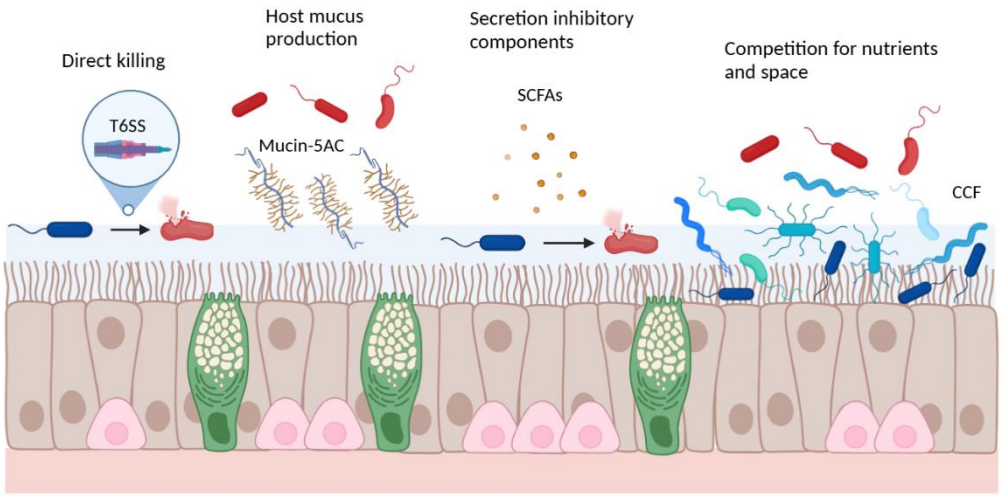

Figure 2. Colonization resistance and pathogen exclusion mechanisms in the mucosa: direct killing of the pathogenic bacteria by the type VI secretion system (T6SS), stimulation of the Mucin-5AC, secretion of inhibitory components such as short-chain fatty acids (SCFAs), and host bile acids and competition for nutrients and space using the conserved commensal colonization factor (CCF). Commensal members of the microbiota are represented in blue while pathogenic bacteria are represented in red.

To date, most of this knowledge has been mainly investigated in the human gastrointestinal microbiota. However, other less-studied microbiotas, including the dermal, oral, respiratory and reproductive ones, have also shown to be determinant in both human and animal health (30–34).

1.2. The pig nasal microbiota

The respiratory tract is responsible for the exchange of oxygen and carbon dioxide and is divided into the upper respiratory tract (URT) and the lower respiratory tract (LRT). The URT is constituted by the nose, the nasopharynx and oropharynx, while the LRT is composed of the trachea, the bronchi, bronchioles and the alveoli (30,35,36). In health, the respiratory microbiota is restricted to the URT, and it is colonized by niche-specific bacteria (30,37). Like gut microbiota, respiratory microbiota is strongly associated to animal health and to essential functions of the host. However, despite its high relevance, it has been less studied (38).

The nasal cavity is the most exposed part of the respiratory tract, and has several physiological functions such as air filtration, warming, humidification and olfaction (39). As it is continuously exposed to the exterior, it is the main entry route for the respiratory pathogens. Hence, the nasal mucosa is the first barrier that, together with the nasal microbiota, confers protection against respiratory pathogens by direct competition (**Figure 3**) (40–43). Besides, the microbiota has a key role in mucosal immunity, being able to modulate the immune system of the host and leading to a better functionality (43).

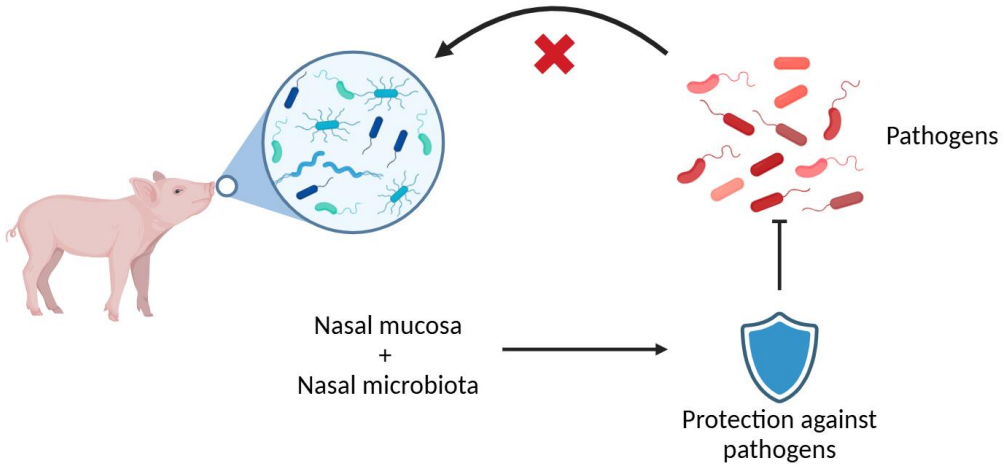

Figure 3. Scheme of the protection that confers the nasal mucosa together with the microbiota against pathogens' colonization.

Pseudomonadota (*Proteobacteria*) and *Bacillota* (*Firmicutes*) are the predominant phyla that colonize the nose of pigs, followed by *Bacteroidota* (*Bacteroidetes*) and *Actinomycetota* (*Actinobacteria*) (44–48). *Moraxella* is the most relative abundant and prevalent genera, but others, as *Streptococcus, Weeksella*, *Staphylococcus*, *Rothia* and *Lactobacillus* are also prevalently found. Strikingly, some anaerobic bacteria have been also identified in the pig nasal microbiota, such as *Clostridium* (44,45,49). This fact is supported by a recent study in which it was observed that anaerobic taxa were not only present, but also active in the nasal microbiota, indicating that they are not merely the result of contamination (50).

The nasal microbiota is a complex ecosystem that is constantly evolving. Indeed, there are remarkable changes in the composition and structure of the piglets' nasal microbiota during the firsts 7 weeks of life, when it reaches a stable stage (47). Besides the dynamic changes, the nasal microbiota can be modulated by a plethora of factors such as sow-piglet contact, diet, antimicrobials, treatments and stress, among others (45,48,51,52).

1.3. The microbiota establishment

In pigs, as well as in all mammals, the early microbial colonization provider is their mother by the direct contact with the vaginal tract during the birth (52–55). Indeed, the delivery by caesarean is considered one of the principal causes of disruption of the normal colonization of the microbiota that can alter its composition (53,56–58). In mammals, breastfeeding is also an important factor that can modulate the correct development of the newborn microbiota due the presence of some oligosaccharides, which potentially stimulate the proliferation of *Bifidobacteria* and *Lactobacilli* species (13,56,59,60). In newborn piglets, breastfeeding is crucial because it provides warmth and energy, while influencing the establishment and development of gut microbiota, similar to humans (61). Since piglets are born more immunologically compromised in comparison to humans, the colostrum intake is also essential to provide them with the antibodies and immune factors they need to protect against infections, support the development of their immune system, and ensure their survival in the early stages of life (55,61).

After birth, a combination of endogenous and exogenous factors, such as the genetic predisposition, the geographical location and the social context can shape the newborn microbiota, affecting the richness and diversity of the commensal bacteria and hence, the pathogen susceptibility (13). In piglets, weaning is the abrupt separation of the newborns from their mothers, which is a stressful moment for them (62,63). This process has a significant impact on the microbiota diversity and composition that may compromise their health and welfare (31,32,55,63). Some of the factors involved in this period that can alter the microbiota are described in **Figure 4** (55,62–66).

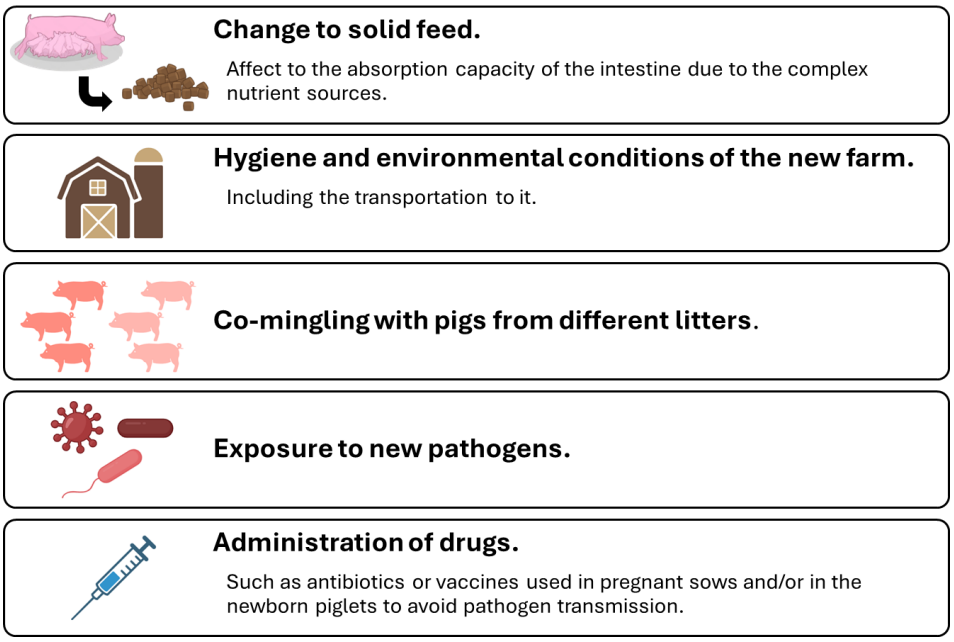

Figure 4. Management practices performed at weaning that can affect to piglet's microbiota.

1.4. Tools to study the microbiota composition

Cultivation techniques have been the most common approach to study the microbiota during the last century (67,68). Bacterial isolation using laboratory media and identification of strains based on physiological or biochemical properties, as Gram staining, have been convenient to describe the phenotypic characteristics of the isolates (67). More recently, culturomics was developed to improve the characterization of these communities. In culturomics, multiple culture conditions are used, coupled with matrix-assisted laser desorption/ionization time-of-flight mass spectrometry (MALDI-TOF) and 16S rRNA gene sequencing for the identification of the microbial species (69). However, all these culture-dependent approaches have the limitation of determining only the bacteria that can grow under the conditions used.

The development of culture-independent methods based on the extraction and sequencing of the DNA has facilitated the study of complex bacterial communities (67). Next-generation sequencing (NGS) started to be exponentially used due to the ability to perform massive parallel sequencing of small DNA fragments amplified by

Polimerase Chain Reaction (PCR) (70,71), in comparison to classic Sanger sequencing, which only analyses one sequence at a time (70,72,73). Some examples of NGS platforms are Illumina and 454-pyrosequencing, among others. More recently, third-generation NGS PCR-independent techniques were developed, which allowed the amplification of longer DNA molecules, such as Pacific Biosciences (PacBio) and Oxford Nanopore Technology (ONT) (70).

To characterize microbial communities, the sequencing of a marker gene is a widespread approach in all sequencing technologies described before. A marker gene should include highly conserved regions (for universal amplification) containing some hypervariable regions (for unique classification). A good example is the 16S rRNA gene, which is the most commonly used gene for studying bacterial populations (74). Another option is whole genome sequencing (WGS) metagenomics, which allows the simultaneous sequencing of all the genetic material in a sample, providing information of other aspects encoded in regions beyond the 16S rRNA gene (70). However, due to the higher economic costs along with the intricacy of the generated data, the 16S rRNA marker gene sequencing has become the preferred technique in the last decades.

2. Role of the nasal microbiota in bacterial diseases in piglets

2.1. Disease and etiological agents

Infectious diseases of animals have a significant impact on global health. In wildlife, emerging infectious diseases are responsible for numerous epidemics and pandemics, while in domestic and farm animals, they are linked to relevant economic loses in the food industry, especially the respiratory pathogens, since they cause higher mortality and growth retardation during the fattening period (75–77). Some respiratory pathogens can be found in the nasal microbiota of healthy piglets. However, depending on different factors such as the virulence of the strains, the animal immunity status and the environmental conditions, they can also produce the associated disease. Due to this duality, they are called pathobionts, and *Glaesserella*

parasuis, *Streptococcus suis* and *Mycoplasma hyorhinis* are some examples. These three bacteria can produce the inflammation of the serous membranes, known as polyserositis (78–82). In agreement, the clinical signs produced are common to the three infections, which make the differentiation of these diseases quite challenging, requiring the identification of the specific agent in the laboratory (83).

2.2.1. *Glaesserella parasuis*

G. parasuis is a pleomorphic Gram-negative bacterium that belongs to the *Pasteurellaceae* family and whose only host is the pig. It is commonly found in the URT of the pig as part of the normal nasal microbiota. However, it is also the etiological agent of the polyserositis called Glässer's disease, a severe disease that causes considerable welfare problems, and production loses in the pig industry (84). The most common clinical signs are fever, anorexia, depression, respiratory problems, nervous signs, lameness, and death (79).

The colonization by *G. parasuis* occurs soon after birth through the direct contact with the sow (85), and piglets normally are protected from Glässer's disease by the maternal immunoglobulin M (IgM) and immunoglobulin G (IgG) antibodies (79). Generally, the disease is produced when virulent strains of *G. parasuis* colonizing the nasal mucosa, can spread systemically to internal organs due to their resistance to the phagocytic activity of the porcine alveolar macrophages (PAMs) and to the serum complement (79). In contrast, the non-virulent strains do not produce disease and can only be isolated from the nose, being restricted to the URT by the innate immunity (78,86,87). Additionally, *G. parasuis* can be found in co-infections with other pathogens, such as the porcine reproductive and respiratory syndrome virus (PRRSV), the swine influenza virus (SIV), the porcine circovirus type 2 (PCV-2) and *S. suis* (88–90).

2.2.2. *Streptococcus suis*

S. suis is a Gram-positive encapsulated coccus that belongs to the *Streptococcaceae* family, and it is considered the most important porcine streptococcal etiological agent due to its impact in swine industry around the world

(80,91). Among all the clinical signs, fever, nervous signs indicative of meningitis, lameness, and anorexia are the most common, even causing the death of the animal (80,92). Lesions found at necropsy include polyserositis and valvular endocarditis. Moreover, *S. suis* is a zoonotic pathogen and, in consequence, a public health concern, especially in Southeast Asia (93,94). Humans in close contact with pigs and/or eat raw pig products are particularly at risk of being infected with this bacterium (92,95,96). The symptoms in humans are similar to the clinical signs observed in the pigs.

The associated systemic disease described above is normally produced by some strains considered virulent, but *S. suis* is also a normal commensal member of the URT microbiota, typically found in the nose and the tonsils of pigs. Normally, colonization of piglets starts at the birth canal, since *S. suis* can colonize the vagina, and continues after birth through direct contact with the sows (80). The pathogenesis and the mechanisms that *S. suis* use to pass though the mucosal barrier and systemically infect the animal are still unknown (97). In some cases, *S. suis* can co-infect and contribute to the pathogenesis of other etiological agents such as the PRRSV, PCV-2, SIV, *G. parasuis*, *Actinobacillus pleuropneumoniae, Pasteurella multocida* and other bacteria (98,99).

2.2.3. *Mycoplasma hyorhinis*

M. hyorhinis is a small wall-less bacteria that belongs to the *Mycoplasmataceae* family (81,100). *Mycoplasma* are the smallest free-living organisms capable of self-replication, and consequently, their genome is very small. This implies a reduced metabolic and enzymatic capacity, which force *Mycoplasma* to be a nutritional parasite (101).

M. hyorhinis is considered a swine colonizer that is normally found in the mucous membranes of the URT and the tonsils (100). This bacterium is transmitted through contact with the sow or with other piglets. It can bind to the ciliated respiratory epithelium using the variable lipoproteins that are found in their cell membrane (81). In some cases, it can produce polyserositis, arthritis, eustachitis,

conjunctivitis and even meningitis in post-weaning piglets (102–105). Indeed, Clavijo et al. (2019) found the same strain in the nose and in the pericardium of sick animals, which indicated that *M. hyorhinis* can disseminate and produce, in this case, pericarditis (106). In addition, few studies have demonstrated that *M. hyorhinis* can produce pneumonia (107,108). Nevertheless, this latter fact is controversial, as other studies have suggested that it may play only a secondary role in pneumonia, together with *Mycoplasma hyopneumoniae,* PCV-2 or PRRSV (109–111). Until now, no clear marker has been identified to differentiate between virulent and non-virulent strains.

2.2. Role of the nasal microbiota in disease development

Alterations in the nasal microbial diversity and relative composition facilitates the development of disease by pathobionts. Correa-Fiz et al. (2016) showed that healthy weaned piglets from farms with recurrent problems of Glässer's disease had a nasal microbiota with relative lower alpha diversity and different composition than piglets from healthy farms (45). In comparison to the diseased farms, an increase of *Moraxella* and *Enhydrobacter*, accompanied by a decrease of *Haemophilus* (*Glaesserella*) and *Streptococcus* genera was associated with health. In agreement with this, Blanco-Fuertes et al. (2021) reported that an altered nasal microbiota composition was associated with the development of polyserositis produced by *M. hyorhinis* as well. For instance, *Moraxella* genus was reduced in the group of animals from farms with recurrent problems with polyserositis associated with *M. hyorhinis* in comparison to the healthy control farms, while *Enhydrobacter* was found in a higher abundance in the *M. hyorhinis* farms (44). Similarly, a recent study has demonstrated that the piglet's tonsillar microbiota influences the development of *S. suis*-associated disease via colonization resistance: *Rothia nasimurium* was reduced in comparison to the healthy animals, while *Fusobacterium gastrosuis*, *Bacteroides heparinolyticus*, *Prevotella* and *Alloprevotella* species were in a higher abundance in diseased animals (112). In global, these studies suggest that the nasal and tonsillar colonizers can have a protective role against respiratory pathogens.

The protective role of the microbiota has been observed also with *Staphylococcus aureus*. This bacterium is responsible of septicaemia, polyarthritis, endocarditis, chronic infections and lesions of the skin (113). Piglets that were not colonized with *S. aureus* showed microbial species with a potential probiotic role in their nasal microbiota, such as *Leuconostop spp.* which produces lactic acid, and members of the *Lachnospiraceae* family, related to butyrate production. By contrast, *S. aureus*-colonized piglets were associated with pathogenic bacteria such as *P. multocida* and *Klebsiella spp*. (46). Moreover, in another study, it was revealed a strong negative correlation between the presence of *S. aureus* and *R. nasimurium*, which is a normal commensal of the pig nose microbiota, among other bacteria (114).

Alterations in the nasal microbiota can also influence the susceptibility to viral diseases, such as SIV and PRRSV (115,116). These viruses, in turn, may be associated with shifts in the microbial diversity, which can further contribute to susceptibility to other infections.

Despite the implications that the nasal microbiota has on pathogen exclusion, the comprehension of the commensal-pathogen interplay remains unclear.

2.3. Impact of the antibiotics in the nasal microbiota

Antibiotics are a type of antimicrobials produced by microorganisms that are commonly used to treat bacterial infections (117). Among all the different antibiotics used to treat respiratory diseases in pigs, penicillin, ceftiofur, ampicillin and enrofloxacin are useful to treat the polyserositis caused by *G. parasuis* and *S. suis* (79), while tetracyclines, fluoroquinolones and macrolides are normally administered when animals are infected with *Mycoplasma* (118,119). Although the discover of antibiotics changed the modern medicine, their inappropriate and excessive use worldwide both in humans and animals has resulted in a dramatic increase of antimicrobial resistances (AMRs), becoming a global public concern that requires an urgent solution. The situation is even worse due to the decline in the development

of new effective antibiotics (120–124). Hence, ensuring animal health to minimize the use of antibiotics must be a priority in the swine industry (124,125).

Another important antibiotic-associated problem is the disturbance that these drugs produce in the microbiota, affecting the host health. Several studies have found that antibiotics produce a decrease of the bacterial diversity in the piglet's nasal microbiota, including a microbial shift in the composition over time (48,126,127). Mou et al. (2019) demonstrated how an oxytetracycline treatment in 2-week-old piglets decreased the nasal bacterial diversity, especially when the antibiotic was administered in the feed. In addition, increased relative abundances of *Actinobacillus* and *Streptococcus* were found, together with decrease of relative abundances of commensal genera such as *Lactobacillus* (128). In agreement, Correa-Fiz et al. (2019) and Blanco-Fuertes et al. (2023) observed higher relative abundance of *Prevotella* and *Lactobacillus*, accompanied by an improvement of the piglet's health, when antibiotic treatments were removed from the management of the farrowing unit (126,127).

Altogether, these problems reflect the urgent need for developing alternative therapies to prevent or treat respiratory bacterial infections, taking into consideration the importance of a good-balanced microbiota.

2.4. Microbiota intervention as an alternative for antimicrobial therapy

Nowadays, the main alternative to the use of antibiotics for controlling respiratory diseases are vaccines. For the three etiological agents that produce polyserositis in pigs mentioned above, there are commercial vaccines available in Europe for *G. parasuis* and for *S. suis*, but not for *M. hyorhinis* (81,129–131), although experimental vaccines are being developed for the three pathogens (132–139).

Nevertheless, vaccines are generally designed to target only one pathogen. Therefore, exploring alternatives that could tackle multiple pathogens simultaneously by competition and stimulation of the piglet's immune system is highly interesting. Modulation of the microbiota emerges as an interesting approach to control disease avoiding or diminishing the use of antimicrobials. A common way

to regulate the microbial communities is by using probiotics, prebiotics and postbiotics (**Figure 5**). Probiotics are microorganisms that modulate the microbiota positively and reduce pathogenic bacteria, while prebiotics are non-digestible substances that can stimulate the growth and establishment of commensal microorganisms, including the considered probiotics (10,140,141). Postbiotics are soluble factors derived from the metabolic activity of bacteria or any released molecule that can provide health benefits to the host, including non-living whole microorganisms o parts of them (10,142,143).

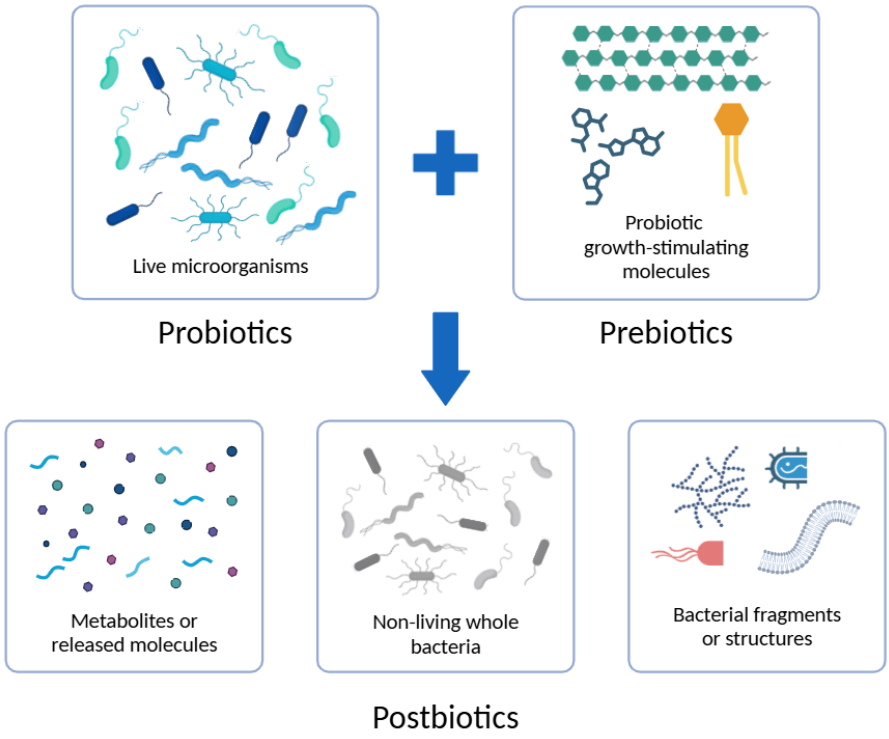

Figure 5. Schematics of microbiota interventions: probiotics, prebiotics and postbiotics.

Until now, only probiotics have been used to modulate the pig respiratory microbiota, demonstrating beneficial effects on the animals' health. For instance, Rattigan et al. (2023) tested the probiotic capacity of an intranasally inoculated *Lactococcus spp.* cocktail, which was well-tolerated and did not have any adverse

effect on the piglet's health, showing a potential immunomodulatory role (144). In another study, the intranasal inoculation of *Bacillus subtilis* on piglets stimulated local immune responses, exhibiting an increased number of immune cells in the nasal mucosa and tonsils along with a stimulated immune system (145). However, both treatments were not assessed to avoid pathogen colonization and infection. A recent study showed the potential probiotic activity of the intranasal inoculation of some commensal colonizers of the pig nasal microbiota. This inoculation that included *Moraxella pluranimalium*, *Vagococcus lutrae*, *Streptococcus pluranimalium*, *R. nasimurium* and a non-virulent strain of *G. parasuis*, not only ameliorated the long-term changes produced by a ceftiofur treatment on the microbiota but also demonstrate that these bacteria were able to modulate the pig nasal microbiota (126).

These strategies have been widely studied in humans, but less applied in animal health, which should be seriously considered due to the importance of zoonotic diseases and increase of AMRs. Hence, understanding the interactions between the members of the piglet's nasal microbiota as well as with the pathobionts will allow the design of rational strategies to improve the protective capacity of the microbiota, supporting efforts to avoid antibiotic use.

3. Approaches to study host-microbiota interactions

3.1. Interactions in the microbiota

Interactions among the members of the nasal microbiota are crucial to shape the community network, as they share and compete for many metabolites found in their niches (42). Importantly, those interactions can also determine and modulate pathogen entry and therefore, the subsequent capacity to disseminate in the host and produce disease. However, the study of the nasal microbiota is not an easy task due to the complexity of this ecosystem. A useful approach to simplify the complexity and understand the network in those communities is the use of synthetic communities. These consortia are well-defined and characterized mixtures of live microorganisms, generally bacteria, that effectively represent the microbiota (146).

Synthetic communities were developed to represent the gut microbiota, such as for example the Oligo-Mouse-Microbiota (OMM12), which has been used to perform pathogen exclusion studies with *Salmonella* in mice (147). In addition, OMM12 has been crucial to understand microbe-microbe metabolic interactions (148–151). For example, Pérez Escriva et al. (2022) unravelled the exchange of nutrients (cross-feeding) between the members of OMM12 to elucidate its network functionality. At the beginning of this thesis, there was not a nasal consortium defined for any animal species to study the interactions within the microbiota and with respiratory pathogens.

In terms of respiratory pathogen exclusion, many studies have been conducted in humans. These studies include techniques such as the use of spent media assays, liquid and side-by-side co-cultures, and metabolomics, to elucidate such interactions (**Figure 6**) (150,152,153). For instance, some investigations have shown that the negative association of the human nasal commensal *Dolosigranulum pigrum* with *Staphylococcus aureus* and *Streptococcus pneumoniae* could be explained by growth inhibition of the pathogens by *D. pigrum* (in synergy with *Coryneobacterium* species in the case of *S. pneumoniae*) (152,154–156). On the other hand, *D. pigrum* showed several auxotrophies and may be dependent on other bacteria and/or the host for obtaining key nutrients (152). Similarly, Stubbendieck et al. (2023) showed that various *Rothia* species inhibited *Moraxella catarrhalis* by secreting a peptidoglycan endopeptidase, explaining why *Rothia* spp. was negatively associated with the presence of *Moraxella catarrhalis* and more abundant in the nasal microbiota of healthy children noses compared to children with cold symptoms (153). These findings support the role of microbe-microbe interactions in shaping the composition of the nasal microbiota and the possibility of designing microbe-targeted interventions to reshape nasal microbiota and exclude pathogens, which could also be relevant for pigs.

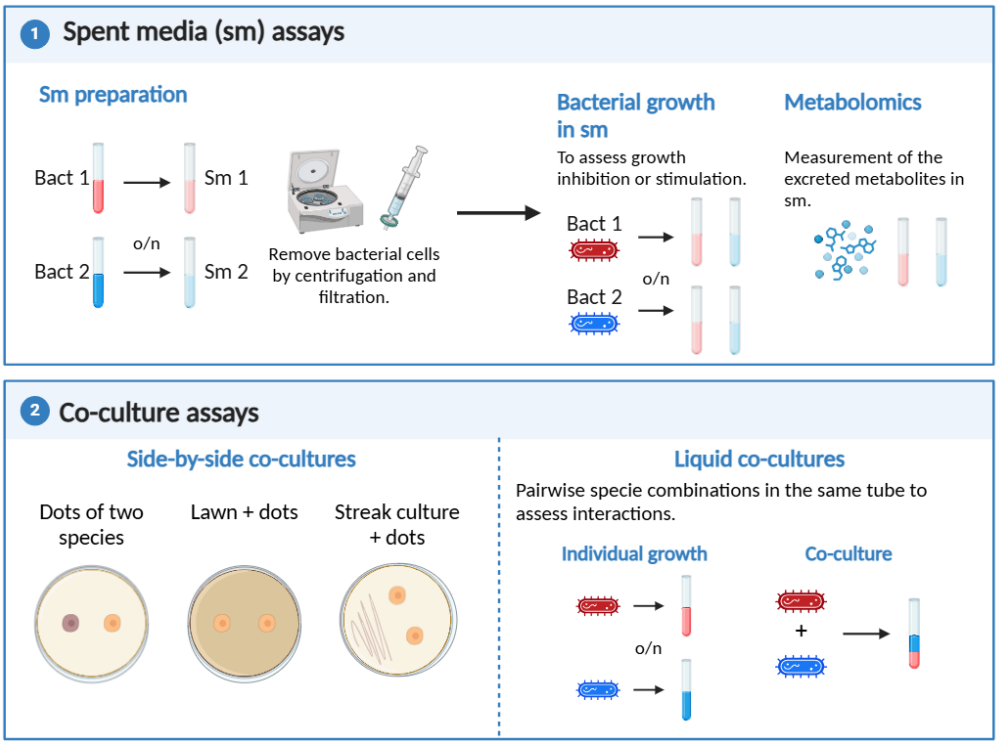

Figure 6. Schematic representation of some techniques used to study microbe-microbe interactions *in vitro*.

3.2. Interactions with the host

While studying isolated microbial communities *in vitro* can provide insights into their basic metabolic and ecological interactions, such studies lack the complexity of the host-microbiota relationship. The microbiota composition, diversity, and functionality are shaped by the host's physiology and immune system, while the microbiota, in turn, influences host health, contributing to processes such as immune modulation and resistance to pathogens in a bidirectional relationship. A comprehensive understanding of the microbiota requires studying it within the host environment, and to achieve this, different approaches have been developed (**Figure 7**).

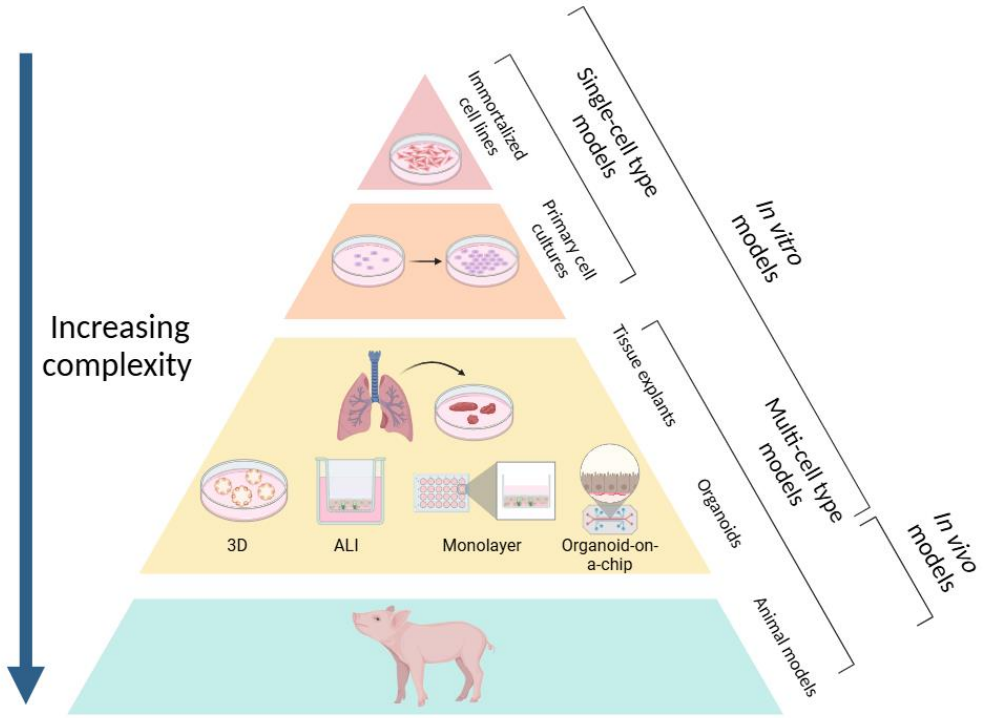

Figure 7. Host models to study host-microbiota interactions. Inspired by Aguilar et al. (2021) (157).

3.2.1. Host models based on a single cellular type

Since the establishment of HeLa cells in the 1950s, immortalized cell lines have proven to be a useful tool to study host-pathogen interactions, primarily due to their relatively cost-effectiveness and ease of handling (157). Cell lines were initially isolated from tumours and embryos, which make them able to escape from the cell cycle restrictions, proliferating and growing constantly without limitations *in vitro* (158,159). Subsequently, methods for obtaining immortalized cell lines were developed, such as physical or chemical stimulation to abolish the regulation of proto-oncogenes or tumour suppressor genes, heterologous expression of viral oncogenes to evade from the cell cycle control or stimulation of the cellular telomerase to overcome the replicative senescence produced by telomere shortening (158).

In pigs, the immortalized epithelial cell line PK-15, isolated from the kidney of an adult pig, was used, for instance, to understand *G. parasuis* and *M. hyorhinis* pathogenesis (160–162). Human immortalized cell lines have been also used to assess the adhesion capacity of some pig nasal commensals, such as the human lung adenocarcinoma A549 cells (163,164). Despite both PK-15 and A549 cell lines were useful, they were not isolated from the swine respiratory tissue. Thus, in order to better simulate the *in vivo* scenario, the swine tracheal epithelial cell and the newborn pig trachea cell lines, among others, were employed to study the infections of swine respiratory bacteria such as *G. parasuis*, *M. hyorhinis*, S*. suis*, *P. multocida* and *A. pleuropneumoniae* (161,165–170).

Although immortalized cell lines were practical and extensively used, they have limitations, since they fail to mimic the functions and structures of the *in vivo* tissue, such as polarization, proper barrier formation or cell differentiation, among other essential aspects of the tissue. Hence, primary cell cultures represented an appealing alternative, as they are directly isolated from the specific tissues, better mimicking their functions *in vitro* (157). Many studies have isolated swine primary cell lines from nasal, tracheal and lung tissues to perform host-pathogen studies (171–174). Nevertheless, primary cell lines have a low expansion and fast differentiation rate, which quickly ends in culture death. In addition, the amount of fresh tissue needed to generate them is remarkably high (157,158).

3.2.2. Host models based on multi-cellular type approaches

The nasal mucosa is a multi-layered structure, where the outermost layer is a pseudostratified epithelium whose integrity and polarity are maintained by intercellular tight junctions. This epithelium contains different cell types as shown in **Figure 7** (41,175–177):

a) Ciliated cells: key to maintain the airway homeostasis by trapping and expelling the external agents by rhythmically beating their cilia in a process that is known as mucociliary clearance (MCC).

b) Goblet cells: responsible of the mucus production, and that together with the ciliated cells, are crucial to maintain the MCC.

c) Proliferative or basal cells: stem cells able to self-renew and responsible for giving rise to most of the other cell types when required.

Below the pseudostratified epithelia, the lamina propria is located, where glands and immune cells are found. These innate immune cells are crucial for the rapid immune surveillance and response in the nasal mucosa (41,175) (**Figure 8**).

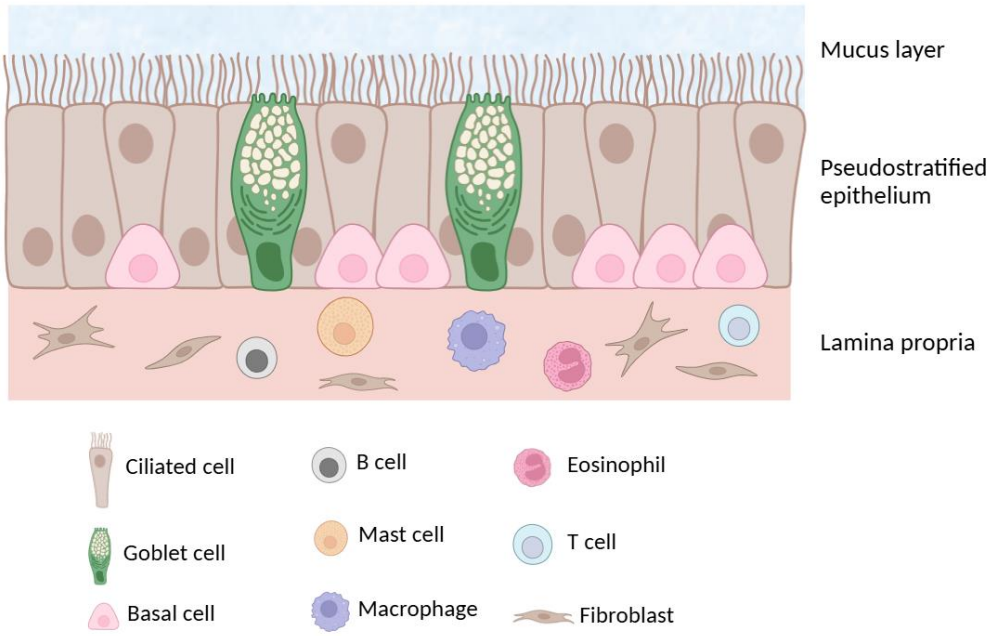

Figure 8. Nasal mucosa, including the mucus layer secreted by the Goblet cells, the pseudostratified epithelium and the lamina propria with the different cell types that constitute the tissue.

Airway explants, which consist in three-dimensional segments of the tissue, containing diverse cell types as well as spatial information, can mimic the physiological environment *in vitro*, normally maintained in air-liquid interface (ALI) conditions (157,178,179). Many studies have shown the value of these models for elucidating host-pathogen interactions, such as SIV, avian influenza virus and African swine fever virus infections using *ex vivo* explants of porcine nasal mucosa, trachea,

bronchi or lung tissues, including precision-cut lung slices (PCLS) (178,180–183). Other studies also used the PCLS to understand interactions between *S. suis* and *Bordetella bronchiseptica* or SIV, which promoted *S. suis* adherence, colonization and invasion (184,185). Moreover, Dumigan et al. (2019) studied the bacterial pathogenesis of *Klebsiella pneumoniae* using the *ex vivo* lung perfusion system, in which they sustain the lungs in the laboratory, allowing the proper study of *K. pneumoniae* pathogenic potential and the inflammatory responses of the subsequent infection (186). However, although explants are a valuable tool that clearly represents the tissue in its entirely, they require fresh tissue obtained few hours before and they are limited by their short-term viability. Recently, Lee-Ferris et al. (2024) have described methods to maintain these explants until 14 days, by using Gelfoam sponge in ALI cultures, enhancing the value of this technique for long-term studies (187).

A more recent strategy is the use of organoids, which are 3D *in vitro* culture systems derived from self-organizing stem cells. Organoids were first developed from the human intestinal tissue by Sato et al. (2009), which showed that intestinal stem cells could proliferate *in vitro* and generate these 3D structures also called mini-guts (188). Organoids recapitulate the *in vivo* architecture and functionality of the parent organ and are phenotypic and genetically stable in long-term cultures. Organoids can be derived from two types of stem cells: from pluripotent stem cells, that can be either embryonic stem cells or induced pluripotent stem cells; and from adult stem cells, which are tissue-specific stem cells (157,189,190).

The use of organoids to elucidate host-microbiota and host-pathogen interaction have been widely applied in different human tissues, mainly in the intestinal tissue (10,191,192), although many studies of respiratory pathogens in organoids derived from different parts of the human respiratory system have been also conducted (193–196). Indeed, a recent study used human nasal organoids to understand the bacterial nasal colonization of some pathogens such as the methicillin-resistant *S. aureus* and *S. pneumoniae* but also tested the colonization of

D. pigrum to elucidate the host-microbiota and host-pathogen interactions (197). In pigs, a plethora of organoids from various organs have been developed, including kidney, airway tract, liver and intestine, and some of them have been used to test host-pathogen interactions (198–201). Some studies have generated porcine airway organoids to study the virulence of SIV strains, as well as the porcine respiratory coronavirus infection (202,203). However, to date no pig nasal organoid model has been developed yet.

Organoids are first isolated in 3D embedded in Matrigel, which is the extracellular matrix (ECM) secreted by the Engelbreth-Holm-Swarm tumour cell line (189,204). In this 3D form, the apical side of the organoids is enclosed within the lumen of the organoid. For most studies, the apical side must be exposed to the environment and, consequently, to the microbes. Different approaches can be applied:

a) Microinjections was the first approach used to colonize organoids. This method consists in injecting microbes directly to the lumen of 3D organoids, which allows to detect the early response of the host cells. As it is relatively labour-intensive and requires a high level of precision, an organoid microinjection platform aided by computer vision was developed. However, microinjections exhibit significant variability due to differences in organoid size and cell number (10,157,189,204).

b) Infection of dissociated organoids, which entails disrupting organoids into single-cell suspensions and incubating them with microbes. When infected cells are seeded again in Matrigel, they reform the organoids. This method is easy to perform but the infection efficiency can vary among different microorganisms, and it is not possible to analyse the initial host-microbe interaction. Additionally, as the incubation with the microbes is carried out during the organoid splitting process, it may affect the infection, as if the organoids are infecting specifically differentiated cell types, because when splitting, cells are mainly adult stem cells. Additionally, as the incubation with microbes is carried out during the

organoid splitting process, it may affect the infection. This is because after splitting, cells in newly formed organoids are mainly adult stem cells, which may be refractory to bacterial infection (157,189,204).

c) Apical-out organoids. This approach aims to expose the apical side of the epithelium to the media by reverting the polarity of the 3D organoids using EDTA to disrupt the polymerization of the ECM. Although this technique preserves an intact barrier and the ability of cells to differentiate, it is not clear if this polarity reversion can have any impact on the functionality of the cells (10,157,204).

d) Organoid-derived monolayers involve the dissociation of the 3D organoids and the incubation of 2D apical-out monolayers on ECM-treated (Matrigel or collagen) wells. This method supports the growth of a single layer of apical-up organoids, that can develop tight junctions, ciliated cells and the rest of different cell types. Monolayers are easy to incubate with microbes, as the addition of them directly into the culture media allows the interaction with the host. However, monolayers do not resemble the *in vivo* 3D structure of the tissues. To improve the structure, monolayers can be seeded in transwells or other permeable inserts. Transwells allow barrier polarization and assessment of the integrity, bacterial adhesion and translocation and invasion of pathogens. Transwells can be used to establish ALI cultures, where cells are in contact with the culture medium by the basolateral side, while the apical side is exposed to the air (10,157,189,204).

e) Organoid-on-a-chip (OrgOC) are devices seeded with 2D-organoids in a chamber subjected to a flow that mimics the physiological organ conditions. Generally, these models include multiple chambers separated by a porous membrane, allowing the presence of different cell types on each chamber (10,157).

3.2.3. Animal models

Animal models have a key role in the research of human and animal diseases. Several species have been adapted for elucidating host-microbe interactions. In pig diseases, murine models have been used due to the easy handling and the availability

of genetic tools. Yang et al. (2022) studied the relation between the gut microbiota dysbiosis, and the lung infection produced by *S. suis* in a mouse model, supporting the idea of the gut-lung axis communication (205). However, most of the bacteria in the microbiota are host-specific, and they can only be properly studied when using the actual host (51,64,109,134,145). Although animal models are a very valuable tool, due to ethical concerns, the number of animals used in research need to be clearly justified and, when possible, reduced. In this context, it was developed the principle of 3Rs (reduce, refine and replace), which is illustrated in **Figure 9** (206–208). For replacement, alternative models based on the *in vitro* approaches previously described should be considered, with careful attention to their limitations and avoiding reliance on a single method. An integrative approach combining different tools with complementary strengths should be used to optimize the interpretation of results (208,209).

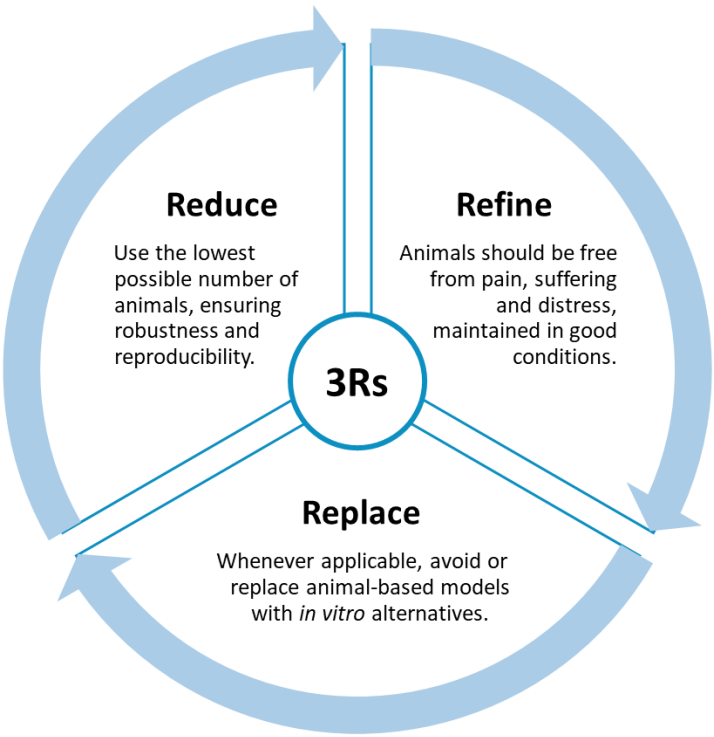

Figure 9. 3Rs principle of animal experimentation: reduce, refine and replace.

Hypothesis and objectives

The importance of a good-balanced nasal microbiota in host health has been demonstrated in previous studies. However, there is a lack of tools for the evaluation of host-microbiota and microbe-microbe interactions in a systematic and rational way, including microbiota functionality studies and the factors that can alter it.

In this thesis, we hypothesized that a model recapitulating the pig nasal complexity could allow the investigation of microbial interactions within the piglet nasal microbiota members and with the host. This approach would also enable the study of the colonization by respiratory pathogens and its modulation by the healthy microbiota. To develop an *in vivo* model, we hypothesize that intensive antibiotic treatments to sows will restrict the microbial transfer to their piglets since we have observed that the sow is the main source of piglet's microbiota. This treatment will eliminate the resident commensals to establish a reliable animal model for microbiota studies.

Objectives

The general objective of this thesis was to develop approaches for studying the interactions within the nasal microbiota of piglets, including pathobionts, with the final goal of elucidating the microbiota functionality and its influence on the host immune response.

With this, the specific objectives were:

1. Assess whether intensive antibiotic treatments can prevent microbiota transfer from sow to piglets.
2. Design an *in vitro* synthetic community that represents the piglet's nasal microbiota.
3. Establish a Porcine Nasal Organoid (PNO) model that recapitulates the pig nasal mucosa.
4. Evaluate interactions between members of the piglet's nasal microbiota as well as with the pathobiont *Glaesserella parasuis.*

Results

Chapter 1

Intensive antibiotic treatment of sows with parenteral crystalline ceftiofur and tulathromycin alters the composition of the nasal microbiota of their offspring

Chapter adapted from the article:

Bonillo-Lopez L*, Obregon-Gutierrez P*, Huerta E, Correa-Fiz F, Sibila M, Aragon V. **Intensive antibiotic treatment of sows with parenteral crystalline ceftiofur and tulathromycin alters the composition of the nasal microbiota of their offspring.** Vet Res. 2023;54(1):112. doi: 10.1186/s13567-023-01237-y.

* Equally contributing first authors.

Abstract

The nasal microbiota plays an important role in animal health and the use of antibiotics is a major factor that influences its composition. Here, we studied the consequences of an intensive antibiotic treatment, applied to sows and/or their offspring, on the piglets' nasal microbiota. Four pregnant sows were treated with crystalline ceftiofur and tulathromycin (CT_{sows}) while two other sows received only crystalline ceftiofur (C_{sows}). Sow treatments were performed at D-4 (four days pre-farrowing), D3, D10 and D17 for ceftiofur and D-3, D4 and D11 for tulathromycin. Half of the piglets born to CT_{sows} were treated at D1 with ceftiofur. Nasal swabs were taken from piglets at 22–24 days of age and bacterial load and nasal microbiota composition were defined by 16 s rRNA gene quantitative polymerase chain reaction (qPCR) and amplicon sequencing. Antibiotic treatment of sows reduced their nasal bacterial load, as well as in their offspring, indicating a reduced bacterial transmission from the dams. In addition, nasal microbiota composition of the piglets exhibited signs of dysbiosis, showing unusual taxa. The addition of tulathromycin to the ceftiofur treatment seemed to enhance the deleterious effect on the microbiota diversity by diminishing some bacteria commonly found in the piglets' nasal cavity, such as *Glaesserella*, *Streptococcus*, *Prevotella*, *Staphylococcus* and several members of the *Ruminococcaceae* and *Lachnospiraceae* families. On the other hand, the additional treatment of piglets with ceftiofur resulted in no further effect beyond the treatment of the sows. Altogether, these results suggest that intensive antibiotic treatments of sows, especially the double antibiotic treatment, disrupt the nasal microbiota of their offspring and highlight the importance of sow-to-piglet microbiota transmission.

Introduction

The animal microbiota is defined as the ecological community of microorganisms found in different body sites, which are considered their niches (3). Several studies have reported positive effects and functions that the microbiota provides to their hosts, including metabolic benefits, immune system maturation, protection against pathogens and other physiological functions (4,55). Due to the importance of the microbiota functions, the stability of the bacterial community is crucial for the health and welfare of their hosts (23,55,127,210). In general, the gut has been the main niche targeted in microbiota studies, but less-studied microbiomes have also proven to be highly important in animal health, as for example, the nasal microbiota (45,47). This microbiota is the first protection against colonization by respiratory pathogens, which need to overcome this barrier to systemically infect the host (211). In fact, it has been demonstrated that the nasal microbiota plays a role in the development of several swine respiratory diseases (31,44,45,212,213).

One of the first sources of microbiota for the piglets are their mothers, firstly through exposure to the vaginal tract during birth and, later, by colostrum and milk intake together with the exposure to their faecal and skin microbiomes (52,214). Hence, the transmission of microorganisms from the dam is determinant for the early microbial acquisition by the piglet and is crucial for the proper development of their microbiome and immune system (52,54,55). Among early colonizers, *Glaesserella parasuis*, *Streptococcus suis* and *Mycoplasma hyorhinis*, are pathobionts found to be transmitted from sows to their offspring (85,96,100).

Weaning, normally done in commercial farms at 3–4 weeks of age (215), is a stressful moment in piglets' lives that has a big impact on their microbiota diversity and composition affecting also their health status (31). Changes caused by the separation from the sows (52), change to solid feed (51), different environmental conditions (52), or vaccination programs (64) have been shown to contribute to increasing the risk of disease development, and to impact the nasal microbiota of

piglets at this stage. Therefore, knowledge on the factors involved in the establishment and those that alter the swine microbiota is key in pig health. Among these factors, the use of antibiotics is one of the most concerning ones, not only for their association with antimicrobial resistances, but also for their deleterious effects on the microbiota (4,31,55). In farms, sows are sometimes treated with antibiotics to control pathogen transmission to their offspring (216); however, these treatments may have an impact on the natural early colonization of their offspring. Indeed, there is a need to reduce the use of these substances in animal production (121).

Ceftiofur and tulathromycin, are two antibiotics used in animal production against respiratory diseases in swine, cattle, and other animals (84,118,128,217–220). Ceftiofur is a broad-spectrum antimicrobial that inactivates penicillin-binding proteins (PBPs) and interferes with the cross-linkage of peptidoglycan chains necessary for building the bacterial cell wall, resulting in the weakening of this structure and the consequent lysis of the bacterial cells (221). Tulathromycin is a macrolide that inhibits bacterial protein synthesis by binding to the ribosomal 50S subunit, which results in a bacteriostatic and bactericidal activity. Due to its positive charge, this drug has a preferential activity against Gram-negative bacteria and *Mycoplasma spp*. (118,119). It has been shown that the administration of crystalline ceftiofur or tulathromycin, among other antibiotics, in 8-week-old piglets has an impact in the nasal microbiota, changing the microbial populations at both phylum and genus level (48). Despite the effect of the use of β-lactams on the nasal microbiota has been assessed in piglets and sows (48,126,222), to our knowledge, the effect of the co-administration of crystalline ceftiofur and tulathromycin on the bacterial transmission from sows to piglets has not been studied.

The goal of this study was to compare the effect of two intensive antibiotic treatments given to sows (crystalline ceftiofur alone or together with tulathromycin) on the nasal microbiota of their piglets. Moreover, we also aimed to assess if the effect of the double antibiotic treatment in sows was enhanced by an additional treatment of crystalline ceftiofur on piglets.

Results

Antibiotic treatment of sows reduces the microbial transfer to their offspring

To investigate whether the antibiotic treatments could reduce the bacterial transmission from sow to piglets, DNA was extracted and quantified from nasal swabs from all sows and piglets of the study. In sows, we found that the total amount of DNA estimated using the absorbance at 260 nm (A260) was numerically lower (mean ± standard deviation, SD) after the first antibiotic treatment in both treated groups (CT_{sows} 202 ± 16.1 ng and C_{sows} 203 ± 6.8 ng) than before this treatment was applied at D-7 (CT_{sows} 500 ± 362.6 ng and C_{sows} 321 ± 132.3 ng). Indeed, the bacterial load (quantity of 16S rRNA gene) was also numerically reduced after the first antibiotic treatment in both CT_{sows} and C_{sows} groups (**Figure 1.1A**). However, these differences were not statistically significant for the CT_{sows} group (Wilcoxon matched-pairs signed rank test, $P = 0.6250$) and not possible to confirm for the C_{sows} group due to the low group size (n = 2). Nevertheless, when considering all treated sows together, the bacterial load after antibiotic treatment was significantly reduced (Wilcoxon matched-pairs signed rank test, $P = 0.0260$).

In piglets, the amount of total DNA extracted from nasal swabs (D22-24) measured at A260 was lower in samples taken from $CT_{sow}N_{piglet}$ (433.8 ± 221.4 ng), $CT_{sow}C_{piglet}$, (432 ± 229 ng) and $C_{sow}N_{piglet}$ (1155 ± 802 ng) than from six age-matched healthy farm animals used as a reference control (1443.4 ± 1250.8 ng). Again, this result is in agreement with the total bacterial load (16S rRNA gene quantification) that also showed a reduction due to the antibiotic treatment (**Figure 1.1B**). All the piglets born to treated sows showed a reduced bacterial load compared with a group of the six age-matched healthy farm animals. The treatment of the sows with the combination of ceftiofur and tulathromycin caused a more pronounced reduction in bacterial load in their offspring than the treatment with only ceftiofur (Kruskal–Wallis test Multiple comparisons adjusting *P* values with a Benjamini, Krieger and Yekutieli correction method). On the other hand, the extra treatment performed to the piglets

with ceftiofur did not result in higher decrease in bacterial load in their nasal cavities (P = 0.9414, $CT_{sow}N_{piglet}$ vs $CT_{sow}C_{piglet}$; **Figure 1.1B**).

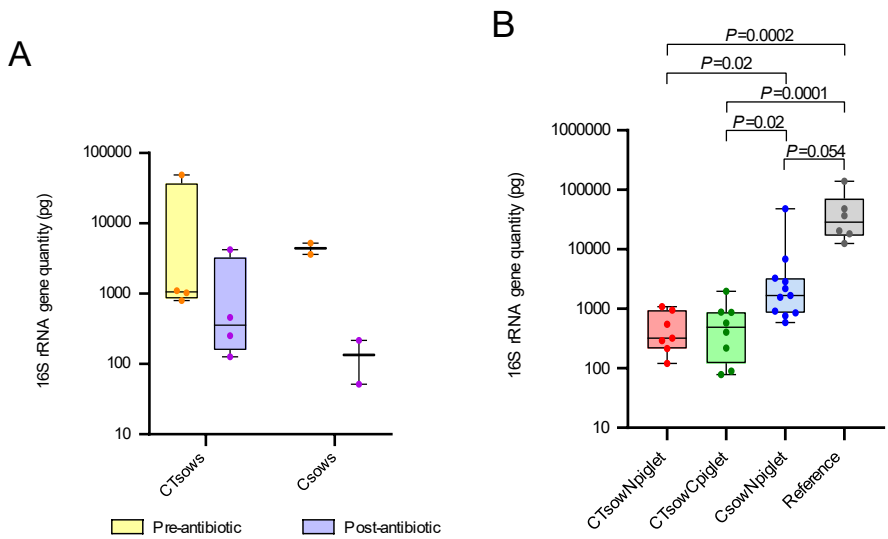

Figure 1.1: Quantitative PCR of 16S rRNA gene in nasal swabs. **A)** 16S rRNA gene quantity (pg) detected by qPCR in nasal swabs taken from sows before (Pre-antibiotic, in yellow) and after (Post-antibiotic, in purple) first administration of their respective antibiotic treatments: crystalline ceftiofur + tulathromycin sows (CT_{sows}) and crystalline ceftiofur sows (C_{sows}). Each dot corresponds to one animal. **B)** 16S rRNA gene quantity (pg) detected by qPCR in nasal swabs from piglets of the groups under study: non-treated piglets born to ceftiofur + tulathromycin treated sows ($CT_{sow}N_{piglet}$, red); ceftiofur treated piglets born to ceftiofur + tulathromycin treated sows ($CT_{sow}C_{piglet}$, green); non-treated piglets born to ceftiofur treated sows ($C_{sow}N_{piglet}$, blue); and the reference group of age-matched farm piglets (grey). Each dot corresponds to one animal. Significant *P* values are shown in upper bars.

The presence of typical pathobionts from the swine nasal microbiota was analysed to evaluate the effect of the antibiotic treatment on the transfer dynamics from sows to piglets. All nasal swabs from sows taken before and after the antibiotic treatment were negative to *S. suis* and *G. parasuis* PCRs, as well as *M. hyorhinis* qPCR. Similarly, all nasal swabs from piglets were negative for *S. suis* and for *M. hyorhinis* by PCR/qPCR. On the other hand, $CT_{sow}N_{piglet}$ piglets were negative for *G. parasuis*, but 4 out of 11 (36%) piglets of $C_{sow}N_{piglet}$ were positive for non-virulent *G. parasuis* strains and 1 out of 8 (12.5%) piglets of $CT_{sow}C_{piglet}$ was positive for virulent *G. parasuis* strains.

The antibiotic treatment on sows altered the nasal microbiota composition of the piglets

In order to assess how the antibiotic treatment impacted the composition of the nasal microbiota of the piglets, we performed 16S rRNA gene sequencing analysis. After raw read pre-processing, a final number of 6666 different amplicon sequence variants (ASVs) were obtained (total frequency of 1374806), with a mean frequency per sample of 52877.15. All ASVs were classified at different taxonomic levels to characterize the nasal microbiota composition of the piglets. Surprisingly, a large percentage of the microbial community was represented by the orders *Burkholderiales* and *Rhizobiales*, with a mean abundance ± SD across all groups of 33.7% ± 17.4 and 11.4% ± 9.3, respectively. The most relatively abundant genera within these orders were *Ralstonia*, *Afipia* and *Hyphomicrobium*, indicating an overabundance of environment-associated taxa. Other relatively abundant taxa belonged mainly to the orders *Clostridiales*, *Pseudomonadales*, *Bacteroidales*, *Lactobacillales* and *Pasteurellales*, including typical nasal associated genera such as *Prevotella*, *Streptococcus*, *Acinetobacter*, *Ruminococcaceae* (uncl.), *Lachnospiraceae* (uncl.) and *Glaesserella* (**Annex 1.1** for the whole composition at genus level and **Figure 1.2** for the most relatively abundant taxa at order level).

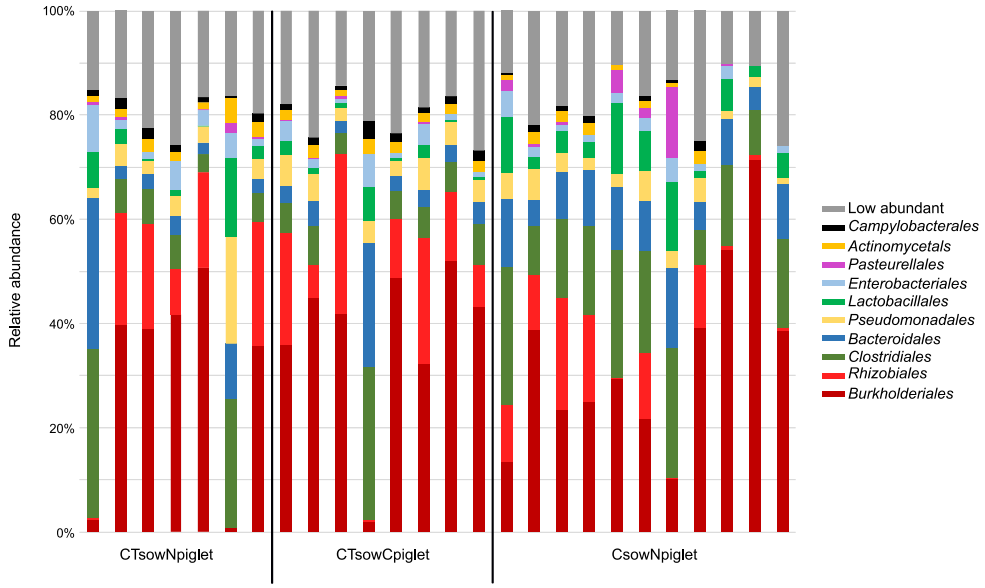

Figure 1.2. Relative abundance (%) of the top 10 most abundant orders in the piglet's nasal microbiota. Microbiota composition is shown for each group included in the present study at order level. $CT_{sow}N_{piglet}$, non-treated piglets born to ceftiofur+tulathromycin treated sows; $CT_{sow}C_{piglet}$, ceftiofur treated piglets born to ceftiofur+tulathromycin treated sows; $C_{sow}N_{piglet}$, non-treated piglets born to ceftiofur treated sows. Each bar represents the microbiota composition in each animal grouped by the study group they belong, where each colour represents one order. Orders under 1% mean relative abundance are summed and represented as "low abundant". Red color scheme was used for the orders *Burkholderiales* and *Rhizobiales*.

Since taxa not commonly found in the nasal microbiota were detected in relatively high abundance (probably due to the low bacterial load in the nasal cavity of these animals caused by the antibiotic treatments), we filtered out the ASVs classified as these uncommon taxa and continued the analyses with only those ASVs belonging to the core-microbiota of healthy farm piglets (see methods). The nasal core-microbiota from farm piglets represented a mean of 30.57% (± 30.46%), 21.89% (± 20.26%), and 39.21% (± 17.13%) of the total abundance for $CT_{sow}N_{piglet}$, $CT_{sow}C_{piglet}$ and $C_{sow}N_{piglet}$ groups, respectively. The final filtered data consisted of 2319 ASVs (total frequency of 385391), with a mean frequency per sample of 14822.7. After filtering, the nasal microbiota was dominated by genera within the orders *Clostridiales* (general abundance of 35.2 ± 5.8%), mainly composed by the families *Lachnospiraceae* and *Ruminococcaceae*; *Bacteroidales* (22.2 ± 6%), with *Prevotella*

and *Bacteroides* as the most prevalent genus; *Pseudomonadales* (16 ± 9.6%) with genera such as *Acinetobacter* and an unclassified member from the *Moraxellaceae* family; *Lactobacillales* (8.65 ± 5%), with *Streptococcus* and *Lactobacillus* within the most relatively abundant genera; *Enterobacteriales* (4.45 ± 4.5%), with *Escherichia* as the most abundant genus; and *Pasteurellales* (3 ± 7%), mainly represented by *Glaesserella*. The abundances of the families and genera after filtering are detailed in **Figure 1.3** and **Annex 1.2**.

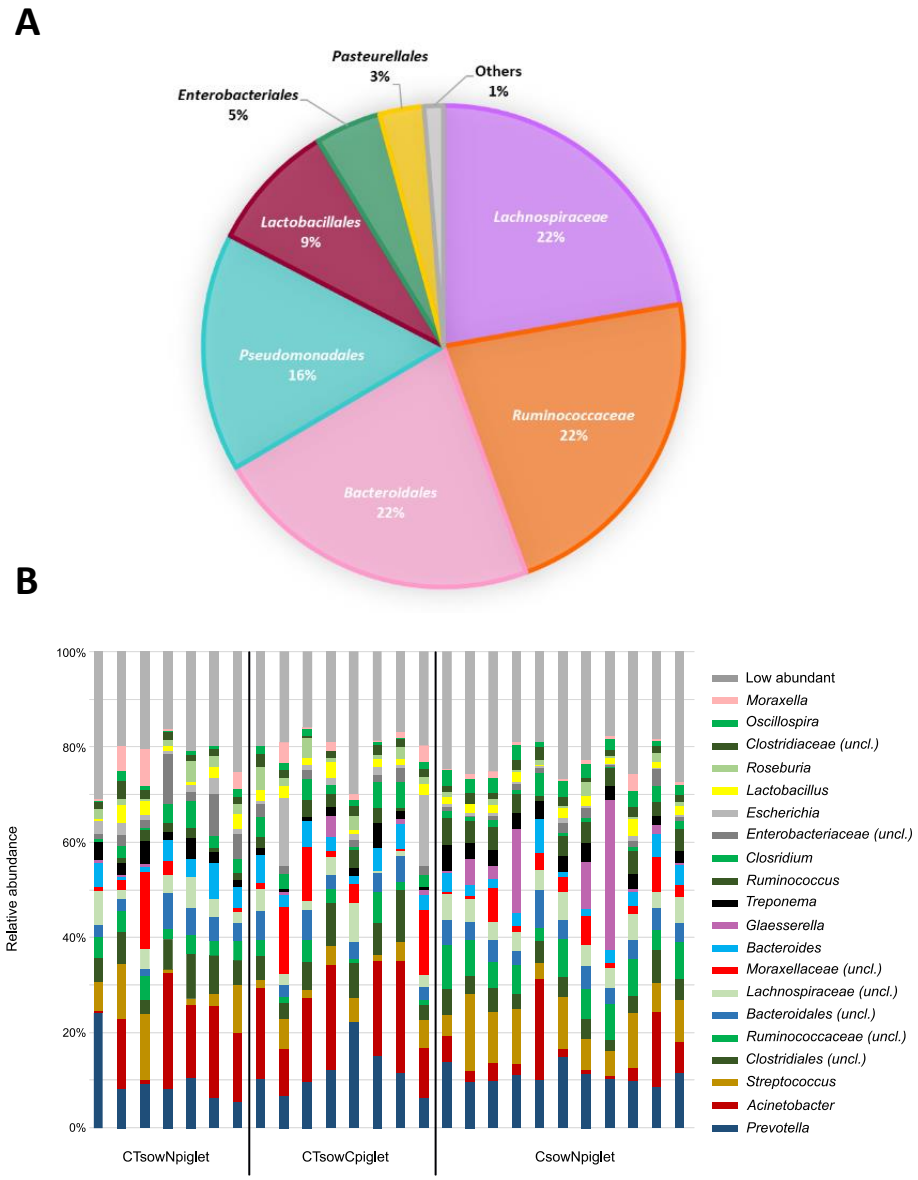

Figure 1.3. **Relative abundance (%) of genera from the piglet's nasal microbiota that are present in the farm core-microbiota. A)** Relative abundance (%) of the dominant families after farm core-microbiota filtering in all the study groups. Each colour of the legend represents the family members found (see **Annex 1.1**). **B)** Relative abundance of the dominant genera (>1% global mean) after farm core-microbiota filtering, shown per sample in the three study groups. $CT_{sow}N_{piglet}$, non-treated piglets born to ceftiofur+tulathromycin treated sows; $CT_{sow}C_{piglet}$, ceftiofur treated piglets born to ceftiofur+tulathromycin treated sows; $C_{sow}N_{piglet}$, non-treated piglets born to ceftiofur treated sows. Each bar represents the microbiota composition in each animal grouped by the study group they belong, where each colour represents one genus. Genera under 1% mean relative abundance are summed as low abundant.

With the aim of quantitatively compare the microbiota composition of animals in this study with that of animals from farms used as reference core-microbiota, we focused on the most abundant taxa in each type of samples (**Figure 1.4**). Eight of the most abundant genera were shared between farms and the groups under study. On the contrary, some typical swine nasal colonizers detected among the most abundant genera in farm samples, such as *Moraxella*, *Bergeyella* or *Lactobacillus*, were not found among the most abundant taxa in this study. At last, we detected some genera that were highly represented in the samples of this study while found in low abundance in farms, including *Acinetobacter*, *Clostridium* or *Treponema*.

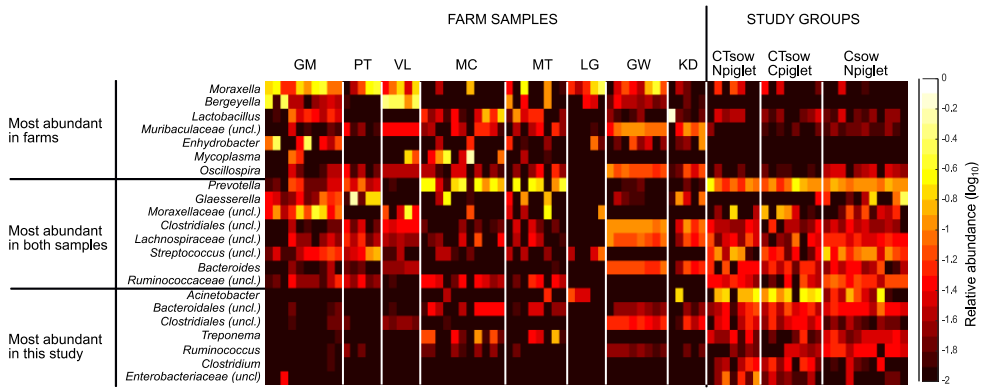

Figure 1.4. Comparison of the most abundant taxa in the study groups and healthy farms. Relative abundances (log scaled) of the top 15 most prevalent genera found in nasal cavities of piglets from the different groups of this study and in age-matched animals from farms from the studies of Correa-Fiz et al., 2019 and Correa-Fiz et al., 2016. Genera have been labelled as found between the most abundant in farms, this study groups, or both. Farms are labelled withs their original ID from their respective studies. Abundances in samples from this study are shown per group: non-treated piglets born to ceftiofur + tulathromycin treated sows ($CT_{sow}N_{piglet}$); ceftiofur treated piglets born to ceftiofur + tulathromycin treated sows ($CT_{sow}C_{piglet}$); non-treated piglets born to ceftiofur treated sows ($C_{sow}N_{piglet}$).

The sow antibiotic treatments differentially altered the nasal microbiota diversity of the piglets

A diversity analysis was performed to understand whether the antibiotic treatments had a different impact on the nasal microbiota of piglets. Higher richness and evenness (Chao1 and Shannon) were found in the $C_{sow}N_{piglet}$ group compared to the groups of piglets born to sows treated with the two antibiotics ($P < 0.05$, **Figure**

1.5A). In the beta diversity analysis, the $C_{sow}N_{piglet}$ group clustered as a different community when it was compared to the two CT_{sow} groups (Jaccard and Bray–Curtis, **Figure 1.5B**, PERMANOVA *P* = 0.001). On the contrary, differences between $CT_{sow}N_{piglet}$ and $CT_{sow}C_{piglet}$ groups were not significative in both qualitative and quantitative analyses.

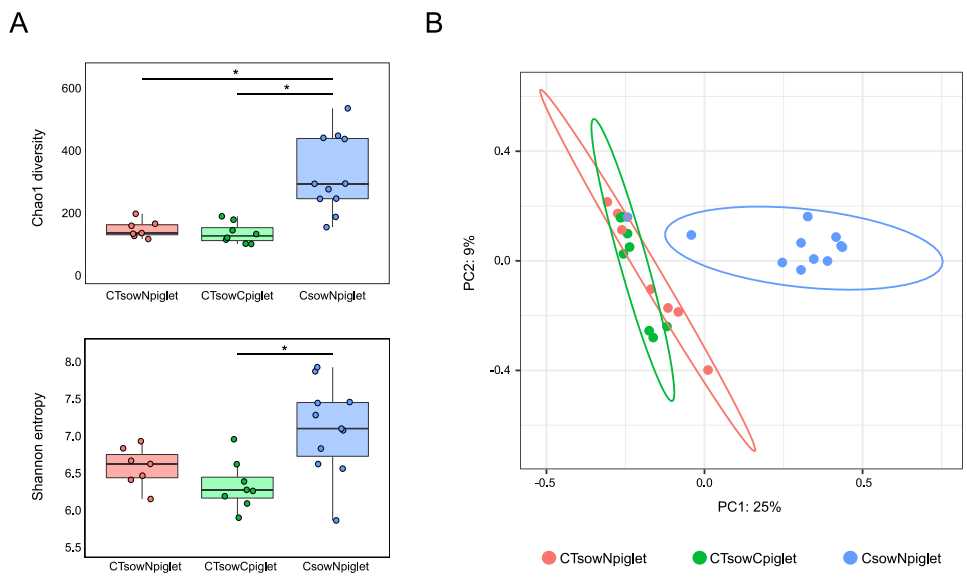

Figure 1.5. Alpha and beta diversity analysis of the groups under study. Non-treated piglets born to ceftiofur+tulathromycin treated sows ($CT_{sow}N_{piglet}$, red); ceftiofur treated piglets born to ceftiofur+tulathromycin treated sows ($CT_{sow}C_{piglet}$, green); non-treated piglets born to ceftiofur treated sows ($C_{sow}N_{piglet}$, blue). **A)** Alpha diversity boxplots estimated with Chao1 and Shannon indexes. Each dot represents a sample. Dots corresponding to outlier simples are coloured in black. **B)** Beta diversity PCoA analysis computed with Bray–Curtis dissimilarity index, of the groups under study. Each dot represents a sample. Ellipses of confidence are calculated using Euclidean distances within the samples of each group

To study the effect of the antibiotic treatments when applied only to sows, $CT_{sow}N_{piglet}$ and $C_{sow}N_{piglet}$ groups were compared, eliminating the treatment of piglets as a potential confounding factor. The beta diversity was significantly different between these groups, where the effect size was estimated to be 13.7% and 20.8% for qualitative and quantitative analyses, respectively (Adonis R2 value, *P* = 0.001,

Figure 1.6). Accordingly, several differently abundant ASVs were found between these two groups (ANCOM-BC and dsf-dr, **Figure 1.6** and **Annex 1.3**).

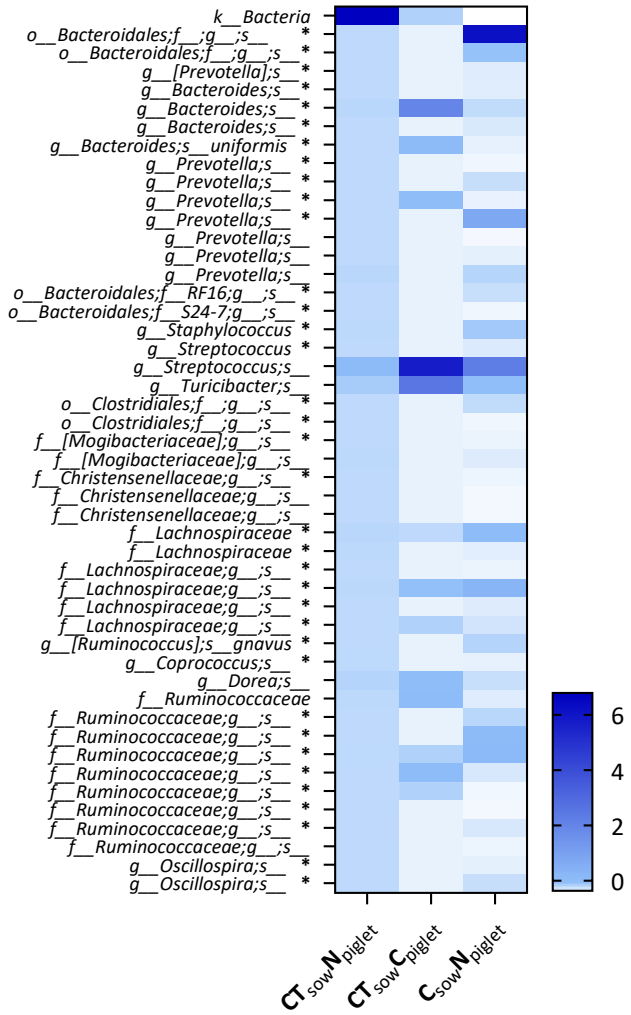

Figure 1.6. Top 50 differentially abundant ASVs between $CT_{sow}N_{piglet}$ and $C_{sow}N_{piglet}$. ASV taxonomical classification is detailed to the lowest known taxonomical level. Z-score was applied to normalize the data. ANCOM-BC and dsf-dr approaches to assess the significance were applied, and an asterisk (*) was added to the taxa that were significant for both tests. All data is shown in **Annex 1.3**.

$C_{sow}N_{piglet}$ group showed increased abundances of different ASVs belonging to Bacteroides and *Prevotella* (*Bacteroidales*); *Staphylococcus* (*Bacillales*); *Streptococcus* (*Lactobacillales*); *Lachnospiraceae* and *Ruminococcaceae* (*Clostridiales*); *Glaesserella* (*Pasteurellales*); *Acinetobacter* (*Pseudomonadales*); and *Succinivibrio* (*Aeromonadales*), among others. The top five most relatively abundant differential ASVs are shown in **Figure 1.7**. Despite this finding at ASV level, similar differences were not reflected at higher taxonomic levels, as very few differences between families, genera were found (**Table 1.1**).

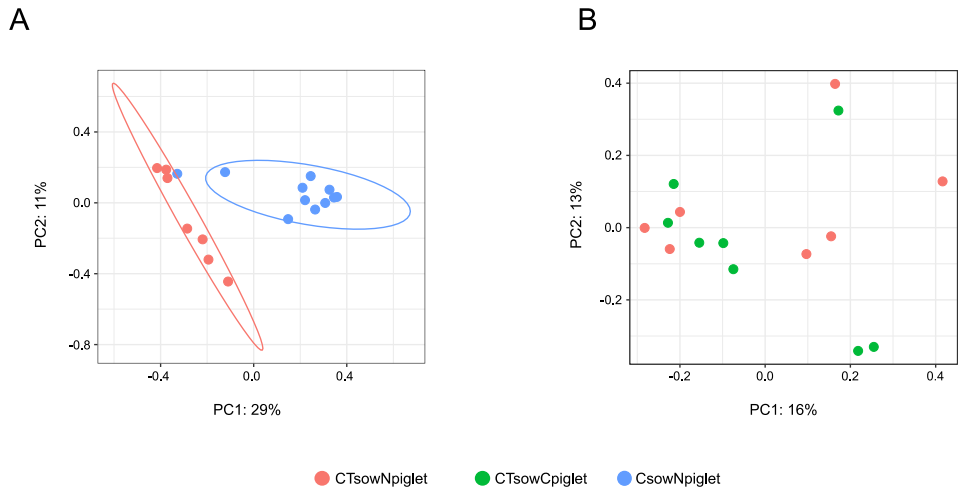

Figure 1.7. Beta diversity on Bray–Curtis dissimilarity index for the groups under study. PCoA was done between $CT_{sow}N_{piglet}$ (in red) and $C_{sow}N_{piglet}$ (in blue) groups in **A)** and between $CT_{sow}N_{piglet}$ (in red) and $CT_{sow}C_{piglet}$ (in green) groups in **B)** $CT_{sow}N_{piglet}$, non-treated piglets born to ceftiofur+tulathromycin treated sows; $CT_{sow}C_{piglet}$, ceftiofur treated piglets born to ceftiofur+tulathromycin treated sows; $C_{sow}N_{piglet}$, non-treated piglets born to ceftiofur treated sows. Each dot represents a sample from a piglet. Ellipses of confidence are not shown because of group convergence.

Table 1.1. Differentially abundant taxa between $CT_{sow}N_{piglet}$ and $C_{sow}N_{piglet}$ groups computed two different approaches. The relative abundance in all study groups and the significance in each test is shown per ASV (NF=not found).

Taxa	Mean relative abundance (%)			ANCOM-BC statistics q-value	Ds-FDR statistics *P*-value
	$CT_{sow}N_{piglet}$	$CT_{sow}C_{piglet}$	$C_{sow}N_{piglet}$		
Order					
Enterobacteriales	0.0631	0.0636	0.0189	0.0002	NF
Flavobacteriales	0.0037	0.0012	0.0003	0.0224	NF
Family					
Aerococcaceae	0.0007	0.0015	0.0029	NF	0.0140
Bacteroidales (uncl.)	0.0405	0.0424	0.0452	NF	0.0160
Campylobacteraceae	0.0018	0.0048	0.0038	NF	0.0080
Christensenellaceae	0.0053	0.0114	0.0101	NF	0.0020
Clostridiaceae	0.0584	0.0631	0.0444	0	NF
Clostridiales (uncl.)	0.0311	0.0381	0.0177	0.0017	NF
Enterobacteriaceae	0.0631	0.0636	0.0189	0	NF
Erysipelotrichaceae	0.0075	0.0044	0.0154	NF	0.0130
[Mogibacteriaceae]	0.0039	0.0035	0.0086	NF	0.0070
Muribaculaceae	0.0054	0.0103	0.0167	NF	0.0070
Pasteurellaceae	0.0025	0.0089	0.0647	NF	0.0170
RF16 (Bacteroidales)	0.0003	0.0006	0.0064	0	0.0020
Ruminococcaceae	0.0843	0.0742	0.1532	NF	0.0080
Succinivibrionaceae	0.0034	0.0082	0.0143	NF	0.0040
Veillonellaceae	0.0158	0.0206	0.0278	NF	0.0070
Verrucomicrobiaceae	0.0012	0.0021	0.0015	NF	0.0030
[Weeksellaceae]	0.0037	0.0012	0.0003	0.0106	NF
Genus					
Akkermansia	0.0012	0.0021	0.0015	NF	0.0050
Christensenellaceae (uncl.)	0.0053	0.0114	0.0101	NF	0.0010
[Eubacterium]	0.0031	0.0011	0.0121	0.0166	0.0010
[Mogibacteriaceae] (uncl.)	0.0039	0.0035	0.0086	NF	0.0030
Oscillospira	0.0097	0.0103	0.0264	0.0000	0.0050
[Paraprevotellaceae] (uncl.)	0.0000	0.0000	0.0007	0.0021	NF
RF16 (uncl.)	0.0003	0.0006	0.0064	0.0000	0.0010
Ruminococcus	0.0140	0.0199	0.0411	NF	0.0040
Succinivibrio	0.0034	0.0082	0.0143	NF	0.0040

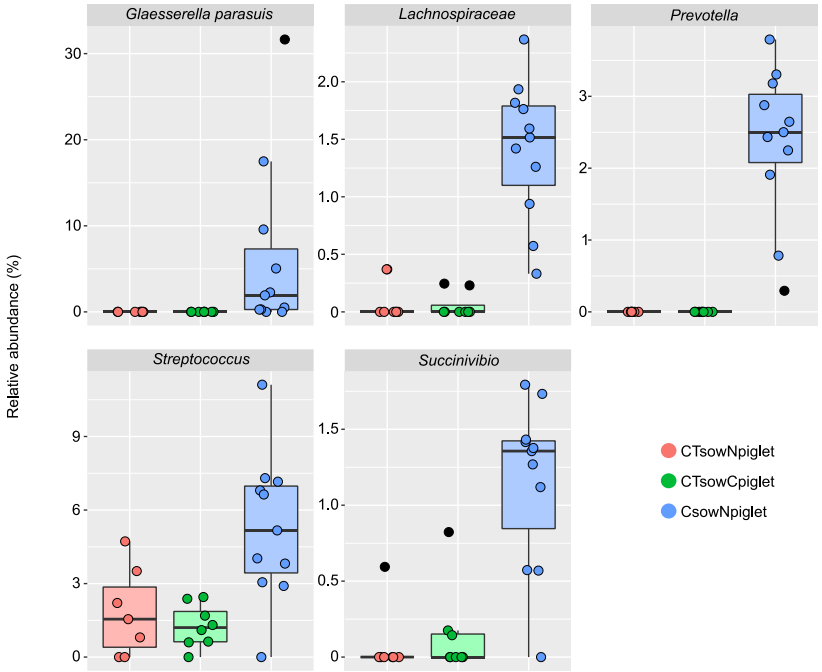

Figure 1.8. Differently abundant ASVs between CT_{sow} and C_{sow} piglets. Top 5 most relatively abundant ASVs within all the differentials found with ANCOM-BC and DSFDR when comparing non-treated piglets born to ceftiofur+tulathromycin treated sows ($CT_{sow}N_{piglet}$, red) and non-treat piglets born to ceftiofur treated sows ($C_{sow}N_{piglet}$, blue). The abundances of these ASVs in ceftiofur treated piglets born to ceftiofur+tulathromycin treated sows ($CT_{sow}C_{piglet}$) are shown too (green). Dots corresponding to outlier samples are coloured in black. All the differently abundant ASVs are listed in **Figure 1.6** and **Annex 1.3**.

The effect of the additional treatment with ceftiofur of the piglets born to sows treated with the two antibiotics was evaluated by comparing the microbiota composition of piglets born to CT_{sows} ($CT_{sow}N_{piglet}$ and $CT_{sow}C_{piglet}$). The clustering of the samples according to the treatment of piglets was not significant in either the qualitative or quantitative beta diversity analysis (PERMANOVA $P > 0.05$, **Figure 1.7B**), confirming that the treatment of the sows was the major driver of the changes observed in the piglets (**Figure 1.5**). Accordingly, no differentially abundant taxa were found between the two groups at any taxonomic level, except for one single low abundant ASV classified as Streptococcus (0.8% in $CT_{sow}N_{piglet}$ and 0.01% in $CT_{sow}C_{piglet}$ groups).

Discussion

Our study shows that intensive antibiotic treatment in sows severely affected the microbial communities in the piglets' nasal cavities. This effect was more pronounced when using a combination of crystalline ceftiofur and tulathromycin than only using crystalline ceftiofur. Sow treatments affected the bacterial transfer from sows to piglets, which showed a nasal microbiota with reduced alpha diversity and decreased populations of commonly found swine nasal colonizers, although were not completely eliminated. The addition of an extra administration of ceftiofur to newborn piglets had no further effect.

The low transfer of microbiota from the sows seemed to increase the detection in the piglets' nasal cavities of uncommon bacteria for this niche, with taxa from the orders *Burkholderiales* and *Rhizobiales* (*Ralstonia*, *Afipia* and *Hyphomicrobium*) among the most abundant ones. These microorganisms are not found in the nasal microbiota of pigs under standard farm conditions and are unlikely to be part of the swine nasal microbiota. These taxa are often associated with plants, as symbionts or pathogens (223,224) and they probably came from the food or the extraction kit in the case of *Ralstonia*, as it has been shown in other studies (225). The detection of environmental microbes in high relative abundance could be caused by the reduced presence of professional colonizers, creating a low-biomass environment prone to be colonized by transit microorganisms, as it has been previously observed (226). In agreement, during the preprocessing of raw reads, we found chloroplast and mitochondrial 16S sequences in unusual high abundances (9.5% and 4.3%, respectively) in comparison with the farm animals evaluated in this study, as well as in previous studies (0.07% and 0.03%, respectively) (45,127).

Besides the unusual microbes described above, the rest of the microbiota was constituted of taxa previously found in the swine respiratory microbiota (45,47,127,128,227–229), which includes aerobic taxa as well as gut-associated anaerobic taxa that are commonly found and have been shown to be active in the pig's nose (50). All of them were initially detected in a very low abundance

(considering also the 16S rRNA gene qPCR) and were represented by an unusual low quantity of ASVs but were not entirely eliminated. Altogether, these results suggest that the antibiotic treatment had a drastic effect on the usual nasal colonizers. This is in agreement with several studies assessing the effect of antibiotic treatments on the microbiota (48,126–128,230). As Mou et al. (2019) have reported, pig nasal microbiota shifted in response to the broad-spectrum antibiotic oxytetracycline treatment, normally used to treat respiratory bacterial diseases in swine (including *Mycoplasma*, *Pasteurella* and *Glaesserella*). They determined that oxytetracycline administered orally had a major impact in the diversity and disturbance of the microbiota than the intramuscular route (128). In the present study, we only assessed the intramuscular administration and observed that ceftiofur and tulathromycin administered by this route was enough to severely disturb the nasal microbiota and avoid the bacterial transfer from sow to piglet. In particular, sow antibiotic treatment reduced drastically the bacterial transfer of natural nasal microbiota members, including the three pathobionts *G. parasuis*, *M. hyorhinis* and *S. suis*. Although *G. parasuis* was not found in any of the sows, it is known that the level of this bacterium in nasal swabs from sows is sometimes too low to be detectable (85). The results obtained by PCR in piglets could be explained if the animals carried *G. parasuis* strains sensitive to tulathromycin but resistant to ceftiofur. This could be attributed to the presence of plasmids that bear resistances to β-lactams, as the ROB-1 β-lactamase reported in the pB1000 and the pJMA-1 plasmids. These plasmids were found in strains recovered from the nasal cavities from healthy animals and considered non-virulent strains (231). In the case of *S. suis*, the transmission of this pathogen from sow to piglet seems to be prevented. However, we cannot discard the presence of *S. suis* in tonsils, since we have not analysed this niche, which is preferentially colonized by this bacterium (229). Similarly, *M. hyorhinis* colonization in piglets seems to have been prevented, but it is also possible that this colonization could occur later in life (100). It is possible that eliminating the transfer of pathobionts and microbiota from sows to piglets may require combining antibiotic treatments with early separation from the sows, as soon as possible after colostrum uptake, to improve piglet survival.

In relation to this, we assessed this gnotobiotic-like model by inoculating a combination of three members of the piglet's nasal microbiota (*Streptococcus pluranimalium*, *Moraxella pluranimalium* and *Rothia nasimurium*) could colonize the piglet's nose after the intensive antibiotic treatment conducted in this study. However, they were not able to settle in the piglet's nose, as we did not detect the specific ASVs of the inoculated strains after the 16s rRNA gene sequence (unpublished results). These findings suggest that the combination of these three commensals was not enough to establish a stable microbial community in this model, which suggest that interactions within more microbiota members seem to be crucial for the early piglet nasal colonization.

If we consider the implications of antibiotic treatments for farms, our results indicate that these interventions can also have negative consequences, since the dysbiosis produced by these drugs could facilitate pathogen colonization, with the consequent higher risk of infection. In fact, we detected in piglets from treated sows some potentials pathogens such as *Acinetobacter* (232,233), *Clostridium* (234) or *Treponema* (235) that were not found in the farm samples. In good health status farms, the colonization of these pathogens is probably controlled by the exclusion provided by the normal nasal microbiota. Other explanation could be the selection of resistant strains from these potential pathogens. In agreement, *Acinetobacter* was detected together with eighteen different antibiotics in the groundwater of areas affected by swine farming (232). Moreover, the poorly establishment of the microbiota in the early ages of the animal live could determine the proper maturation of their immune system (236).

Several studies have demonstrated that the use of antimicrobial drugs in sows have an important impact on the establishment of the microbiota in the first weeks of life of their offspring (47), and that this effect lasted longer when administered to the sows than directly to their piglets (126). In the present study, the long-term effect was not evaluated, as we only had piglet nasal swabs from one timepoint (D22-24).

It would have been very interesting to elucidate the impact of the transitory effect of these antimicrobials in an extended period of time.

In conclusion, our results evidence the importance of the maternal microbiota in the establishment of the respiratory microbiota of piglets, which can have a subsequent impact in the control of potential pathogens. This should be taken into consideration when setting treatment plans and routines in swine industry. In addition, further attempts to obtain gnotobiotic piglets need to consider other interventions besides the antibiotic treatments described here.

Materials and methods

Experimental design and sampling

Animal experimentation was performed following proper veterinary practices, in accordance with European (Directive 2010/63/EU) and Spanish (Real Decreto 53/2013) regulation and with the approval of the Ethics Commission in Animal Experimentation of the Generalitat de Catalunya (Protocol Number 11150). Six pregnant sows were moved to IRTA-CReSA facilities 2 weeks pre-farrowing. Two sows were treated with 15 mL of 5 mg/kg crystalline ceftiofur (C_{sow}) four days before farrowing (D-4), and at D3, D10 and D17 and four sows received the same treatment in addition to 6 mL of 2.5 mg/kg tulathromycin (CT_{sows}) at D-3, D4 and D11 (**Table 1.2**).

Table 1.2. Study design: groups, number of animals and treatments administrated to sows and piglets. (Crystalline ceftiofur + tulathromycin treated sows, non-treated piglets, $CT_{sow}N_{piglet}$; crystalline ceftiofur + tulathromycin treated sows, crystalline ceftiofur treated piglets, $CT_{sow}C_{piglet}$; crystalline ceftiofur treated sows, non-treated piglets, $C_{sow}N_{piglet}$).

Group	Number of sows	Sow treatment day		Number of piglets	Piglet treatment day
		Crystalline ceftiofur	Tulathromycin		Crystalline ceftiofur
$CT_{sow}N_{piglet}$	n=2	D-4, D3, D10 and D17	D-3, D4 and D11	n=7	-
$CT_{sow}C_{piglet}$	n=2	D-4, D3, D10 and D17	D-3, D4 and D11	n=8	D1
$C_{sow}N_{piglet}$	n=2	D-4, D3, D10 and D17	-	n=11	-

Farrowing was induced by injecting 1 mL of 0.075 mg/mL Veteglan to the sows. At birth (D0), piglets took colostrum from their biological mothers for at least 2 h and were cross-fostered to avoid the bias from the sow to their litter. Afterwards, piglets born to sows from CT_{sows} were randomly distributed in two groups: group $CT_{sow}C_{piglet}$ (*n* = 8), where animals were treated at D1 with a dose of 0.1 mL 5 mg/kg of crystalline ceftiofur, and group $CT_{sow}N_{piglet}$ (n = 7), in which piglets remained untreated (**Table 1.2**). Piglets born to sows from C_{sow} did not receive any antibiotic treatment ($C_{sow}N_{piglet}$, n = 11). Piglets from all groups were observed until weaning for clinical signs.

Nasal sampling was performed with thin aluminium cotton swabs on both nostrils before (D-7) and after (D0) the first antibiotic administration on sows and on piglets at weaning (D22-D24). Moreover, nasal swabs from six age-matched animals (21 days of age) from healthy farms were sampled as a control for reference value of the total bacterial load. All nasal swab samples from piglets and sows were resuspended in 500 µL of PBS and stored at −80 °C until processed.

DNA extraction and PCR/qPCR testing

DNA extraction from all nasal swabs taken from sows and piglets was performed using the NucleoSpin Blood kit (Machinery Nagel, GmbH & Co, Duren; Germany) following the manufacturer's protocol instructions. DNA concentration was measured using absorbance at 260 nm (A260) with BioDrop DUO (BioDrop Ltdre). Moreover, to assess the total bacterial load present in the samples, a real-time (RT) qPCR targeting the 16S rRNA gene was performed. This reaction was prepared in a volume of 20 µL consisting in 2 µL of the template DNA and 18 µL of Femto Bacterial qPCR Premix (Femto Bacterial DNA Quantification Kit, Zymo Research) and run following the manufacturer's protocol. Samples were quantified using different dilutions of DNA from *Escherichia coli* strain JM109 provided as a standard in the kit. Following manufacturer's recommendations, samples were considered negative with a cycle threshold (Ct) > 33. Graphpad 8.3 (538) Prism software (Dotmatics, San Diego, CA, USA) was used for statistical analysis. Wilcoxon matched-pairs signed rank test

(237) was used to compare the bacterial quantity in sow samples before and after the antibiotic treatment. Kruskal–Wallis multiple comparison (238) with Benjamini, Krieger and Yekutieli post-hoc test (239) was used to compare the bacterial quantity among the three different groups of piglets. $P < 0.05$ were considered statistically significant.

The presence of early colonizers (*G. parasuis, S. suis* and *M. hyorhinis*) in the piglet's nasal cavities was tested by specific PCR/qPCR to confirm the possible reduction in bacterial transfer. The PCR used for the detection of *G. parasuis* allows the discrimination between virulent and non-virulent strains (240). For *S. suis*, a conventional PCR was performed following a previously described protocol (Ishida et al., 2014) modifying the annealing temperature (from 55 °C to 60 °C) and using 1 U GoTaq polymerase (Promega). Amplicons from both conventional PCRs were analysed by electrophoresis on 2% agarose gels. *M. hyorhinis* qPCR was performed using a previously described protocol (241) modifying the number of cycles (from 35 to 40). Samples were considered negative when the Ct > 39 cycles.

16S rRNA gene sequencing and microbiota analysis

From the total extracted DNA from piglets' nasal swabs at D22-D24, the 16S rRNA gene libraries were prepared and sequenced in two runs with Illumina MiSeq pairended (2X300 bp, MS-102–2003 MiSeq Re-agent Kit v2, 500 cycle) at the Servei de Genòmica, Universitat Autònoma de Barcelona (Spain). The amplicon sequences corresponding to V3-V4 hypervariable regions of the 16S rRNA gene were demultiplexed and used as input for downstream bioinformatics analyses.

The analyses of the nasal microbiota of piglets were performed using quantitative insights into microbial ecology (QIIME) 2 software version 2022.2 (242). First, raw reads were imported in QIIME2 and quality assessed using q2 demux plugin. Primers were trimmed out from forward and reverse reads using Illumina V3V4 adapter sequences with q2 cutadapt plugin. DADA2 (243) was used to denoise the reads, i.e. quality-filtering, read-merging and chimera removal, and sort them into Amplicon Sequence Variants (ASVs) for each run. Additionally, low-quality 3' end

positions were truncated from the reads. After, ASVs not matching the 88% preclustered Greengenes database Vs. 13.8. (244,245) at 65% identity and 50% query coverage were filtered out using VSEARCH (246) within *q2 quality control* plugin (247), to eliminate spurious nonprokaryotic features (unspecific contaminants). Furthermore, non-bacterial sequences classified as *Archaea*, *Chloroplast* or *Mitochondria* were also removed from the data set. Since the reads included in this analysis were obtained in two different runs, after all these denoising and filtering steps, all data was merged for the downstream analysis. Curated merged sequences were aligned with MAFFT (248) and hypervariable positions were masked (249) with *q2 alignment* plugin. Finally, the phylogenetic tree was built using Fastree (250). For the first diversity analysis, the depth used was 17,348, corresponding to the lowest sample depth evaluated through rarefaction curves (251).

The farm core-microbiota was calculated at genus level considering nasal samples of same-aged healthy animals from Spanish (n = 39) and British (n = 18) farms from previous studies (45,127). All genera present in at least 80% of all farm samples were considered as farm core microbiota and hence, common members of the swine nasal microbiota. In this study, we excluded all ASVs whose classification did not match the defined genera using the QIIME2 software options to filter the data. As the core-microbiota also contained taxa with unresolved classification to genus level (i. e. *Bacteroidales* or *Moraxellaceae*), we also kept those ASVs with such unresolved classifications. After eliminating the ASVs absent from the farm core-microbiota, the lowest sample depth to be used in the diversity analyses was 3,629.

Alpha diversity (diversity found within each sample) was estimated with Chao (Chao, 1984) and Shannon (Weaver, 1949) indexes, and the significance between groups was computed by pairwise non-parametric t-tests (999 random permutations) with *q2 diversity alpha-group-significance* plugin (238). The distance matrices to estimate beta diversity (diversity between samples) were computed using *q2 core-metrics plugin* and used to perform principal coordinate (PCoA) analysis (252,253). Jaccard (254) and Bray Curtis (255) dissimilarity measures were

used to estimate beta diversity qualitatively and quantitatively respectively and visualized using Emperor (256). To quantify the group variation of the variables under study (R2), we used Adonis function from Vegan package in R software (257), where the significance was calculated by PERMANOVA pairwise test (999 random permutations) using *q2 diversity beta-group-significance* plugin (258). PERMANOVA test was also performed to estimate the significance of the clustering on both qualitative and quantitatively distance matrices. ASVs were taxonomically classified with scikitlearn (Python module for machine learning) using a naive Bayes classifier (Dubourg et al., 2011), previously trained against V3-V4 regions from 16S rRNA gene with Greengenes database vs. 13.8 pre-clustered at 99% sequence identity, to improve its performance as suggested by Werner et al. (2012) (259). To perform differential abundances estimation, we used two complementary approaches to compare the groups: discrete False-Discovery Rate (dsf-dr) (260) and Analysis of Compositions of Microbiomes with Bias Correction (ANCOM-BC) (261). In all tests, *P* values lower than 0.05 were considered significant.

Annexes

Annex 1.1

Nasal microbiota composition, ordered by global abundance (50 more abundant taxa), of the study groups at three weeks of age: non-treated piglets born to ceftiofur + tulathromycin treated sows ($CT_{sow}N_{piglet}$), Ceftiofur treated piglets born to ceftiofur + tulathromycin treated sows ($CT_{sow}C_{piglet}$); non-treated piglets born to ceftiofur treated sows ($C_{sow}N_{piglet}$).

Genera	$CT_{sow}N_{piglet}$		$CT_{sow}C_{piglet}$		$C_{sow}N_{piglet}$	
	Mean	SD	Mean	SD	Mean	SD
Ralstonia	0.293	0.200	0.368	0.158	0.327	0.180
Prevotella	0.042	0.062	0.032	0.051	0.043	0.018
Afipia	0.048	0.039	0.045	0.039	0.028	0.030
Hyphomicrobium	0.038	0.032	0.041	0.036	0.022	0.023
Streptococcus	0.027	0.039	0.009	0.011	0.038	0.029
***Phyllobacteriaceae*;__**	0.020	0.015	0.027	0.014	0.012	0.011
Acinetobacter	0.017	0.009	0.022	0.012	0.016	0.011
***Ruminococcaceae*;g__**	0.014	0.016	0.004	0.002	0.027	0.014
***Lachnospiraceae*;g__**	0.015	0.019	0.010	0.020	0.018	0.008
Haemophilus	0.001	0.002	0.001	0.001	0.033	0.056
***Moraxellaceae*;__**	0.020	0.048	0.013	0.013	0.010	0.008
***Bacteroidales*;f__;g__**	0.008	0.005	0.009	0.007	0.016	0.004
Bradyrhizobium	0.012	0.010	0.012	0.011	0.009	0.008
Ruminococcus	0.004	0.006	0.005	0.009	0.017	0.009
Treponema	0.011	0.015	0.004	0.004	0.013	0.006
Bacteroides	0.010	0.012	0.007	0.003	0.011	0.005
Sphingomonas	0.010	0.006	0.012	0.006	0.006	0.003
Arcobacter	0.011	0.008	0.010	0.006	0.006	0.006
***Clostridiales*;f__;g__**	0.009	0.010	0.006	0.006	0.010	0.004
Pedomicrobium	0.008	0.007	0.010	0.014	0.004	0.004
***Chitinophagaceae*;g__**	0.010	0.012	0.005	0.003	0.007	0.005
***Clostridiales*;__;__**	0.006	0.002	0.009	0.011	0.006	0.002
***Pirellulaceae*;g__**	0.008	0.004	0.009	0.006	0.004	0.003
Oscillospira	0.003	0.002	0.003	0.003	0.011	0.007
Moraxella	0.011	0.023	0.003	0.004	0.004	0.006
Lactococcus	0.004	0.006	0.002	0.003	0.010	0.008
Lactobacillus	0.006	0.007	0.004	0.002	0.007	0.005
k__*Escherichia*	0.006	0.007	0.009	0.012	0.003	0.002
***Lachnospiraceae*;__**	0.006	0.014	0.002	0.003	0.007	0.005
***Clostridiaceae*;g__**	0.005	0.005	0.004	0.004	0.007	0.004
Pseudomonas	0.007	0.002	0.006	0.002	0.004	0.002

[*Prevotella*]	0.008	0.014	0.004	0.007	0.004	0.002
***Enterobacteriaceae*;__**	0.008	0.004	0.004	0.003	0.004	0.003
***JG30-KF-CM45*;f__;g__**	0.004	0.004	0.007	0.004	0.003	0.004
Clostridium	0.004	0.001	0.005	0.002	0.005	0.002
Phascolarctobacterium	0.003	0.004	0.004	0.009	0.006	0.003
Roseburia	0.005	0.005	0.006	0.006	0.003	0.002
S24-7;g__	0.003	0.006	0.003	0.005	0.006	0.003
SMB53	0.003	0.003	0.003	0.003	0.005	0.003
Succinivibrio	0.001	0.002	0.003	0.006	0.006	0.004
Staphylococcus	0.004	0.004	0.002	0.004	0.005	0.003
***Coxiellaceae*;g__**	0.003	0.003	0.004	0.002	0.003	0.002
Blautia	0.003	0.002	0.003	0.003	0.004	0.002
Coprococcus	0.004	0.004	0.003	0.002	0.003	0.002
Faecalibacterium	0.005	0.009	0.003	0.004	0.003	0.002
Rothia	0.008	0.017	0.002	0.002	0.001	0.001
***Coriobacteriaceae*;g__**	0.002	0.003	0.007	0.012	0.001	0.001
Citrobacter	0.006	0.011	0.002	0.002	0.002	0.002
***Christensenellaceae*;g__**	0.001	0.001	0.003	0.005	0.004	0.002
***Caldilineaceae*;g__**	0.003	0.003	0.004	0.002	0.002	0.002

Annex 1.2

Relative abundance of the genera from nasal microbiota of the piglets included in this study including only the ASVs present in the farm core-microbiota. Non-treated piglets born to ceftiofur+tulathromycin treated sows ($CT_{sow}N_{piglet}$); ceftiofur treated piglets born to ceftiofur+tulathromycin treated sows ($CT_{sow}C_{piglet}$); non-treated piglets born to ceftiofur treated sows ($C_{sow}N_{piglet}$). Genera with global relative abundance below 0.5% are summed as low abundant.

Genus	**$CT_{sow}N_{piglet}$**		**$CT_{sow}C_{piglet}$**		**$C_{sow}N_{piglet}$**	
	Mean	SD	Mean	SD	Mean	SD
g__Prevotella	0.1031	0.0634	0.1178	0.0518	0.1104	0.0185
g__Acinetobacter	0.1271	0.0893	0.1532	0.0789	0.0573	0.0673
g__Streptococcus	0.0661	0.0535	0.0376	0.0198	0.0863	0.0392
f__Ruminococcaceae;g__	0.0393	0.0096	0.0274	0.0198	0.0658	0.0187
o__Bacteroidales;f__;g__	0.0405	0.0211	0.0424	0.0154	0.0452	0.0141
f__Lachnospiraceae;g__	0.0426	0.0200	0.0309	0.0248	0.0465	0.0078
f__Moraxellaceae;__	0.0324	0.0581	0.0574	0.0617	0.0313	0.0254
g__Bacteroides	0.0391	0.0242	0.0397	0.0160	0.0320	0.0176

g__Haemophilus	0.0025	0.0033	0.0089	0.0148	0.0647	0.0999
o__Clostridiales;__;__	0.0311	0.0182	0.0381	0.0140	0.0177	0.0056
o__Clostridiales;f__;g__	0.0315	0.0080	0.0262	0.0150	0.0260	0.0078
g__Treponema	0.0288	0.0132	0.0180	0.0144	0.0334	0.0085
g__Ruminococcus	0.0140	0.0079	0.0199	0.0156	0.0411	0.0125
g__Clostridium	0.0272	0.0183	0.0338	0.0171	0.0155	0.0139
f__Enterobacteriaceae;__	0.0448	0.0390	0.0180	0.0094	0.0125	0.0088
g__Escherichia	0.0183	0.0104	0.0456	0.0626	0.0064	0.0028
g__Lactobacillus	0.0204	0.0126	0.0191	0.0075	0.0171	0.0081
g__Roseburia	0.0204	0.0125	0.0246	0.0157	0.0099	0.0082
f__Clostridiaceae;g__	0.0180	0.0096	0.0168	0.0071	0.0169	0.0048
g__Oscillospira	0.0097	0.0068	0.0103	0.0058	0.0264	0.0087
g__Moraxella	0.0245	0.0312	0.0155	0.0153	0.0090	0.0098
g__Coprococcus	0.0150	0.0063	0.0205	0.0118	0.0075	0.0030
g__[Prevotella]	0.0180	0.0181	0.0114	0.0091	0.0117	0.0042
f__Lachnospiraceae;__	0.0118	0.0191	0.0064	0.0049	0.0175	0.0071
f__Clostridiaceae;g__SMB53	0.0132	0.0125	0.0125	0.0095	0.0121	0.0045
o__Bacteroidales;f__S24-7;g__	0.0054	0.0086	0.0103	0.0076	0.0167	0.0041
g__Phascolarctobacterium	0.0084	0.0048	0.0105	0.0120	0.0138	0.0045
g__Faecalibacterium	0.0142	0.0105	0.0088	0.0052	0.0098	0.0111
g__Staphylococcus	0.0123	0.0094	0.0062	0.0051	0.0108	0.0050
g__Succinivibrio	0.0034	0.0033	0.0082	0.0100	0.0143	0.0064
g__Anaerovibrio	0.0049	0.0036	0.0088	0.0062	0.0127	0.0065
f__Christensenellaceae;g__	0.0053	0.0052	0.0114	0.0072	0.0101	0.0039
g__Rothia	0.0147	0.0214	0.0081	0.0045	0.0035	0.0022
g__Turicibacter	0.0074	0.0077	0.0070	0.0070	0.0079	0.0070
g__Dorea	0.0109	0.0129	0.0036	0.0028	0.0061	0.0034
f__Erysipelotrichaceae;g__[Eubacterium]	0.0031	0.0044	0.0011	0.0018	0.0121	0.0043
f__Ruminococcaceae;__	0.0046	0.0052	0.0058	0.0052	0.0065	0.0038
f__[Mogibacteriaceae];g__	0.0039	0.0040	0.0035	0.0055	0.0086	0.0027
k__Bacteria;__;__;__;__;__	0.0109	0.0114	0.0073	0.0060	0.0012	0.0016
k__Bacteria;p__;c__;o__;f__;g__	0.0065	0.0082	0.0066	0.0054	0.0018	0.0039
f__Lachnospiraceae;g__[Ruminococcus]	0.0027	0.0047	0.0027	0.0052	0.0066	0.0044
g__Desulfovibrio	0.0059	0.0084	0.0059	0.0052	0.0016	0.0013
g__Campylobacter	0.0018	0.0024	0.0048	0.0084	0.0038	0.0029
g__Parabacteroides	0.0026	0.0035	0.0030	0.0033	0.0034	0.0028
o__Bacteroidales;f__RF16;g__	0.0003	0.0005	0.0006	0.0016	0.0064	0.0038
g__Butyricicoccus	0.0026	0.0033	0.0020	0.0029	0.0035	0.0023
;g__Sutterella	0.0025	0.0038	0.0015	0.0013	0.0024	0.0022

f__Erysipelotrichaceae;g__p-75-a5	0.0009	0.0024	0.0026	0.0047	0.0025	0.0022
g__Aerococcus	0.0007	0.0018	0.0015	0.0016	0.0029	0.0026
c__Alphaproteobacteria;o__RF32;f__;g__	0.0028	0.0048	0.0032	0.0040	0.0002	0.0004
g__Mucispirillum	0.0012	0.0021	0.0026	0.0037	0.0013	0.0021
g__Megasphaera	0.0026	0.0028	0.0013	0.0017	0.0014	0.0008
g__Akkermansia	0.0012	0.0023	0.0021	0.0028	0.0015	0.0006
o__Flavobacteriales;f__[Weeksellaceae];__	0.0037	0.0031	0.0012	0.0013	0.0003	0.0004
f__Erysipelotrichaceae;g__	0.0035	0.0033	0.0006	0.0017	0.0008	0.0010
c__Mollicutes;o__RF39;f__;g__	0.0018	0.0031	0.0004	0.0012	0.0009	0.0015
g__Enhydrobacter	0.0006	0.0011	0.0021	0.0031	0.0003	0.0010
g__Mycoplasma	0.0023	0.0030	0.0004	0.0013	0.0001	0.0002
g__Clostridium	0.0005	0.0010	0.0000	0.0000	0.0013	0.0013
g__Delftia	0.0009	0.0015	0.0007	0.0021	0.0001	0.0003
g__Anaeroplasma	0.0000	0.0000	0.0009	0.0023	0.0005	0.0014
f__Desulfovibrionaceae;g__	0.0011	0.0028	0.0000	0.0000	0.0003	0.0005
o__Bacteroidales;f__p-2534-18B5;g__	0.0005	0.0012	0.0002	0.0003	0.0005	0.0006
o__Bacteroidales;f__[Paraprevotellaceae];g__	0.0000	0.0000	0.0000	0.0000	0.0007	0.0006
f__Neisseriaceae;g__	0.0009	0.0021	0.0000	0.0000	0.0000	0.0000
g__Ruminococcus	0.0004	0.0011	0.0003	0.0009	0.0000	0.0000
g__Bacteroides	0.0000	0.0000	0.0002	0.0005	0.0003	0.0009
k__Bacteria;p__TM7;c__TM7-3;o__CW040;f__F16;g__	0.0000	0.0000	0.0000	0.0000	0.0004	0.0008
g__Fusobacterium	0.0006	0.0015	0.0000	0.0000	0.0000	0.0001
o__Lactobacillales;__;__	0.0005	0.0011	0.0000	0.0000	0.0000	0.0000
g__Neisseria	0.0000	0.0000	0.0000	0.0000	0.0001	0.0002

Annex 1.3

Differentially 50 more abundant ASVs between $CT_{sow}N_{piglet}$ and $C_{sow}N_{piglet}$ computed by two different approaches. ASV taxonomical classification is detailed to the lowest known taxonomical level. The relative abundance in all study groups and the significance in each test is shown per ASV (NF=not found).

ASV taxonomical classification	Relative abundance (%)			ANCOM-BC statistics	Ds-FDR statistics (%)
	CT_{sow} N_{piglet}	CT_{sow} C_{piglet}	C_{sow} N_{piglet}	*q*-value (%)	*p*-value
k__Bacteria	0.4390	0.0004	0.0002	NF	0.0100
o__Bacteroidales; f__; g__; s__	0.0000	0.0000	0.1299	0.0000	0.0040

o__Bacteroidales; f__; g__; s__	0.0000	0.0000	0.0072	0.0000	0.0020
g__[Prevotella]; s__	0.0000	0.0000	0.0023	0.0001	0.0080
g__Bacteroides; s__	0.0000	0.0000	0.0022	0.0000	0.0020
g__Bacteroides; s__	0.0010	0.0048	0.0043	0.0123	0.0060
g__Bacteroides; s__	0.0000	0.0000	0.0027	0.0000	0.0040
g__Bacteroides; s__uniformis	0.0000	0.0009	0.0018	0.0000	0.0010
g__Prevotella; s__	0.0000	0.0000	0.0012	0.0004	0.0090
g__Prevotella; s__	0.0000	0.0000	0.0039	0.0000	0.0010
g__Prevotella; s__	0.0000	0.0007	0.0017	0.0011	0.0070
g__Prevotella; s__	0.0000	0.0000	0.0236	0.0000	0.0010
g__Prevotella; s__	0.0000	0.0000	0.0009	0.0407	NF
g__Prevotella; s__	0.0000	0.0000	0.0019	0.0230	NF
g__Prevotella; s__	0.0010	0.0000	0.0050	NF	0.0120
o__Bacteroidales; f__RF16; g__; s__	0.0000	0.0000	0.0038	0.0000	0.0030
o__Bacteroidales; f__S24-7; g__; s__	0.0000	0.0000	0.0012	0.0000	0.0030
g__Staphylococcus	0.0003	0.0000	0.0063	0.0007	0.0020
g__Streptococcus	0.0000	0.0000	0.0025	0.0000	0.0030
g__Streptococcus; s__	0.0183	0.0127	0.0527	NF	0.0130
g__Turicibacter; s__	0.0049	0.0060	0.0079	NF	0.0040
o__Clostridiales; f__; g__; s__	0.0000	0.0000	0.0043	0.0000	0.0010
o__Clostridiales; f__; g__; s__	0.0000	0.0000	0.0012	0.0131	0.0100
f__[Mogibacteriaceae]; g__; s__	0.0000	0.0000	0.0015	0.0001	0.0110
f__[Mogibacteriaceae]; g__; s__	0.0003	0.0000	0.0024	NF	0.0020
f__Christensenellaceae; g__; s__	0.0000	0.0000	0.0014	0.0004	0.0080
f__Christensenellaceae; g__; s__	0.0000	0.0000	0.0010	0.0224	NF
f__Christensenellaceae; g__; s__	0.0000	0.0000	0.0010	0.0262	NF
f__Lachnospiraceae	0.0010	0.0003	0.0093	0.0002	0.0030
f__Lachnospiraceae	0.0003	0.0000	0.0021	NF	0.0120
f__Lachnospiraceae; g__; s__	0.0000	0.0000	0.0015	0.0014	0.0120
f__Lachnospiraceae; g__; s__	0.0005	0.0006	0.0141	0.0000	0.0010
f__Lachnospiraceae; g__; s__	0.0000	0.0000	0.0024	0.0007	0.0100
f__Lachnospiraceae; g__; s__	0.0000	0.0004	0.0032	0.0001	0.0090
g__[Ruminococcus]; s__gnavus	0.0000	0.0000	0.0051	0.0000	0.0010
g__Coprococcus; s__	0.0002	0.0000	0.0018	0.0038	0.0040

g__Dorea; s__	0.0019	0.0007	0.0038	NF	0.0130
f__Ruminococcaceae	0.0004	0.0008	0.0023	NF	0.0090
f__Ruminococcaceae; g__; s__	0.0000	0.0000	0.0048	0.0000	0.0010
f__Ruminococcaceae; g__; s__	0.0000	0.0000	0.0099	0.0000	0.0010
f__Ruminococcaceae; g__; s__	0.0001	0.0004	0.0112	0.0000	0.0010
f__Ruminococcaceae; g__; s__	0.0000	0.0008	0.0028	0.0007	0.0070
f__Ruminococcaceae; g__; s__	0.0000	0.0004	0.0011	0.0034	0.0020
f__Ruminococcaceae; g__; s__	0.0000	0.0000	0.0010	0.0008	0.0070
f__Ruminococcaceae; g__; s__	0.0000	0.0000	0.0028	0.0001	0.0090
f__Ruminococcaceae; g__; s__	0.0000	0.0000	0.0014	0.0230	NF
g__Oscillospira; s__	0.0000	0.0000	0.0019	0.0001	0.0130
g__Oscillospira; s__	0.0000	0.0000	0.0039	0.0000	0.0040

Chapter 2

Design of an *in vitro* Porcine Nasal Consortium (PNC8) synthetic community

This chapter is part of the article:

Bonillo-López L.*, Rouam-el Khatab O.*, Obregon-Gutierrez P., Almansa Fernandez-Villacañas J., Florez-Sarasa I., Correa-Fiz F., Sibila M., Aragon V., Kochanowski K. ***In vitro* metabolic interaction network of a rationally designed nasal microbiota community.** 2025, under review in iScience. Pre-print available at bioRxiv. doi: 10.1101/2024.10.23.619785

* Equally contributing first authors.

Abstract

Mounting evidence suggests that interactions among microbiota members are key drivers of a well-balanced microbial composition and pathogen exclusion. Regarding pig nasal microbiota, current efforts to study these interactions are hampered by a lack of tools for examining them under *in vitro* conditions. To address this issue, we developed the Porcine Nasal Consortium (PNC8), a rationally designed microbial synthetic community of eight strains representing the most *in-vivo* abundant and prevalent genera found in the nasal microbiota of healthy piglets. We used this consortium to systematically examine the metabolic capabilities of nasal microbiota members. We found that PNC8 strains differed substantially in their metabolic functions repertoire and ability to grow across various *in vitro* conditions. Moreover, we conducted an interaction proof-of-concept experiment with some of the PNC8 members, and we determined that it existed cooperation among some consortia members. Overall, this work provides a valuable resource for studying the nasal microbiota under experimentally tractable *in vitro* conditions and is a key step towards mapping its metabolic interaction network.

Introduction

Animals are hosts to a myriad of microorganisms found in different body sites, collectively known as the microbiota (3). Given the importance of the commensal microbiota in the host health, there have been extensive efforts to understand the mechanisms that determine microbiota composition. Indeed, several studies have shown that interactions within the human gut microbiota are key to avoid pathogen's colonization by blocking the nutrients available to them (262–265). An approach that can provide a way to simplify the complexity of microbial ecosystems while still capturing the dynamics of microbial interactions, are the synthetic communities. For instance, the OMM12, a simplified community of 12 bacterial species from gut mice (147), have been critical in enabling the identification of metabolic interactions within the gut microbiota (148–151,266–268).

In the respiratory tract, the nasal microbiota constitutes the first line of defence against respiratory pathogens and pathobionts, acting as the gatekeeper (30,269). However, it remains unclear whether interactions between the members of this microbiota play a similar role in pathogen's protection. Some studies in humans have determined pivotal metabolic interactions, as for example the inhibition of the pathogens *Streptococcus pneumoniae* and *Staphylococcus aureus* by the nasal commensal members *Dolosigranulum pigrum* and *Coryneobacterium* species (152,154). Nevertheless, the full network interaction is not clearly understood yet, mainly because of the lack of adequate experimental tools, as the few currently available nasal communities only cover a small fraction (3 strains) of the diversity present in the *in vivo* human nasal microbiota (270,271). Until date, there is no gut neither nasal microbial consortium for pigs.

To tackle this, we have rationally designed, for the first time, an *in vitro* community called the Porcine Nasal Consortium (PNC8) that represents the aerobic fraction of the piglet's nasal microbiota. We further characterized the growth patterns of each member of the consortium. Finally, as a proof-of-concept, we

conducted side-to-side microbe-microbe interaction experiments with some PNC8 members as well as with the pathobiont *Glaesserella parasuis.*

Materials and methods

Identification of most abundant nasal microbiota genera

To identify the most abundant genera in the piglet nasal microbiota, 16S sequencing data were collected from 94 nasal swab samples from healthy animals from farms of several previous studies conducted in our laboratory and analysed jointly in a recent publication from our group (50). All the taxa composing these samples were sorted (at genus level) by mean relative abundance across all samples. Gut-microbiota associated taxa (i. e. taxa belonging to *Clostridiales* and *Bacteroidales* orders) were excluded, and the relative abundance of the remaining taxa was recalculated accordingly.

Strain selection

To ensemble de defined consortium, we took advantage of our strain internal collection constituted by bacterial isolates from noses of healthy 3-4-week-old piglets coming from previous studies (87,126,163,164,272) (**Table 2.1**). We chose one strain per genus considering the previous information regarding low antibiotic resistances, low virulence traits (sensitivity to serum, phagocytosis susceptibility and biofilm formation positive), availability of a fully sequenced genome, and the ability to grow *in vitro.* For the *Moraxella* and *Bergeyella* genus, previous work showed that isolates predominantly belong to two species, namely *Moraxella pluranimalium* and *Bergeyella zoohelcum* (majority of isolates) and *Moraxella porci* and *Bergeyella porcorum* respectively. From these isolates, we selected the strain *M. pluranimalium* LG6-2 and *B. zoohelcum* AR-9 due to its low virulence traits and antibiotic resistances (163,164). In our collection, only *Rothia nasimurium* was available within *Rothia.* We selected UK1-9 strain due to its high susceptibility to phagocytosis (272), and the lack of adverse effects during *in vivo* inoculation experiments (126). In concordance, for *Streptococcus* genus, we identified three predominant species among our isolates, *Streptococcus pluranimalium*, *Streptococcus suis*, and *Streptococcus hyovaginalis*.

We discarded *S. suis* due to its pathogenic potential (273), and *S. hyovaginalis* since it is normally found in the sow genital tract (274). We selected the strain *S. pluranimalium* LG3-6 due to its high susceptibility to phagocytosis and a lack of adverse effects during *in vivo* inoculation experiments (126,272). F9 *Glaesserella parasuis* strain was picked to represent non-virulent *Glaesserella* since previous studies found this strain to be phagocytosis and serum sensitive and non-virulent in colostrum-deprived piglets (86,87,275,276). Regarding *Staphylococcus*, we had a plethora of species in our strain collection (*Staphylococcus aureus*, *Staphylococcus haeomolyticus*, *Staphylococcus chromogenes*, *Staphylococcus hyicus*, *Staphylococcus agnetis*, *Staphylococcus simulans*, *Staphylococcus saprophyticus*, *Staphylococcus succinus* and *Staphylococcus petrasii*). Although *S. aureus* is an opportunistic pathogen, we selected the strain EJ41-2 since it is the most abundant species from *Staphylococcus* in the nose and skin of piglets (unpublished results from a new strain collection from newborn piglets in our laboratory). Finally, for *Neisseria* and *Lactobacillus* genus, we only had one strain in our collection for each one, *Neisseria shayeganii* GM3-3 and *Lactobacillus plantarum* KD9-5. The full list of strains used in this study, including the virulent *G. parasuis* Nagasaki strain used as a representative pathobiont, is shown in **Table 2.1**.

The genome sequences of the PNC8 strains generated in this study were deposited in the NCBI database (BioProject ID: PRJNA1175893) (**Table 2.1** for biosample numbers of each strain) except for *G. parasuis* F9, which was previously sequenced (NCBI RefSeq Assembly GCF_000731865.1).

Table 2.1. Bacteria used in this study.

Species	Strain	Source	PNC8 member	Biosample number
Bergeyella zoohelcum	AR-9	Lorenzo de Arriba et al., 2018	Yes	SAMN44375914
Glaesserella parasuis	F9	Olvera et al., 2006	Yes	N/A*
	Nagasaki	Amano et al., 1994	No	N/A
Lactobacillus plantarum	KD9-5	This thesis	Yes	SAMN44375915
Moraxella pluranimalium	LG6-2	López-Serrano et al. 2020	Yes	SAMN44375912
Neisseria shayeganii	GM3-3	This thesis	Yes	SAMN44375913
Rothia Nasimurium	UK1-9	This thesis, Lorenzo, 2016	Yes	SAMN44375910
Staphylococcus aureus	EJ41-2	This thesis	Yes	SAMN44375916
Streptococcus pluranimalium	LG3-6	Blanco-Fuertes et al., 2023; Lorenzo, 2016	Yes	SAMN44375911

*NA: Not applicable.

Analysis of KEGG module completeness

KEGG module completeness of individual PNC8 strains was determined with the "reconstruct" function of the KEGG-mapper tool (available online at https://www.genome.jp/kegg/mapper/), using the list of KO identifiers inferred with the eggNOG-mapper, and considering also incomplete modules and modules with missing blocks. To determine KEGG module completeness when considering all PNC8 strains together, the lists of KO identifiers from each strain were first merged before using the KEGG-mapper tool. To infer KEGG module completeness found in *in vivo* samples, a recently identified pig nasal core-microbiota was used as a starting point (Bonillo-Lopez et al., 2023), and ASVs found in this pig nasal core-microbiota (or only ASVs belonging to the 8 genera included in the PNC8 consortium, see Figure 1) were used to predict KO identifiers using PICRUSt2 (Douglas et al., 2020; Czech et al., 2020; Mirarab et al., 2011; Barbera et al., 2019; Louca et al., 2018; Ye et al., 2009 A parsimony approach to biological) using its default parameters, and the KEGG reference database (Kanehisa et al., 2017). Finally, the resulting KO identifier list was used to determine KEGG module completeness as described above. In each case, results from the KEGG-mapper tool were parsed using a python script available at

(https://github.com/JulieMarieCharmillon/kegg_parser) as well as custom bash scripts.

Growth experiments across different conditions

For all *in vitro* cultivation experiments, strains were first plated on chocolate PolyVitex agar plates (Biomérieux), except *L. plantarum*, which was plated on MRS agar, directly from -80ºC stocks and were incubated overnight (o/n) at 37ºC in a 5% CO_2-enriched atmosphere.

To characterize the *in vitro* growth of bacterial strains across diverse metabolic environments, bacterial suspensions were freshly prepared from agar plates (at OD_{600} of 0.3 in sterile PBS) and used 1:30 diluted to inoculate 150 μL cultures of 23 different growth media (listed in **Table 2.2**) in 96-well plate format (Greiner Cat. No 655 180). Subsequently, 100 μL mineral oil (M3516, Sigma-Aldrich) was added to each well to prevent evaporation without affecting the aeration of the culture, as described previously (277,278). Bacterial growth was monitored at OD_{600} every 10 min for around 24h with an automated plate reader (Tecan Nano M+) using an incubation temperature of 37ºC and an intermittent shaking protocol (alternating 10 sec of linear shaking with 1 mm amplitude and 50 sec without shaking) to support the growth of aerobic as well as microaerophilic strains, as described previously (279).

Table 2.2. Cultivation media (conditions) used in this study.

Medium	Composition
BHI	Brain Heart Infusion broth (53286, Sigma-Aldrich)
BHI+	Brain Heart Infusion broth + 80 µg/mL NAD^+ (N0632, Sigma-Aldrich) + 1% pig serum heat-deactivated (P9783, Sigma-Aldrich)
M9 base salts	11.33 g/L sodium phosphate dibasic heptahydrate (S9390, Sigma-Aldrich) + 3 g/L potassium phosphate monobasic (P0662, Sigma-Aldrich) + 0.5 g/L sodium chloride (1.06404.1000, Millipore) + 1 g/L ammonium chloride (12125-02-9, Millipore)
M9 + Glc	M9 base salts + 2 g/L glucose (16301, Sigma-Aldrich)
M9 + Glc + Vit	M9 base salts + 2 g/L glucose + 2% RPMI vitamin solution (R7256, Sigma-Aldrich) + 80 µg/mL NAD^+ + 1 mg/mL pyridoxal-HCl (P9130, Sigma-Aldrich) + 1 mg/mL pyridoxamine-2HCl (P9158, Sigma-Aldrich)
M9 + Glc + CAA	M9 base salts + 2 g/L glucose + 2 g/L Casamino acids (N4642, Sigma-Aldrich)
M9 + Glc + RPMI	M9 base salts + 2 g/L glucose + 1% RPMI amino acid solution (R7131, Sigma-Aldrich) + 2 mM L-Glutamine (G7513, Sigma-Aldrich)
M9 + Glc + CAA + Vit	M9 base salts + 2 g/L glucose + 2 g/L CAA + 2% RPMI vitamin solution + 80 µg/mL NAD^+ + 1 mg/mL pyridoxal-HCl + 1 mg/mL pyridoxamine-2HCl
M9 + Glc + RPMI + Vit	M9 base salts + 2 g/L glucose + 1% RPMI amino acid solution + 1% L-Glutamine + 2% RPMI vitamin solution + 80 µg/mL NAD^+ + 1 mg/mL pyridoxal-HCl + 1 mg/mL pyridoxamine-2HCl
M9 + Glc + CAA + Vit + pig serum	M9 base salts + 2 g/L glucose + 2 g/L CAA + 2% RPMI vitamin solution + 80 µg/mL NAD^+ + 1 mg/mL pyridoxal-HCl + 1 mg/mL pyridoxamine-2HCl + 1% pig serum heat-inactivated
M9 + Glc + CAA + Vit + yeast extract	M9 base salts + 2 g/L glucose + 2 g/L CAA + 2% RPMI vitamin solution + 80 µg/mL NAD^+ + 1 mg/mL pyridoxal-HCl + 1 mg/mL pyridoxamine-2HCl + 0.2 g/L yeast extract (70161, Sigma-Aldrich)
M9 + Glc + CAA + Vit + BHI	M9 base salts + 2 g/L glucose + 2 g/L CAA + 2% RPMI vitamin solution + 80 µg/mL NAD^+ + 1 mg/mL pyridoxal-HCl + 1 mg/mL pyridoxamine-2HCl + 1% BHI
M9 + Glc + CAA + Vit + THB	M9 base salts + 2 g/L glucose + 2 g/L CAA + 2% RPMI vitamin solution + 80 µg/mL NAD^+ + 1 mg/mL pyridoxal-HCl + 1 mg/mL pyridoxamine-2HCl + 1% THB
M9 + Glc + CAA + Vit + MRS	M9 base salts + 2 g/L glucose + 2 g/L CAA + 2% RPMI vitamin solution + 80 µg/mL NAD^+ + 1 mg/mL pyridoxal-HCl + 1 mg/mL pyridoxamine-2HCl + 1% MRS
M9 + NAD^+ + pig serum	M9 base salts + 80 µg/mL NAD^+ + 1% pig serum heat-inactivated
MH	Müller-Hinton broth (212322, BD)

THB	Todd-Hewitt Broth (T1438, Millipore)
THB+	Todd-Hewitt Broth (T1438, Millipore) + 80 µg/mL NAD^+ (N0632, Sigma-Aldrich) + 1% pig serum heat-deactivated (P9783, Sigma-Aldrich)
THY	Todd-Hewitt Broth (T1438, Millipore) + 0.2 g/L yeast extract
MRS	De Man, Rogosa and Sharpe broth (69966, Sigma-Aldrich)
LB	Luria-Bertani broth (L3022, Sigma-Aldrich)
HPLM	Human Plasma-Like Medium (A4899101, Gibco)
BHI + NAD^+ + CAA	BHI + 80 µg/mL NAD^+ + 2 g/L CAA
BHI + NAD^+ + yeast extract	BHI + 80 µg/mL NAD^+ + 0.2 g/L yeast extract
BHI + Vit	BHI + 1% RPMI vitamin solution + 80 µg/mL NAD^+ + 1 mg/mL pyridoxal-HCl + 1 mg/mL pyridoxamine-2HCl

Microbial growth curves in 96-well plate format were analysed using custom MATLAB scripts (Version R2021a) following procedures described previously (Gerosa et al., 2013). Briefly, raw OD_{600} time courses from each well were blank-corrected and smoothed using a moving average window with size 3. Area-under-the-growth-curve (AUC) was calculated using the *trapz* function, and the maximal growth rate of each curve during exponential growth was calculated using a slide window of six consecutive time points and an OD_{600} threshold of > 0.02.

Side-to-side agar plate interaction experiments

Dilutions 1:100 in PBS were prepared from dense suspensions of *R. nasimurium* UK1-9, *S. pluranimalium* LG3-6, *S. aureus* EJ41-2, *G. parasuis* F9, *G. parasuis* Nagasaki and *L. plantarum* KD9-5, individually. Dots of 1.5 µl were cultured in BHI and chocolate agar alone or next to the other bacteria. All plates were incubated o/n at 37ºC in a 5% CO_2-enriched atmosphere.

Results

Development of a defined consortium of the pig nasal microbiota

To identify the taxa highly abundant and most prevalent in the nasal microbiota of healthy piglets, we analysed the 16S rRNA gene sequence from nasal swabs from

94 animals sampled at several farms from previous studies in our laboratory. Since we were interested in nasal colonizers that can be grown under aerobic conditions, we excluded taxa belonging to *Clostridiales*/*Bacteroidales* (gut-associated anaerobic microbes which can frequently be found in nasal microbiota samples) from further analyses and re-calculated the relative abundance of all other taxa accordingly (50).

First, we analysed the complexity of these nasal microbiota samples in terms of the number of abundant taxa. We found that individual samples were typically dominated by a small set of highly abundant taxa at genus level (**Figure 2.1A**).

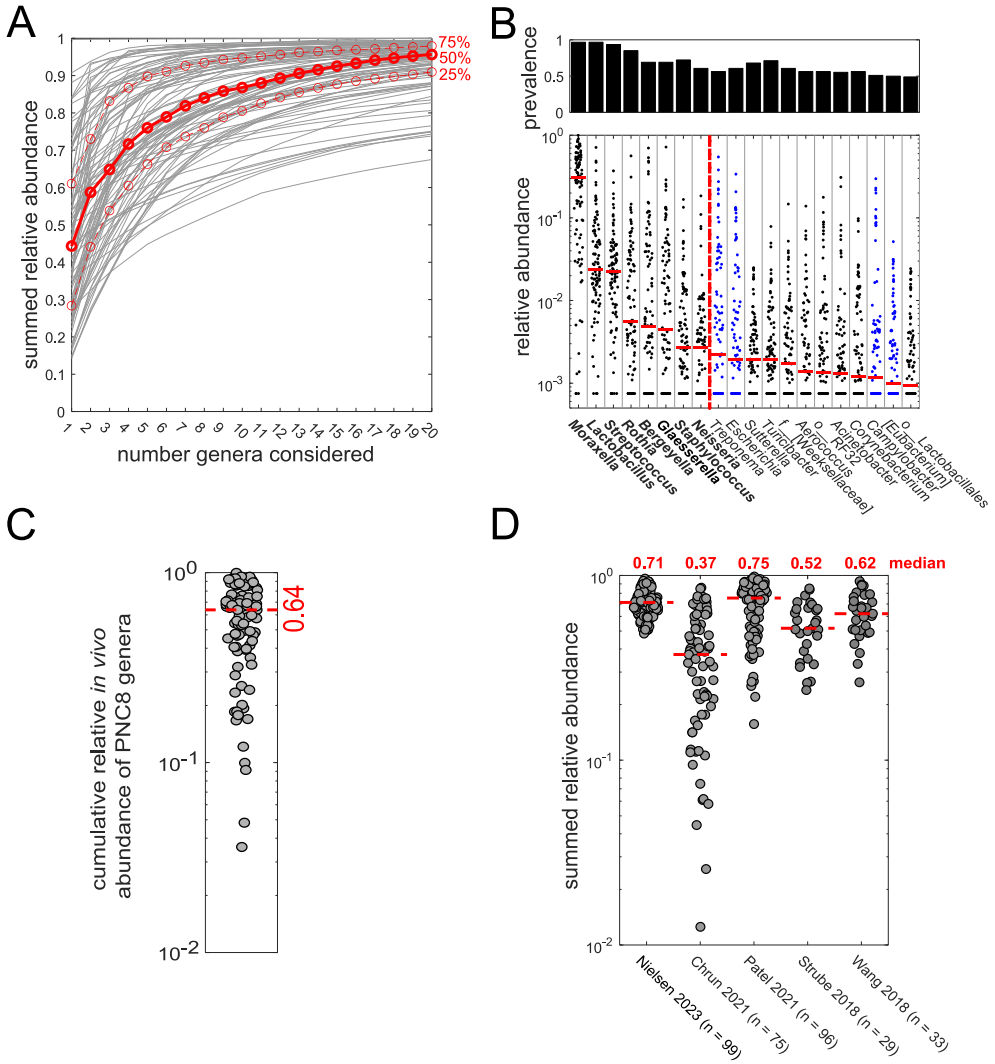

Figure 2.1. Rational design of the Porcine Nasal Consortium (PNC8) using *in vivo* nasal microbiota samples. A) Summed relative abundance as a function of the number of taxa considered at genus level in nasal microbiota samples obtained from 94 piglets (after removing gut-microbiota associated taxa). Gray lines represent samples from individual animals. Red dashed lines denote the 75 and 25 percentiles, and the red continuous line represents the median. **B)** Prevalence (fraction of samples with relative abundance > 0.1%, top) and relative abundance (bottom) of the twenty most abundant genera (sorted by median abundance across samples, shown as red horizontal lines). Each circle denotes an individual animal. Blue: respective genus is prevalent (>10% prevalence) in a reference pig gut microbiota data set (Chrun et al., 2021). Vertical red dashed line: cut-off of genera included in the PNC8 (shown in bold). Wherever the taxonomical assignment was not possible at genus level, the lowest resolved annotation is shown. **C)** Summed *in vivo* relative abundance of PNC8 genera (dashed line denotes median: 64%). Each circle represents an individual animal. **D)** Summed relative abundance of PNC8 genera in five publicly available pig nasal microbiota data sets (using in each case the non-treated control group animals). n denotes the number of samples used for each data set. Red dashed lines: median summed relative abundance (values are listed above).

It is conceivable that, although there were few dominant genera in the nasal microbiota samples, these could be different across individuals. To assess this question, we next determined the relative abundance of different taxa (at genus level) across individuals. *Moraxella*, *Lactobacillus*, and *Streptococcus* were the most abundant genera found with close to 100% prevalence, consistent with previous reports (32). In addition, we detected five other genera (*Rothia*, *Bergeyella*, *Glaesserella*, *Staphylococcus* and *Neisseria*), which were ranked just below (rank 4-8). Beyond these eight genera, we largely detected genera associated with the gut microbiota (e. g. *Treponema*, *Escherichia*), genera with low relative abundance/prevalence, or unclassified genera. As a compromise between completeness (how many of the genera found in the pig nasal microbiota are included in the consortium) and size (enabling *in vitro* tractable experiments in 96-well plate format), we decided to consider the highest ranked eight genera for the defined consortium (**Figure 2.1B**). Collectively, these eight genera, ranking among the 40 most abundant genera in individual animals by relative abundance, constitute the majority of the pig nasal microbiota, (median: 64% summed relative abundance, with many samples reaching > 90% summed relative abundance, **Figure 2.1C**) both in this dataset, as well as in five additional publicly available datasets of pig nasal microbiota samples (**Figure 2.1D**) (117,228,280–282).

The result of these efforts is the Porcine Nasal Consortium (PNC8) consisting of eight genetically diverse strains (**Figure 2.2A**). The assembled PNC8 genomes were used to predict the corresponding KEGG. The KEGG modules inferred for these 8 genomes were compared with the metabolic modules inferred for the previously described healthy nasal core-microbiota (defined as genera present in at least 80% samples (283). The KEGG modules completeness was estimated considering all genera from the core microbiota, and also for the combined ASVs belonging to these 8 genera. As shown in **Figure 2.2B**, the PNC8 consortium can collectively cover a large fraction of the predicted metabolic repertoire found in the *in vivo* pig nasal microbiota. Thus, these analyses suggested that this consortium is a good

representation not only of the overall genetic diversity (in terms of included genera), but also of the metabolic capabilities found in the pig nasal microbiota.

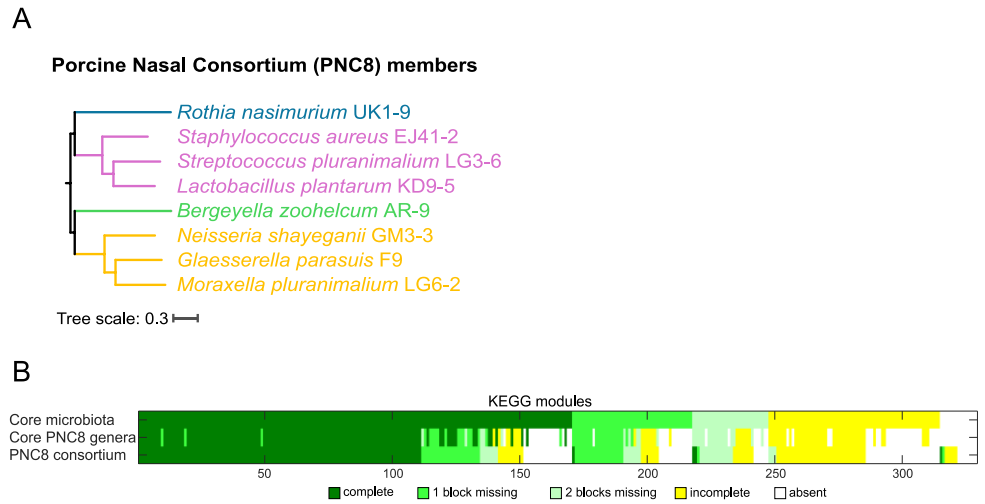

Figure 2.2. Development of the Porcine Nasal Consortium (PNC8). A) Codon phylogenetic tree was built from translated genomes of PNC8 members, using 100 rounds of rapid bootstrapping was done. PNC8 members are color-coded by phylum (Blue: *Actinobacteria*, Purple: *Firmicutes*, Green: *Bacteroidota*, Orange: *Proteobacteria*). B) Comparison of inferred KEGG completeness within *in vivo* samples. Inferred using core nasal microbiota or only PNC8 genera based on 16S ASVs (top and middle rows) and the combined PNC8 strains (bottom row). To aid visual comparison KEGG modules were sorted according to completeness first for core nasal microbiota, and then for PNC8 strains.

Characterization of the *in vitro* growth capabilities of the PNC8

We aimed to characterize the metabolic capacities of the PNC8 species and assess the differences between them. To do that, we examined the ability of each PNC8 strain to grow in 23 metabolically diverse *in vitro* cultivation media, varying their composition and richness (conditions described in **Table 2.2**). Individual bacterial growth is shown in **Figure 2.3**, confirming that all the PNC8 strains had distinct metabolic requirements, and thus, substantial differences in growth patterns. All tested strains grew well in only one or few conditions, which tended to differ across PNC8 strains. Interestingly, only *S. aureus* EJ41-2 was able to grow in most of the tested conditions, being the less-specialized strain. In contrast, *G. parasuis* F9 and *S. pluranimalium* LG3-6 were only able to grow well in 3-4 conditions, suggesting that

they need more specific requirements to grow, and thus, showing a higher level of metabolic specialization. Notably, none of the strains grew in a minimal medium supplemented only with glucose (and inorganic nitrogen/phosphor/sulphate), indicating that all PNC8 strains require at least some external metabolites, while all of them grew well in BHI+, which is a rich medium (**Figure 2.3**). Thus, these data showed that PNC8 members tend to be metabolic specialists with distinct nutrient requirements, which suggests that the *in vivo* nasal microbiota members could also exhibit this specialization.

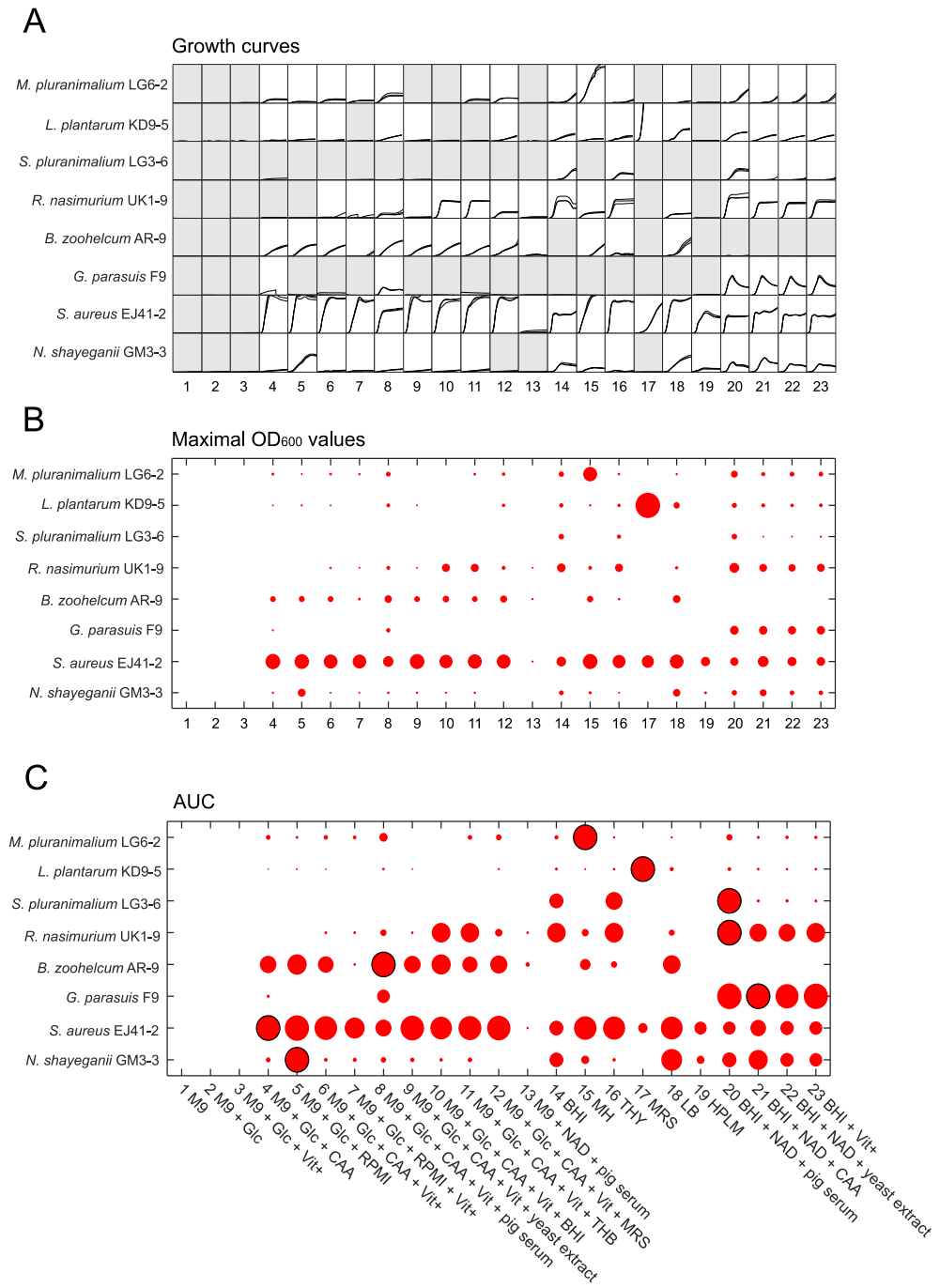

Figure 2.3. Over-time growth patterns of PNC8 members across various *in vitro* conditions. A) Growth curves of all PNC8 members in 23 different cultivation media. Each line is a replicate culture. Gray: no growth detected (maximal OD_{600} < 0.02). X-axis range (h): 0-24h. Y-axis range (OD_{600}): 0 to 0.6. **B)** Maximal OD_{600} value (mean across 2-3 replicates) shown as red circle size for all eight PNC8 members in 23 different cultivation media. **C)** Area-under-growth-curve (AUC) of PNC8 members in 23 different cultivation media (normalized to the condition with maximal AUC for each PNC8 member, which is denoted with a black edge).

Finally, to examine if the virulence correlated with the metabolic capacities of the strains, we evaluated the bacterial growth of the virulent *G. parasuis* Nagasaki strain and compared it with the non-virulent F9 strain of the PNC8 consortium. We selected 12 of the 23 conditions described in **Table 2.2** based on the growth results of F9 obtained in **Figure 2.3**. We observed that both strains grew in the same 4 conditions shown in **Figure 2.4A**. Additionally, Nagasaki strain could slightly grow in M9 + Glc + CAA + Vit, while F9 did not (**Figure 2.3** and **Figure 2.4A**). These results suggest that, under the conditions tested, virulence is not a determinant factor for metabolic characteristics. Both strains did not grow in M9 base salts, HLPM, BHI, MH, THB, MRS and LB. On the other hand, we observed differences in the growth rate, as the virulent Nagasaki strain showed a slower and less-abundant growth in comparison to the non-virulent F9 strain (**Figure 2.4B and 2.4C**).

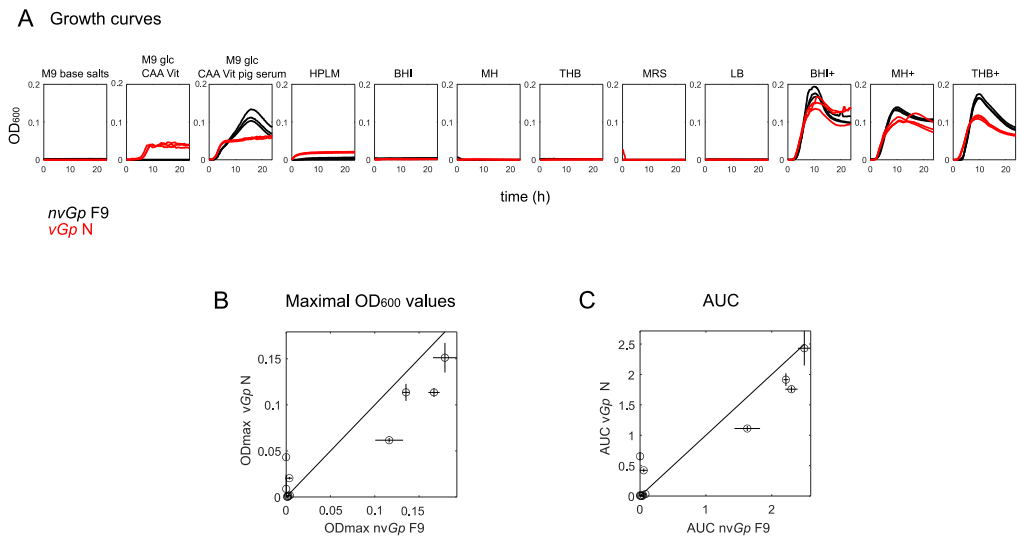

Figure 2.4. Over-time growth patterns of *Glaesserella parasuis* F9 and Nagasaki strains across various *in vitro* conditions. A) Growth curves of *G. parasuis* non-virulent F9 and virulent Nagasaki strains (nv*Gp* F9 and v*Gp* N respectively) in 12 of the conditions described in **Table 2.2**. Each line is a replicate culture. (maximal OD_{600} < 0.02). X-axis range (h): 0-24h. Y-axis range (OD_{600}): 0 to 0.6. **B)** Maximal OD_{600} value and **C)** Area-under-growth-curve (AUC) (normalized to the condition with maximal AUC for each strain) for the two *Glaesserella* strains, in which each circle represents one condition shown in panel **A**. Standard deviation (SD) is represented by horizontal/vertical lines (n=3).

PNC8 allowed the elucidation of a cooperative interaction between *G. parasuis*, *R. nasimurium* and *S. aureus*

As a proof-of-concept, to explore possible interactions within the PNC8 bacterial consortium, we performed a side-to-side experiment in which dotted suspensions of selected PNC8 members were inoculated in agar plates alone and next to the others. Thus, we evaluated the potential interaction between the two strains of *G. parasuis* (virulent Nagasaki and non-virulent F9) and three of the PNC8 strains **(Figure 2.5A)**. We cultured *G. parasuis* in BHI agar plates (which did not contain nicotinamide adenine dinucleotide, NAD^+) in close proximity to *S. pluranimalium* LG3-6, *S. aureus* EJ41-2 and *R. nasimurium* UK1-9, to assess if any of these strains could supply this essential factor for *G. parasuis* growth. When both *G. parasuis* strains were cultured next to *S. aureus* EJ41-2 and *R. nasimurium* UK1-9, a polarized growth towards these two bacteria was observed, showing a cooperative interaction between them, independently of their virulence. In contrast, *S. pluranimalium* LG3-6 did not show interaction with *G. parasuis*, as both strains (Nagasaki and F9) could not grow close to *S. pluranimalium*, similar to the observed when cultured alone (**Figure 2.5B**). As a growth control, we replicated the experiment in chocolate agar, showing that *G. parasuis* alone can grow in this condition and that none of the strain inhibited its growth, confirming that there is not a competitive interaction within these selected PNC8 strains (**Figure 2.5C**). Finally, we also assessed the possible interactions between *L. plantarum* KD9-5 and the same PNC8 members explained before (**Figure 2.5A**). Unlike for *G. parasuis*, we did not observe any interplay between *L. plantarum* KD9-5 and the other 3 PNC8 strains in the conditions tested (**Figure 2.5B** and **Figure 2.5C**).

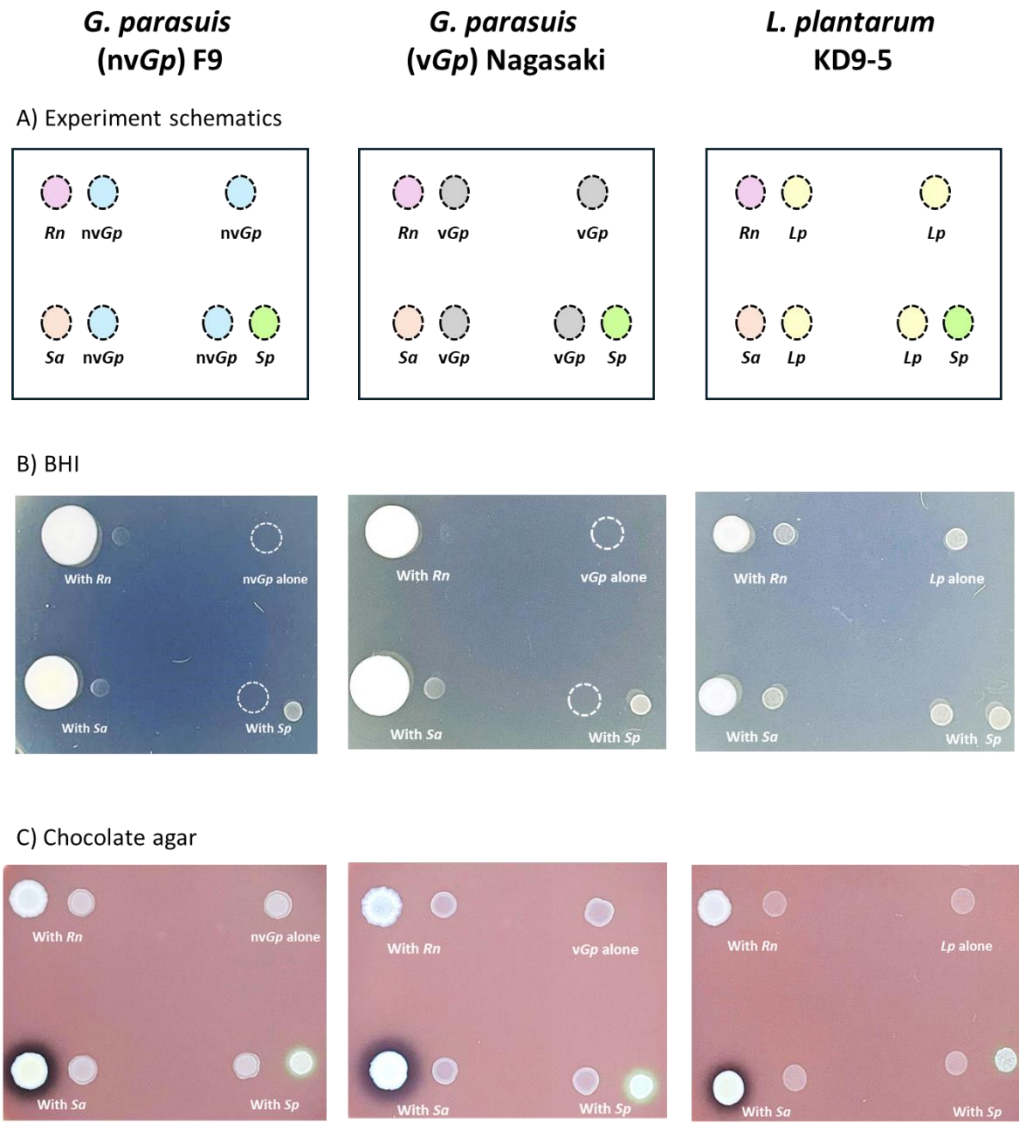

Figure 2.5. Side-by-side interaction experiment in agar plates with some PNC8 members. *Glaesserella parasuis* non-virulent (nv*Gp*, F9), virulent (v*Gp*, N) and *Lactobacillus plantarum* (*Lp*) growth are shown in the columns respectively. A) Schematics of the experiment: *Rothia nasimurium* in pink (*Rn*), *Staphylococcus aureus* in orange (*Sa*), *Streptococcus pluranimalium* in green (*Sp*), F9 in blue, N in grey and *Lp* in yellow. B) Experiment performed in BHI agar plates. C) Experiment performed in chocolate agar plates.

Discussion

In this study, we developed a synthetic nasal community, the Porcine Nasal Consortium (PNC8), to represent the nasal microbiota of piglets. PNC8 will allow the study of the interaction network of the nasal microbiota, which is a critical first hurdle

for respiratory pathogen invasion. The consortium consists of 8 strains representing the most prevalent and/or abundant genera found in the nasal microbiota of healthy piglets, covering a large fraction of the *in vivo* nasal composition, as described in previous studies (45,64,126). This low number of genera dominating the nasal microbiota of individual pigs is in agreement with some findings in the human nasal microbiota (284,285). Indeed, there is a high overlap between the genera selected for the PNC8 and the most abundant taxa in the human nasal microbiota, as *Moraxella*, *Staphylococcus*, *Neisseria* and *Streptococcus* were also identified among the 10 most abundant genera in the human nasal microbiota (285). Moreover, the consortium strains reflect the metabolic network complexity of the *in vivo* community, exhibiting substantial differences in their nutrient requirements, as indicated by the growth assays across various *in vitro* cultivation media. Our results suggest that the nasal microbiota is composed of diverse specialist microorganisms, which is in coherence with the fact that the nose is a poor-nutrient environment, and microorganisms need to find their own metabolic niche to survive (269).

Within this restrictive habitat that is the nasal passage, two different interaction patterns have been observed: cooperation and competition. Cooperation normally occurs between bacteria with different nutritional requirements. For instance, energy-rich fermentation products of one microorganism can be consumed by other. Competition, on the other hand, takes place when closely related bacteria need similar metabolites (269). Understanding the interactions within the nasal microbiota may provide opportunities for developing strategies against respiratory pathogens, as recently suggested (286). In fact, epidemiological studies in humans have shown a negative correlation between the nasal commensals *Corynebacterium spp.* and *D. pigrum*, and the pathogens methicillin-resistant *S. aureus* and *S. pneumoniae* (152,287). In humans, seminal work has demonstrated that pathogens could indeed be eliminated from the nasal passage by the introduction of commensal microbiota members (288). Similar negative interactions may occur in the porcine nasal microbiota and should be identified to leverage this knowledge for pathogen control. For example, a recent study showed that the inoculation with some members of the

swine nasal microbiota (*M. pluranimalium*, *Vagococcus lutrae*, *S. pluranimalium*, non-virulent *G. parasuis* and *R. nasimurium*) to piglets from farms with respiratory problems modulated the microbiota composition and diminished the presence of pathogenic strains of *G. parasuis*, reducing as well the number of animals with lameness (126). In relation to this, we performed an interaction experiment in two different conditions to assess the interplay within some PNC8 members, as a representation of the piglet nasal microbiota, as well as with a pathogenic strain of *G. parasuis*. Our results suggested a cooperation between both *R. nasimurium* and *S. aureus* strains with *G. parasuis*. Moreover, virulence did not affect this cooperation, as both non-virulent and virulent *G. parasuis* strains seemed to behave in the same way in the *in vitro* conditions tested. This cooperative interaction could be explained by the capacity of *S. aureus* to produce NAD^+ using the NAD^+ synthetase enzyme, as this factor is essential for *G. parasuis* growth (289,290). In fact, in some cases *G. parasuis* is cultured in blood agar near to a "nurse streak" of *S. aureus* which will provide the NAD^+ factor (291). We confirmed by sequencing that this *S. aureus* EJ41-2 strain had the NAD^+ synthetase enzyme in its genome. The same explication could be given to the *R. nasimurium* – *G. parasuis* interaction, since we also verified the presence of this enzyme in the UK1-9 genome. All these results correlate with previous human nasal studies, which showed that nasal commensals can interact between them and with pathogens, cooperating or competing in the nose (155,287,292,293). Further research to elucidate PNC8 interaction network must be conducted involving the host to examine if a similar effect may be happening.

Our study has some limitations. First, although the PNC8 consortium enables the systematic characterization of the main nasal microbiota members, and it covers not only the most *in vivo* abundant taxa, but also a large fraction of the metabolic pathways present within the piglet nasal microbiota, it cannot capture the full complexity of the nasal microbiota, as any synthetic microbial consortium. Future efforts may use complementary approaches, such as the *in vitro* cultivation of nasal microbial communities directly from swabs, as recently demonstrated for the gut microbiota (294), to corroborate the findings obtained with our synthetic

consortium. However, this approach faces the challenge of maintaining a representative environment and preserve the selection of one bacterium over the others. Second, as a proof-of-concept, we evaluated only few interactions within the members of the PNC8. This research line needs to be extended to a systematic study of interactions among all the members of the PNC8, not only in pairwise, but also including combination of three and more species in different *in vitro* conditions. It could allow us to elucidate the minimum number of PNC8 strains needed to stablish the nasal community, as well as to fully comprehend the type of interactions (positives or negatives) that can be found in this restrictive environment. In addition, further commensal-pathogen interactions need to be examined, such as with *S. suis*, *A. pleuropneumoniae, Mycoplasma spp.*, among others, as these bacteria are a major concern in pig farms (80,81,91,295). Moreover, other interaction assays such as spent media experiments, liquid co-culture or metabolomics could provide complementary information to better understand the microbial network interaction and the pathogens interplay. Another limitation is the lack of a realistic representation of the in *vivo* environment. One approach well applied in humans is the use of nasal secretions as a growth medium (296,297). Future efforts are needed to adapt to pigs the currently available human protocols to obtain these samples. Alternatively, it would be interesting to characterize the composition of piglet's nasal secretions to obtain an *in vitro* media that recapitulated the nasal environment. In addition, upcoming research may include the relationship between the bacteria and the host, as for example taking advantage of models such as explants, which are tissue segments maintained *in vitro*, or organoids, which are 3D *in vitro* cultures derived from self-organizing stem cells. Both approaches mimic the physiological conditions in an *in vivo*-like environment. In conclusion, in this work we developed and characterized the synthetic community PNC8, a new resource for studying the nasal microbiota under experimental *in vitro* conditions. PNC8 represents a convenient tool to explore the interaction network of the pig nasal microbiota and its role in pathogen exclusion. These studies could serve as a stepping stone to study

alternatives to antibiotic, such as microbiota interventions to promote a healthy microbiota, aiming to reinforce the protective role of the nasal microbiota.

Chapter 3

Porcine Nasal Organoids (PNOs) to model interactions between the swine nasal microbiota and the host

Chapter published in:

Laura Bonillo-Lopez*, Noelia Carmona-Vicente*, Ferran Tarrés-Freixas, Karl Kochanowski, Jorge Martínez, Mònica Perez, Marina Sibila, Florencia Correa-Fiz, Virginia Aragon. **Porcine Nasal Organoids as a model to study the interactions between the swine nasal microbiota and the host.** 2025, accepted in Microbiome. Pre-print available at bioRxiv. doi: 10.1101/2024.08.13.606910

* Equally contributing first authors.

Abstract

Interactions between the nasal epithelium, commensal nasal microbiota, and respiratory pathogens play a key role in respiratory infections. Currently there is a lack of experimental models to study such interactions under defined *in vitro* conditions. Here, we developed a Porcine Nasal Organoid (PNO) system from nasal tissue of pigs as well as from cytological brushes. PNOs exhibited similar structure and cell types than the nasal mucosa, as evaluated by immunostaining. PNOs were inoculated with porcine commensal strains of *Moraxella pluranimalium, Rothia nasimurium* and the pathobiont *Glaesserella parasuis* for examining host-commensal-pathogen interactions. All strains adhered to the PNOs, although at different levels. *M. pluranimalium* and *G. parasuis* strains stimulated the production of proinflammatory cytokines, whereas *R. nasimurium* induced the production of IFNγ and diminished the proinflammatory effect of the other strains. Overall, PNOs mimic the *in vivo* nasal mucosa and can be useful to perform host-microbe interaction studies.

Introduction

The nasal epithelium is the first barrier in direct contact with the external environment providing protection from viral, bacterial, and fungal pathogens, as well as pollutants in the air (40,298). This tissue is responsible for mucociliary clearance and, together with the nasal microbiota, acts as a physical, chemical, and immunological defence to preserve the homeostasis of the nasal cavity and limit the invasion of microorganisms (31,41,176,292,299–302). It is also considered an integral part of the innate immune system as it produces antimicrobial agents, danger-associated molecular patterns (DAMPs) and recognize pathogens via pattern recognition receptors (PRRs) (299). Integrity alteration of the nose epithelium has been related to inflammation with severe consequences for animal health (39,176,299).

Traditionally, models to study basic and clinical aspects of the airway pathophysiology have been cells and explants from nose, trachea, or bronchia. These models were either hard to maintain *in vitro* (like primary cells and explants) or not physiologically relevant enough (like immortalised cell lines) (303–307). The recent emergence of both human and animal organoids are promising systems to model the respiratory epithelium and study immunological parameters or host-pathogen interactions. To date, airway organoids established in humans (190,195,196) as well as in some animal species (203,308,309) have shown to represent a robust system for airway modelling, since they retain the *in vivo* architecture of the nasal epithelium forming a complex pseudostratified epithelium with most of the cell types from the original tissue (ciliated, mucus-secreting goblet, basal and club cells) (40,298). To our knowledge, only lung organoids have been set up for the porcine respiratory tract (308). Despite the burden of respiratory diseases for the porcine sector, there is no nasal organoid model currently available for pigs, which would enable experiments under defined *in vivo*-like conditions. Moreover, cross-species transmission from pigs to humans are continuously posing a major challenge to public health and this model could be extended to investigate the potential transmission of many zoonotic

pathogens, using pigs as asymptomatic carriers, to humans preventing outbreaks of disease in both host species.

To tackle this issue, we have successfully established and characterized the first Porcine Nasal Organoids (PNOs) cultures and used this model to study the interactions with the host and between members of the nasal microbiota. Understanding the interplay between the host with its microbiota, and the pathogens will facilitate the design of preventative and therapeutic interventions to promote respiratory health.

Results

Generation and characterization of Porcine Nasal Organoids (PNOs)

Several lines of PNOs were established from nasal turbinates by isolation of the cells and embedding in Matrigel (basement membrane matrix), adapting published protocols for human and swine tissues (195,203,310). After 7-10 days in culture, PNOs were formed showing the typical cystic shape with visible lumen, showing the cellular types normally found in the nasal mucosa (**Figure 3.1A and 3.1B**). Moreover, beating cilia were observed inside the lumen (**Annex 3.1**) under light microscopy. PNO cultures were treated with 1% penicillin-streptomycin and 10 µg/ml of primocin to avoid bacterial growth, but they were positive for *Mycoplasma spp.* Since *M. hyorhinis* can be found in the nasal cavity of pigs, we performed a specific PCR for this pathogen and confirmed that the PNOs were positive to this species.

To verify if the generated organoids recapitulated the histology of the nasal mucosa, organoids were expanded, differentiated, and characterized. Thus, PNOs from non-differentiated 3D cultures were seeded as monolayers (2D cultures) with the apical side exposed, cultured for 1 week and differentiated for one more week (**Figure 3.1C**). PNOs were also established from nasal samples taken with cytology brushes yielding comparable PNOs. The only difference noted was that they required more time to form 3D PNO structures, specifically 2 to 3 weeks after initial adaptation to the growth medium. Early passages from non-differentiated 3D PNOs were frozen

to keep a stock of the different PNO cultures and maintained viability after at least 3 freeze-thaw cycles.

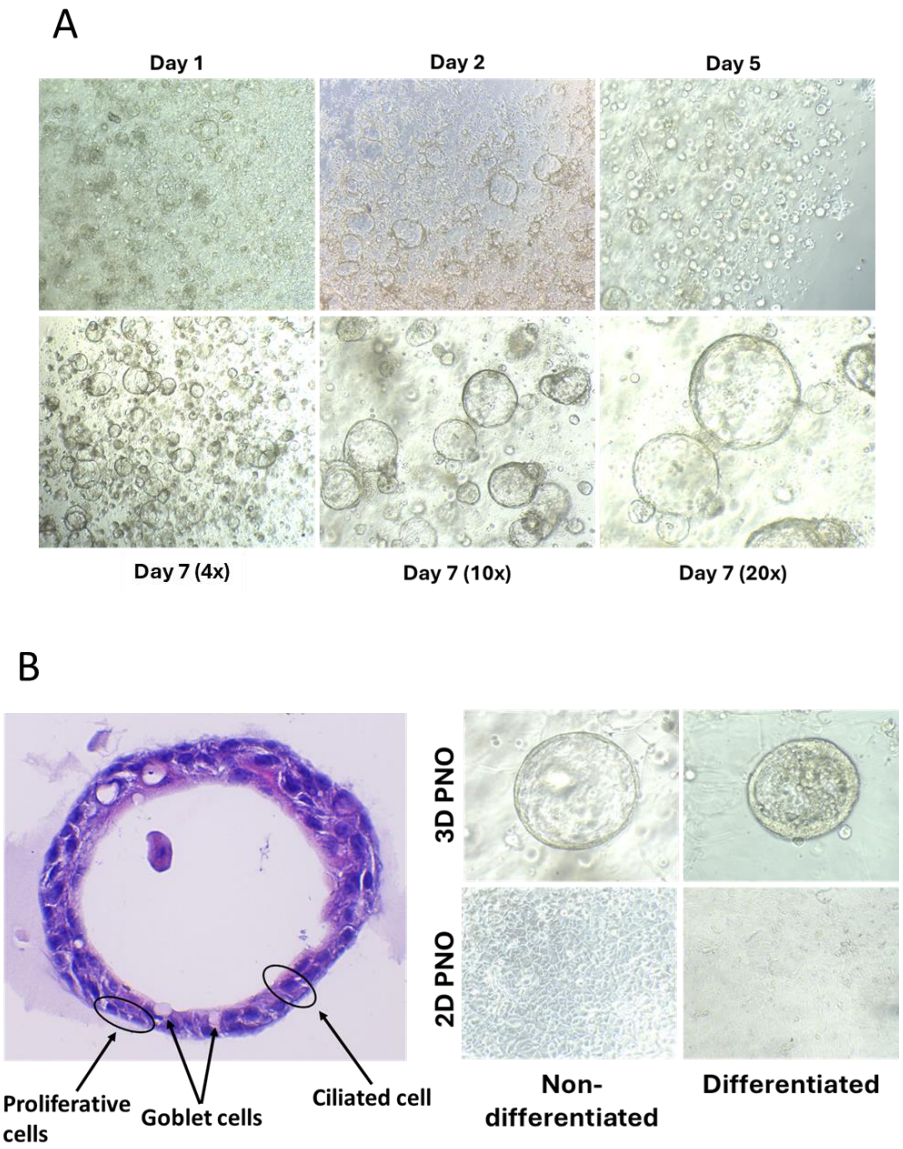

Figure 3.1. Establishment of porcine nasal organoids (PNOs) from nasal turbinates. A) Representative images of PNOs morphology at different time points by bright field microscopy at 4x, 10x and 20x magnification, respectively. B) Haematoxylin and eosin (H&E) staining of 3D paraffin-embedding PNOs in which proliferative, goblet and ciliated cells are marked with arrows. C) Comparison between differentiated and non-differentiated 3D PNOs (top) and monolayers (bottom).

To evaluate whether 3D and/or 2D PNO cultures maintained and mimicked the characteristics and the organization of the nasal respiratory epithelium, as well as the response to differentiative stimuli, the expression of several cell markers was analysed at different time points by reverse transcription polymerase chain reaction (RT-PCR) and immunofluorescent assays (IFA). Similar to nasal turbinates from pigs, 3D PNOs and 2D non-differentiated and 2D differentiated PNOs expressed the markers for club cells (*scgb1a1*), goblet cells (*muc5ac*), basal cells (*tp63*), ciliated cells (*foxj1*) and tight junctions (*zo-1*). An increase in the expression of *muc5ac*, *zo-1* and *foxj1* genes was observed in organoids that underwent a longer period of differentiation (**Figure 3.2**).

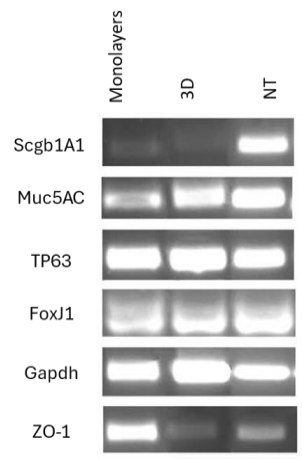

Figure 3.2. RT-PCR of nasal epithelial cell marker genes expressed on porcine nasal organoids (PNOs). In monolayers, 3D organoids and nasal turbinate (NT) as a positive control for club cells (*scgb1a1*), goblet cells (*muc5ac*), basal cells (*tp63*), ciliated cells (*foxj1*), housekeeping gene (*gapdh*) and tight junctions (*zo-1*).

Gene expression of the cellular markers was confirmed by immunostaining, showing that both 3D and 2D PNO cultures did cover all major airway epithelial cell types, including proliferative cells (Ki67+), goblet cells (Muc5AC+) and ciliated cells (AceαTub+, FOXJ1+), and exhibited an *in-vivo* like stratification, as illustrated by the increased expression and organized localization of ZO-1 protein (**Figure 3.3**). Few Ki67 positive cells were detected while acetylated α-tubulin appeared highly expressed in the differentiated cultures. Goblet cells were also detected.

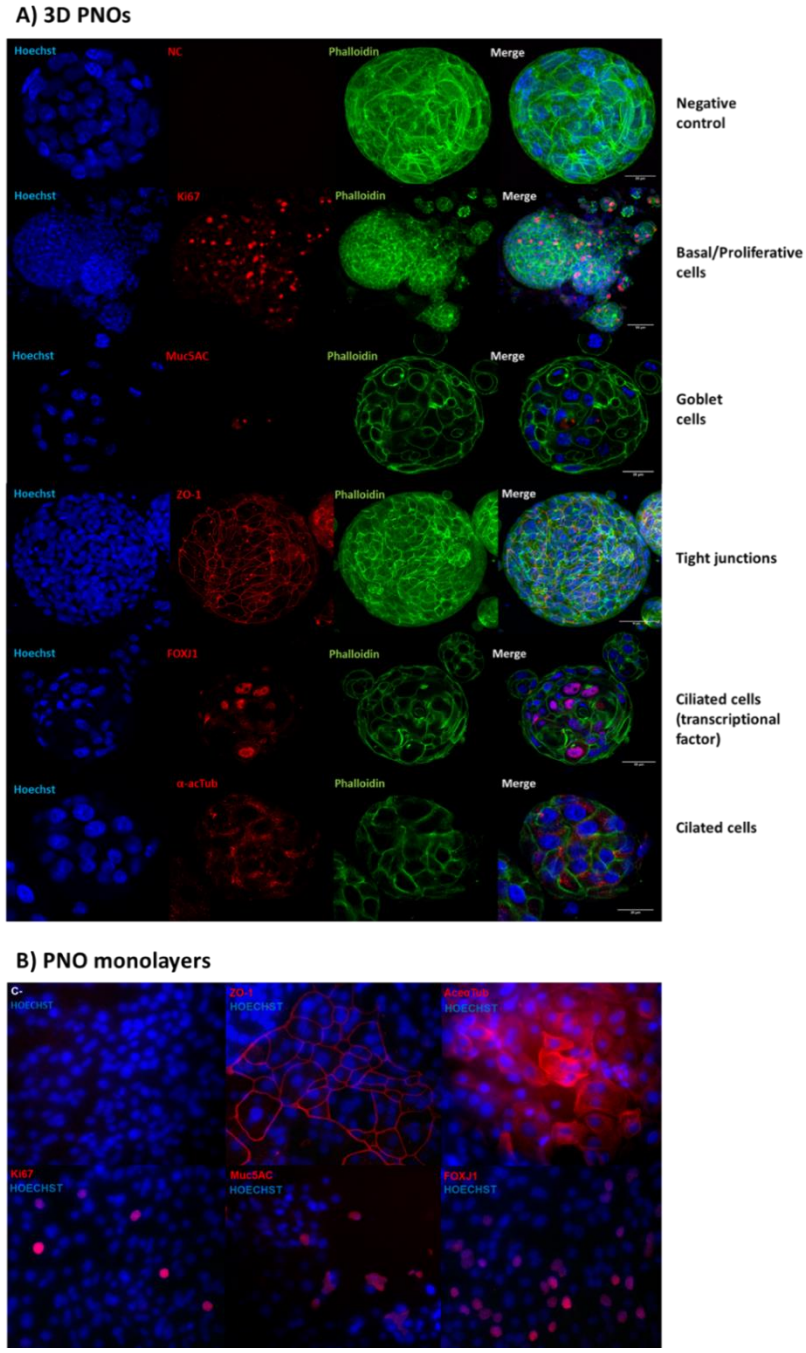

Figure 3.3. Cell marker analysis expressed on porcine nasal organoid (PNO) surface by immunofluorescent assay (IFA). A) Cell marker expression in PFA-fixed differentiated 3D PNOs and B) PFA-fixed differentiated monolayers by IFA. ZO-1 protein (tight junctions) highlighted the tightness of the epithelial monolayer. Few proliferative Ki67 positive cells were detected indicating a mature epithelium. Muc5AC (goblet cells) and airway-specific markers acetylated α-tubulin (AceαTub) and FOXJ1 (ciliated cells) were expressed at high levels. All markers were detected in red. Nuclei were counterstained with Hoechst 33342 (blue). In the 3D PNO, IFA phalloidin (green) was also added to the incubation with the secondary antibody.

Taken together, these results suggest that the generated PNO cultures recapitulate the nasal pseudostratified airway epithelium, retaining *in vivo* morphological and functional characteristics as shown in the immunohistochemistry assay (IHC) of the nasal turbinate (**Figure 3.4**).

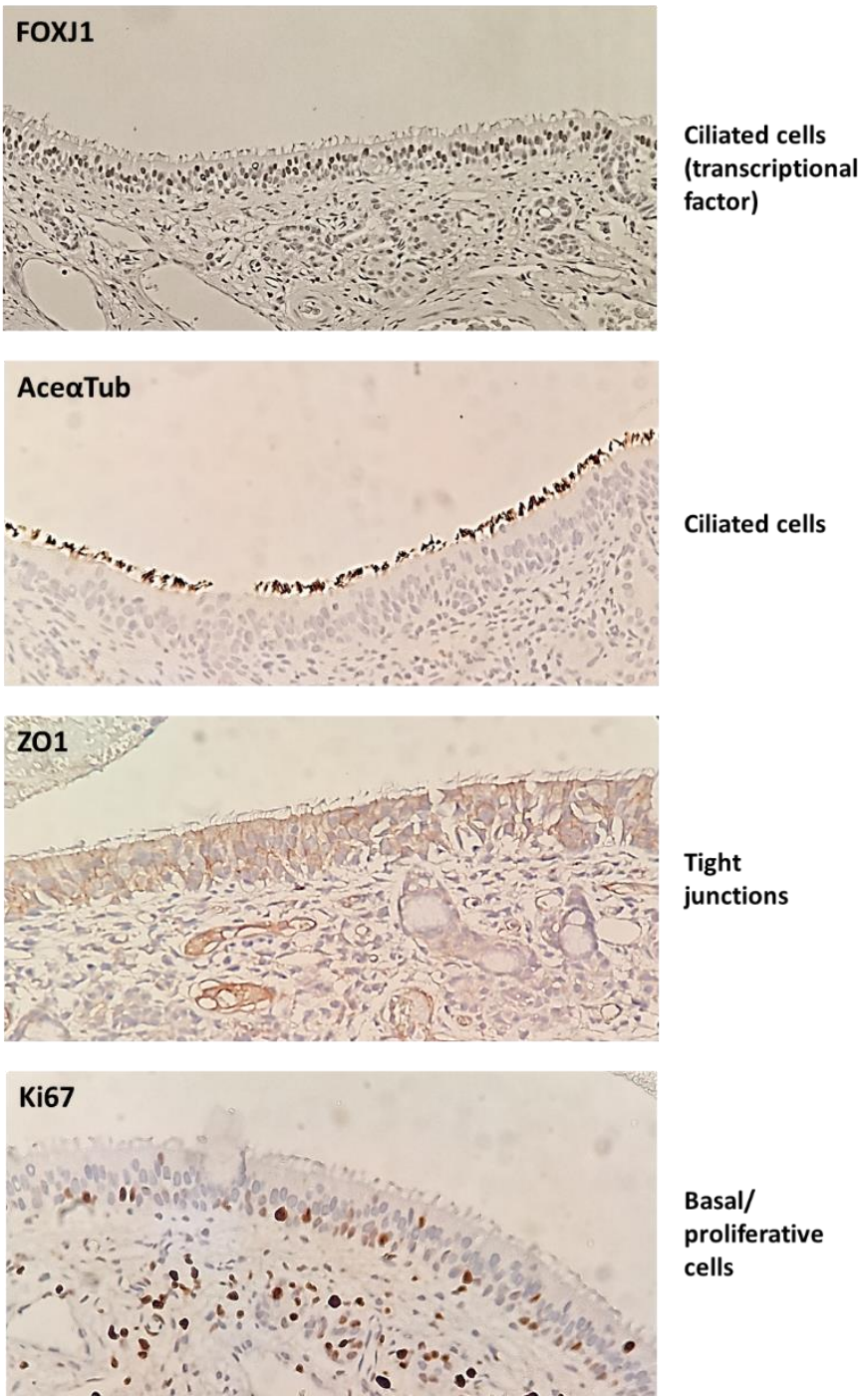

Figure 3.4. Characterization and cell marker expression in paraffin-embedded nasal turbinate from pigs by immunohistochemistry (IHC). Nasal turbinate tissue was used for IHC staining. Antibodies against FOXJ1 (transcriptional factor of ciliated cells), acetylated α-tubulin (ciliated cells), ZO-1 (tight junctions) and Ki67 (proliferative cells) were used to visualize the different cells markers expressed on the nasal airway epithelium from pigs. Images (40x) are representative of at least five similar images.

Nasal microbiota members were able to colonize PNO monolayers maintaining monolayer integrity

The colonization of the host mucosal surfaces by the microbiota is fundamental in host homeostasis. To evaluate the nasal colonization with the organoid model, we selected some bacterial isolates commonly found in the nasal cavity of pigs (126,311). We used two prevalent and abundant members of the nasal microbiota: *Moraxella pluranimalium* (*Mp*) and *Glaesserella parasuis* (*Gp*). From the latter, we included two strains with different virulence capacities (non-virulent, nv*Gp*; and virulent, v*Gp*). Finally, *Rothia nasimurium* (*Rn*) was also inoculated to PNOs as a prevalent but not abundant member of the nasal microbiota. The colonization capacity was assessed through the evaluation of bacteria attachment to the organoids after o/n incubation. As a control, we also incubated the monolayers with all these strains for 2 h to analyse their adhesion capacity. All individual strains were able to adhere and colonize the nasal organoids and were also recovered from the culture supernatants after o/n incubation (**Figure 3.5**).

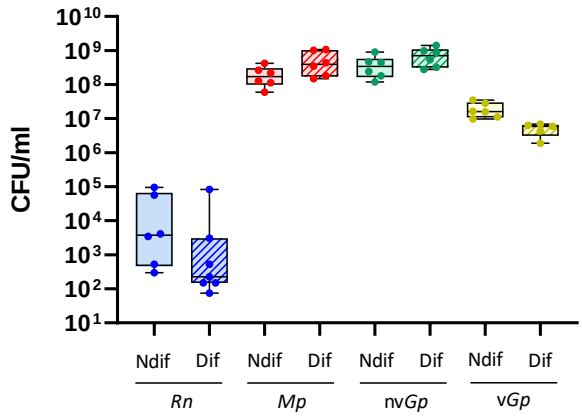

Figure 3.5. Bacteria found in the supernatant of non-differentiated and differentiated Porcine Nasal Organoids (PNOs) after o/n incubation. Non-differentiated (Ndif, plain pattern) and differentiated (Dif, stripped pattern) PNOs were o/n incubated with approximately 10^4-10^5 CFU/ml of *R. nasimurium* (*Rn*, in blue), 10^3 CFU/ml of *M. pluranimalium* (*Mp*, in red), 10^3 CFU/ml of non-virulent *G. parasuis* (nv*Gp*, in green) or 10^5-10^6 CFU/ml of virulent *G. parasuis* (v*Gp*, in yellow). After incubation, bacteria present in the supernatant were quantified by dilutions and plating. Each dot represents a replicate from three different experiments of PNOs coming from two animals. Two replicates were included in each experiment.

Rn adhered (2h) to both non-differentiated and differentiated PNOs (**Figure 3.6**). This association occurred during the first hours of incubation and did not increase in time, while *Mp* and both nv*Gp* and v*Gp* strains colonized the PNOs in a time dependent manner in both non-differentiated and differentiated PNOs (**Figure 3.6**). For nv*Gp* and v*Gp* strains, adhesion at 2h was higher on differentiated than non-differentiated PNOs. Although no differences in adhesion were detected among the strains, o/n colonization by Rn was less efficient than the colonization by the other strains (**Figure 3.6**), probably related to the lower capacity of this strain to grow in the conditions of the assay, as reflected by the lower number of bacteria recovered from the supernatant (**Figure 3.5**).

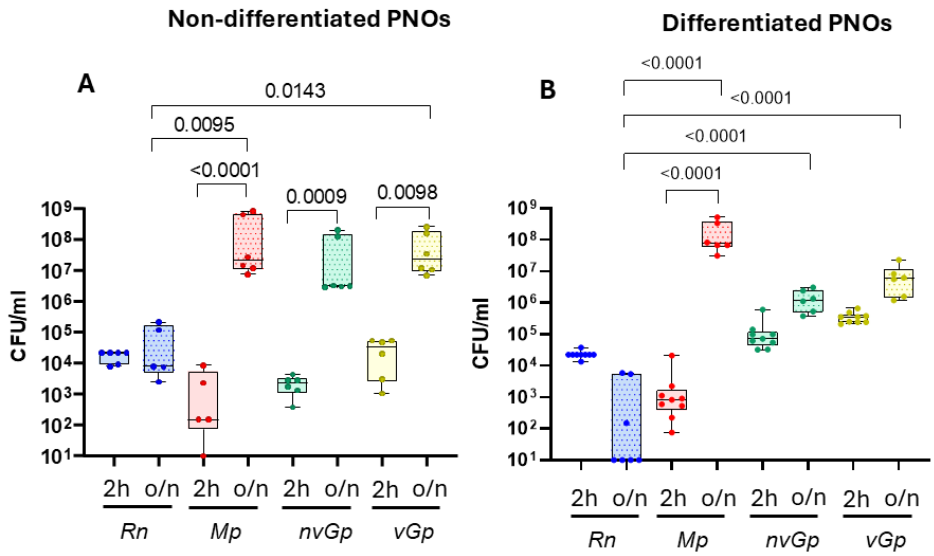

Figure 3.6. Quantity of bacteria associated with Porcine Nasal Organoids (PNOs) after 2h (adhesion) and o/n (colonization) incubation. PNOs coming from two animals were incubated with approximately 10^5 CFU/ml of *R. nasimurium* (*Rn*, in blue), 10^3 CFU/ml of *M. pluranimalium* (*Mp*, in red), 10^3 CFU/ml of non-virulent *G. parasuis* (nv*Gp*, in green) or 10^6 CFU/ml of virulent *G. parasuis* (v*Gp*, in yellow) for 2 h to assess the bacterial adhesion capacity (plain pattern) or o/n to evaluate the colonization (dotted pattern). After incubation, non-attached bacteria were eliminated by washing, and attached bacteria were quantified by dilutions and plating after lysis of the cells with saponin. Three independent experiments were performed with duplicate wells and each dot in the plot represents individual well results. A) Non-differentiated PNOs, B) Differentiated PNOs. Significant differences are shown with the associated *P* values using Kruskal-Wallis multiple comparison with Benjamini, Krieger and Yekutieli post-hoc test.

Finally, the similar level of expression of the different marker genes in differentiated PNOs, together with morphology observation, indicated that the commensal bacterial inoculation did not affect the monolayer integrity (**Figure 3.7**).

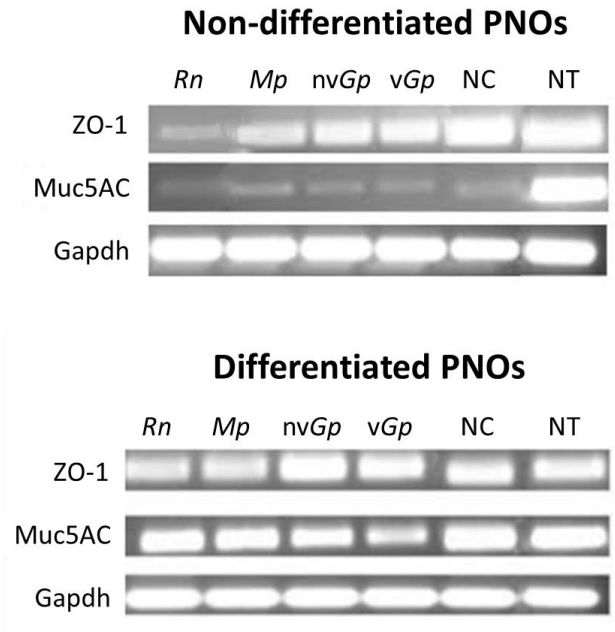

Figure 3.7. Reverse transcription polymerase chain reaction (RT-PCR) of nasal epithelial cell marker genes expressed on porcine nasal organoids (PNOs) after 2 h of bacterial incubation. Presence of mucus (Muc5A gene, (indicating mucus secretion by goblet cells) and ZO-1 gene (tight junctions) after 2 h of incubation with *Rothia nasimurium* (*Rn*), *Moraxella pluranimalium* (*Mp*), *Glaesserella parasuis* non-virulent (nv*Gp*) and virulent (v*Gp*) strains in non-differentiated and differentiated PNOs, respectively. NC represents negative control, consisting in PNOs without bacteria, and NT represents the positive control, nasal turbinate.

PNOs enabled to evaluate interactions within the nasal microbiome and a respiratory pathogen

Rothia has recently received attention for its role in host health and interaction with other members of the microbiota (312). To explore if the PNO model can be useful for elucidating interactions between nasal microbiota members, differentiated PNOs were inoculated with combinations of the commensal *Rn* and the other bacteria under study. The colonization of *Mp*, nv*Gp* and v*Gp* was not affected by the

presence of Rn in the co-culture (**Figure 3.8A**) and likewise, *Rn* colonization was not affected by the presence of any of the other strains (**Figure 3.8B**).

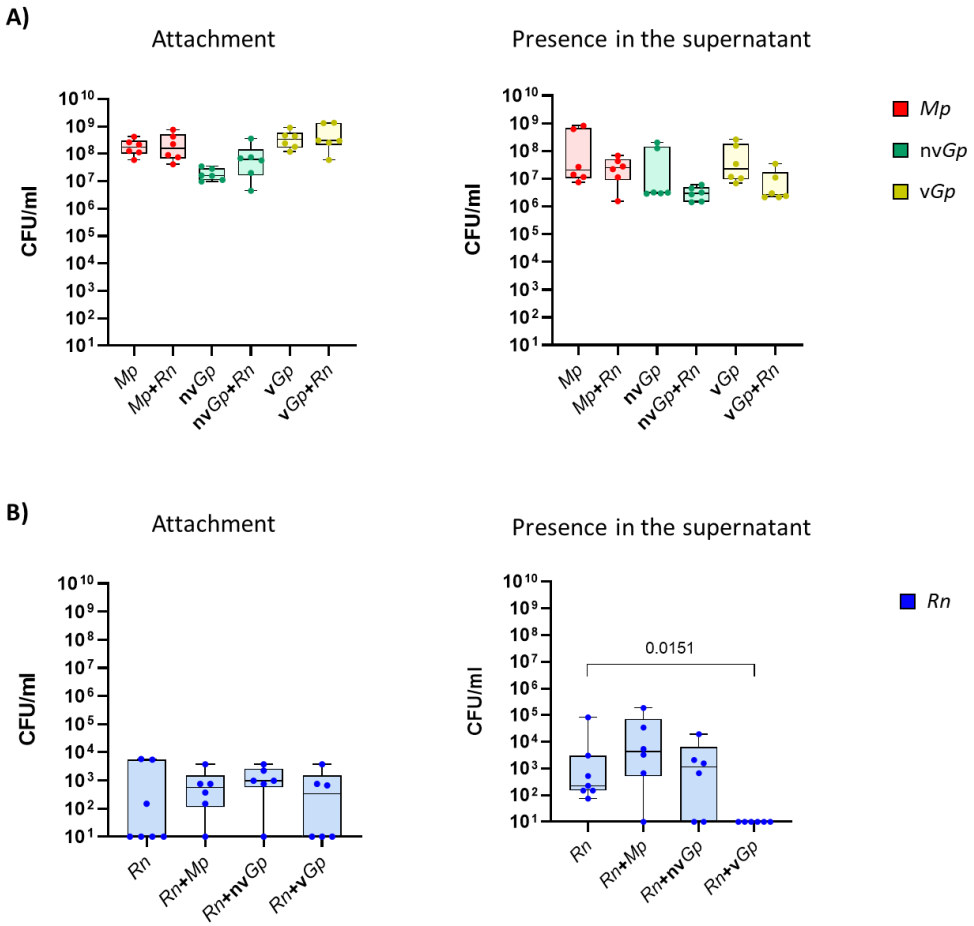

Figure 3.8. Bacterial colonization on differentiated Porcine Nasal Organoids (PNOs). PNOs were incubated o/n with approximately 10^3 CFU/ml of *Mp*, 10^3 CFU/ml of nv*Gp* or with 10^6 CFU/ml of v*Gp* individually or in combination with 10^5 CFU/ml of *Rn* and colonization capacity (attachment) and presence in the supernatant were quantified by dilutions and plating. A) Co-culture of *Moraxella pluranimalium* (*Mp*, red), *Glaesserella parasuis* non-virulent (nv*Gp*, green) and virulent (v*Gp*, yellow) strains with *Rothia nasimurium* (*Rn*, blue) in the PNOs. B) Co-culture of *Rn* with *Mp*, nv*Gp* and v*Gp* in the PNOs. Each dot represents a replicate from three different experiments of PNOs coming from two animals. Two replicates were included in each experiment. Kruskal-Wallis multiple comparison with Benjamini, Krieger and Yekutieli post-hoc test was used to compare the bacterial concentrations. Significant difference is shown with the associated *P* value.

Adhesion at 2 h of either *Mp* or nv*Gp* in co-culture with *Rn* was not affected (**Figure 3.9A**). However, a small reduction in the adhesion of v*Gp* was observed when co-cultured with Rn (**Figure 3.9A**), which was accompanied by a reduction in the recovery of Rn from the supernatant ($P = 0.0151$; **Figure 3.8B**), and this could not be explained by competition of the strains in the culture media alone (**Figure 3.10**). *Rn* adhesion at 2h was not affected by any of the strains (**see Figure 3.9B**).

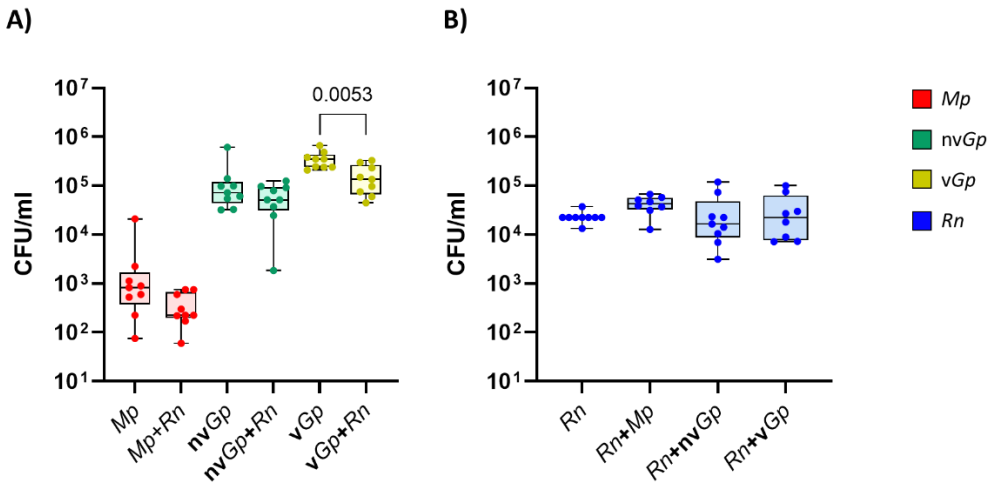

Figure 3.9. Bacterial adhesion after 2 h of incubation in differentiated Porcine Nasal Organoids (PNOs). PNOs were incubated for 2 h with approximately 10^3 CFU/ml of *Mp*, 10^3 CFU/ml of non-virulent nv*Gp*, 10^6 CFU/ml of virulent v*Gp* and with 10^5 CFU/ml of Rn. Adherent bacteria were quantified (CFU/ml) after eliminating non-attached ones by washing. A) Adhesion of *Moraxella pluranimalium* (*Mp*, red) and *Glaesserella parasuis* non-virulent (nv*Gp*, green) and virulent (v*Gp*, yellow) strains co-cultured with *Rothia nasimurium* (*Rn*) in PNOs. B) Adhesion of *Rn* (blue) co-cultured with *Mp*, nv*Gp* and v*Gp* in PNOs. Each dot represents a replicate from three different experiments of PNOs coming from two animals. Two replicates were included in each experiment. Significant difference is shown with the associated *P* value using Welch's t test.

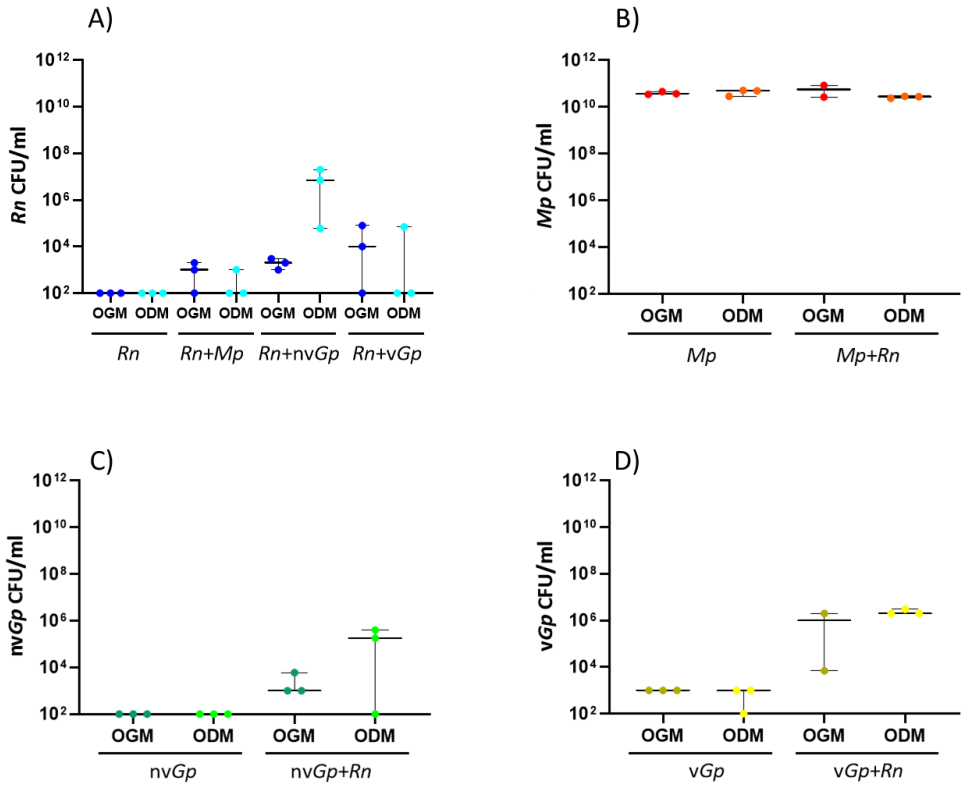

Figure 3.10. o/n co-culture of bacterial strains in fresh organoid media. Bacterial growth (CFU/ml) after o/n incubation in fresh Organoid Growth Medium (OGM) and fresh Organoid Differentiation Medium (ODM). A) *Rothia nasimurium* (*Rn*) individually grown as well as in co-culture with *Moraxella pluranimalium* (*Mp*, *Rn*+*Mp*), non-virulent *Glaesserella parasuis* strain (nv*Gp*, *Rn*+nv*Gp*) and virulent *G. parasuis* strain (vGp, *Rn*+v*Gp*) in OGM (dark blue) and ODM (turquoise). B) *Mp* individually grown and in co-culture with *Rn* (*Mp*+*Rn*) in OGM (red) and ODM (orange). C) nv*Gp* individually grown and in co-culture with *Rn* (nv*Gp*+*Rn*) in OGM (dark green) and ODM (light green). D) v*Gp* individually grown and in co-culture with *Rn* (v*Gp*+*Rn*) in OGM (dark yellow), ODM (light yellow).

Minor differences in colonization patterns were observed in non-differentiated PNOs. A reduction of *Rn* colonization was observed when co-cultured with both nv*Gp* and v*Gp* strains (P = 0.0410 and P = 0.0009 respectively, **Figure 3.11A**), but the adhesion at 2h was not affected (**Figure 3.11C**). In the supernatants from the co-cultures, a reduction in the number of *Rn* was observed when co-cultured with the v*Gp* strain (P = 0.0055), but not with the nv*Gp*, similarly to what was observed with differentiated PNOs (**Figure 3.11B**).

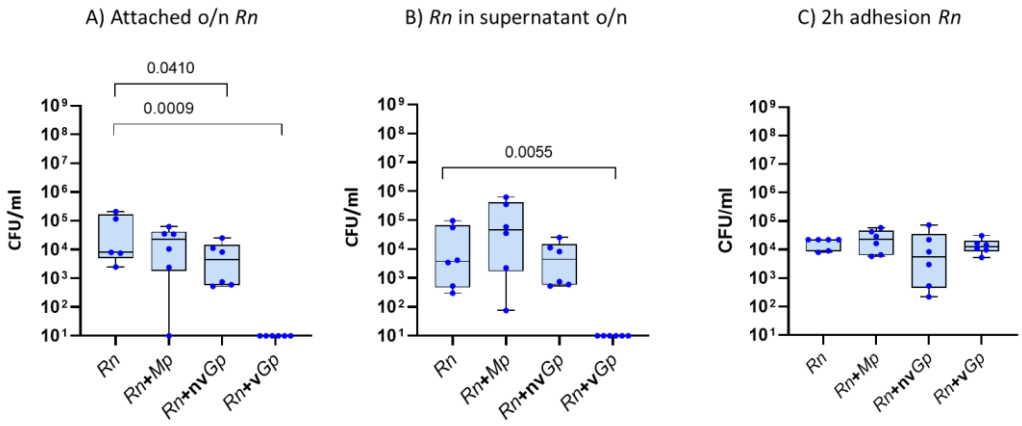

Figure 3.11. *Rothia nasimurium* load in non-differentiated porcine nasal organoids (PNOs) individually or in co-culture with selected strains. PNOs were inoculated with 10^4 CFU/ml of *Rn* alone or in combination with approximately 10^3 CFU/ml of *Moraxella pluranimalium* (*Mp*), 10^3 CFU/ml of non-virulent *Glaesserella parasuis* (nv*Gp*) or with 10^5 CFU/ml of virulent *G. parasuis* (v*Gp*). A) *R. nasimurium* (*Rn*) attachment after o/n incubation. B) *Rn* found in the supernatant after o/n incubation. C) *Rn* adhesion after 2 h of incubation. Three independent experiments were performed with duplicate wells and each dot in the plot represents individual well results. Kruskal-Wallis multiple comparison with Benjamini, Krieger and Yekutieli post-hoc test was used to compare the bacterial concentrations. Significant differences are shown with the associated *P* value.

Considering that the initial *Rn* inoculum was 10^5 CFU/ml, *Rn* did not grow in the conditions used for PNO culture. In fact, when *Rn* was grown as control in fresh Organoid Growth Medium (OGM) and Organoid Differentiation Medium (ODM) without PNOs, no colonies were recovered after o/n incubation (**Figure 3.10A**). However, when co-culturing *Rn* with *Mp* either nv*Gp* or v*Gp* strains, the quantity of Rn recovered after incubation was similar to the inoculum used (**Figure 3.10A**). By contrast, no differences between individual growth and growth with Rn in co-culture were observed in *Mp* when inoculated in fresh OGM and ODM (**Figure 3.10B**), as this bacterium could grow in the same way in all conditions tested. Interestingly, when inoculating ~10^3 CFU/ml of n*vG*, no growth was detected in single culture in fresh OGM or ODM but reached to approximately 10^4 and 10^5 CFU/ml when co-cultured o/n with *Rn* in OGM and ODM respectively, indicating a metabolic cooperation between these strains (**Figure 3.10C**). Similar results were observed with v*Gp*, as it reached a higher concentration of bacteria when co-cultured with Rn in the absence of PNOs (**Figure 3.10D**). Overall, these results indicate that the PNOs are providing a

substrate for *Rn*'s growth, but also that v*Gp* outcompetes *Rn* in these conditions. By contrast, it seemed to be a cooperation between nv*Gp* and *Rn*. Similar to differentiated PNOs, colonization of non-differentiated PNOs by *Mp* and either nv*Gp* or v*Gp* strains was not affected by the presence of Rn (**Figure 3.12A** and **3.12B**). However, *Rn* reduced the initial adhesion of nv*Gp* (2 h of incubation) in the non-differentiated PNOs (*P* = 0.0189, **Figure 3.12C**).

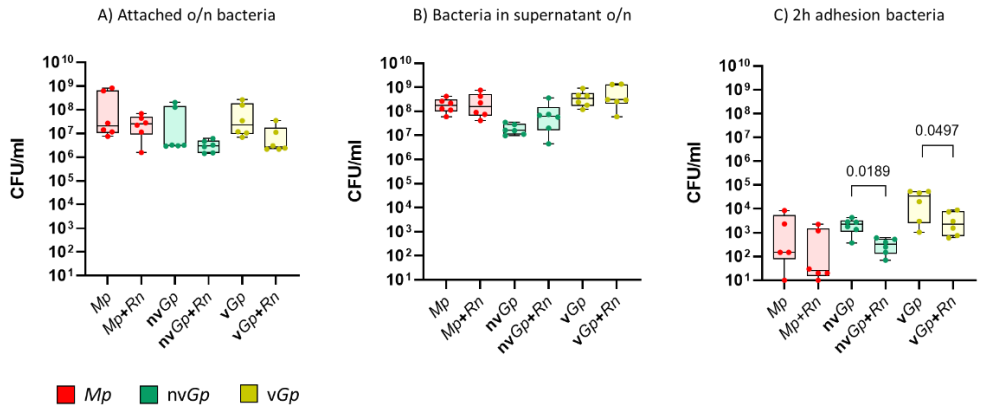

Figure 3.12. *Moraxella pluranimalium* and *Glaesserella parasuis* strains load in non-differentiated porcine nasal organoids (PNOs) individually or in co-culture with *Rothia nasimurium*. PNOs were inoculated with 10^3 CFU/ml of *Moraxella pluranimalium* (*Mp*), 10^3 CFU/ml of non-virulent *Glaesserella parasuis* (nv*Gp*) or with 10^5 CFU/ml of virulent *G. parasuis* (v*Gp*) alone or in combination with 10^4 CFU/ml of *Rn*. A) *M. pluranimalium* (*Mp*, red), non-virulent *G. parasuis* (nv*Gp*, green) and virulent *G. parasuis* (v*Gp*, yellow) attachment after o/n incubation. B) *Mp*, nv*Gp* and v*Gp* found in the supernatant after o/n incubation. C) *Mp*, nv*Gp* and v*Gp* adhesion after 2 h of incubation. Three independent experiments were performed with duplicate wells and each dot in the plot represents individual well results. Kruskal-Wallis multiple comparison with Benjamini, Krieger and Yekutieli post-hoc test was used to compare the bacterial concentrations. Significant differences are shown with the associated *P* value.

R. nasimurium modulated cytokine secretion by PNOs and had an anti-inflammatory role

The results described above indicated that, contrary with the reported interaction described for *Rothia mucilaginosa* and *Moraxella catarrhalis* (153), *Rn* did not have a major direct impact on other microbiota members (i. e. by altering their abundance).

To explore a possible interaction through immunomodulation, we quantified cytokine release by PNOs in presence/absence of *Rn* and the other members of the nasal microbiota. For that, multiple cytokines (interferon alpha, IFNα; interleukin 1 beta, IL-1β; interleukin 4, IL-4; interleukin 10, IL-10; interleukin 17A, IL-17A, interleukin 8, IL-8 (CXCL8); interleukin 12, IL-12; interleukin 6, IL-6, tumour necrosis alpha, TNFα; and interferon gamma, IFNγ) associated with inflammation and colonization were assessed. In general, two different patterns were detected in the stimulation by the individual strains of the differentiated PNOs. The first one produced by *Rn* and characterized by the induction of IFNγ (**Figure 3.12A**). The second one, the stimulation by the rest of the strains, characterized by a proinflammatory pattern with induction of IL-8, IL-12 and TNFα (**Figure 3.12B, 3.12C and 3.12D** respectively). Interestingly, the pro-inflammatory effect produced by *Mp* and both nv*Gp* and v*Gp* was abolished by co-incubation with *Rn* (**Figure 3.12**), despite the low numbers of *Rn* in the co-cultures (~10^3 CFU/ml) in comparison to the high abundance of nv*Gp* and v*Gp* (107 CFU/ml for both strains) and *Mp* (10^8 CFU/ml). On the contrary, the stimulation of IFNγ by *Rn* was not affected by incubation with the other two commensal strains (*Mp* and nv*Gp*), but it was abolished by the pathogenic one, the v*Gp* strain (**Figure 3.12A**).

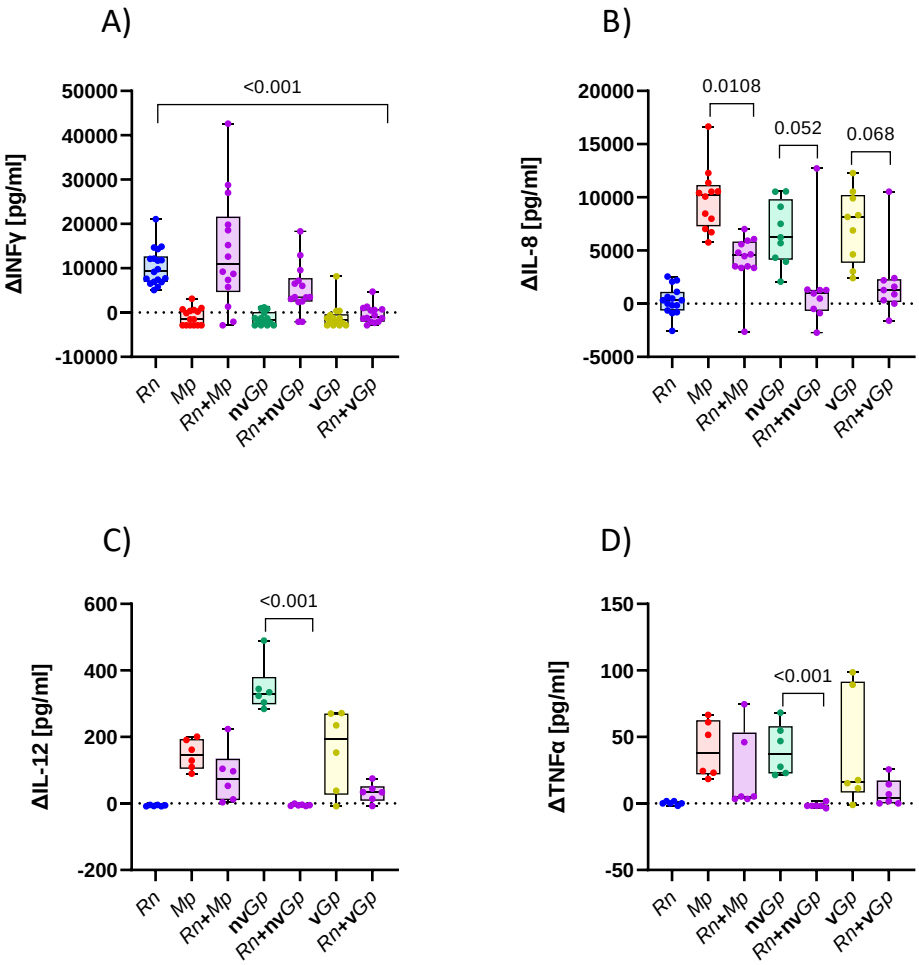

Figure 3.12. Cytokine concentrations secreted by the differentiated Porcine Nasal Organoids (PNOs) when stimulated with the bacteria. Differentiated PNOs were incubated with 10^5 CFU/ml of *R. nasimurium* (*Rn*), 10^3 CFU/ml of *Moraxella pluranimalium* (*Mp*), 10^3 CFU/ml of non-virulent *Glaesserella parasuis* (nv*Gp*) or with 10^6 CFU/ml of virulent *G. parasuis* (v*Gp*) individually or in combinations. After o/n incubation supernatants were recovered for cytokine quantification. Results are shown as the delta of each interleukin and cytokine, subtracting the negative control (PNOs without inoculation, basal levels of the secretion) in pg/ml. A) Secretion of interleukin 8 (IL-8), B) Secretion of interleukin 12 (IL-12), C) Secretion of Tumor Necrosis Factor alpha (TNFα) and D) Secretion of Interferon gamma (IFNγ). Each dot represents a replicate from three different experiments of PNOs coming from two animals. Two replicates were included in each experiment. Kruskal-Wallis multiple comparison with Benjamini, Krieger and Yekutieli post-hoc test was used to analyze the data. Significant differences are shown as horizontal lines with the associated *P* value.

Similar results in the expression of cytokines were obtained with non-differentiated PNOs (**Figure 3.13**), with the addition of the ability of secrete IL-6 (**Figure 3.14**).

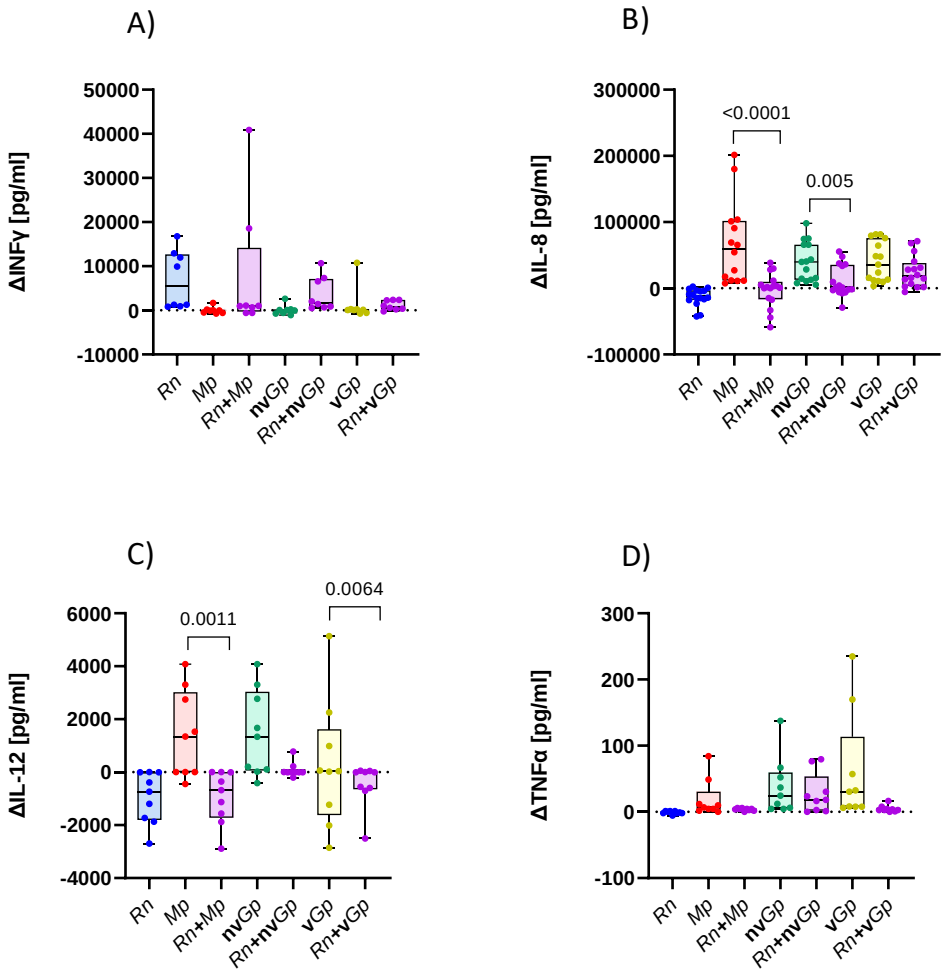

Figure 3.13. Interleukins and cytokines concentrations secreted by the non-differentiated Porcine Nasal Organoids (PNOs) when stimulated with the bacteria. Non-differentiated PNOs were incubated with 10^4 CFU/ml of *R. nasimurium* (*Rn*), 10^3 CFU/ml of *Moraxella pluranimalium* (*Mp*), 10^3 CFU/ml of non-virulent *Glaesserella parasuis* (nv*Gp*) or with 10^5 CFU/ml of virulent *G. parasuis* (v*Gp*) individually or in combinations. After o/n incubation supernatants were recovered for cytokine quantification. Results are shown as the delta of each interleukin and cytokine, subtracting the negative control (PNOs without inoculation, basal levels of the secretion) in pg/ml. a) Secretion of interleukin 8 (IL-8), b) Secretion of interleukin 12 (IL-12), c) Secretion of Tumor Necrosis Factor alpha (TNFα) and d) Secretion of Interferon gamma (INFγ). Each dot represents a replicate from three different experiments of PNOs coming from two animals. Two replicates were included in each experiment. Kruskal-Wallis multiple comparison with Benjamini, Krieger and Yekutieli post-hoc test was used to analyze the data. Significant differences are shown as horizontal lines with the associated *P* value.

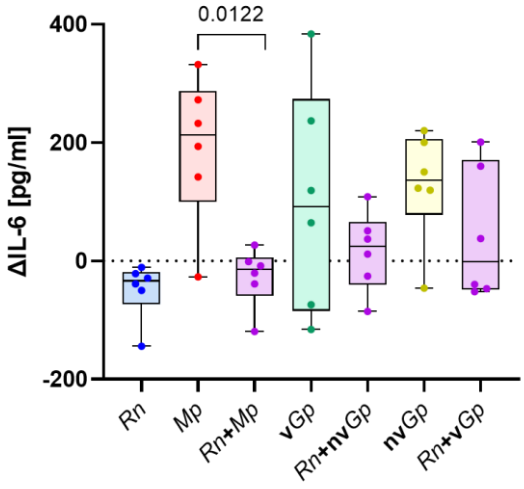

Figure 3.14. Interleukin 6 (IL-6) concentrations by the non-differentiated Porcine Nasal Organoids (PNOs) when stimulated with the bacteria. Non-differentiated PNOs were incubated with 10^4 CFU/ml of *Rothia nasimurium* (*Rn*), 10^3 CFU/ml of *Moraxella pluranimalium* (*Mp*), 10^3 CFU/ml of non-virulent *Glaesserella parasuis* (nv*Gp*) or with 10^5 CFU/ml of virulent *G. parasuis* (v*Gp*) individually or in combinations. After o/n incubation supernatants were recovered for cytokine quantification. Results are shown as the delta of interleukin 6 (IL-6), subtracting the negative control (PNOs without inoculation, basal levels of the secretion) in pg/ml. Each dot represents a replicate from three different experiments of PNOs coming from two animals. Two replicates were included in each experiment. Kruskal-Wallis multiple comparison with Benjamini, Krieger and Yekutieli post-hoc test was used to analyze the data. Significant difference is shown as a horizontal line with the associated *P* value.

Finally, IFNα, IL-1β, IL-4, IL-10 and IL-17A were below the detection limits in all tested samples, suggesting that these cytokines are not released in this PNO model under the tested conditions.

Discussion

In this study, for the first time, we have established long-term cultures of porcine nasal organoids (PNOs) derived from nasal turbinates by isolating the basal epithelial cells. These 3D “mini-noses” exhibited a centralised lumen surrounded by a polarised airway epithelial cell layer, showing cilia oscillations with proliferative activity and tight junction function, which are physiologically similar to the pig airway epithelium *in vivo*. This model recapitulates key histological and functional aspects of the in vivo tissue, suggesting that it is an excellent proxy of the porcine nasal

epithelium and can be used to model respiratory diseases. As a proof-of-concept, we used the PNOs to study host-bacterial interactions using nasal colonizers of pigs.

The culture conditions used to generate and maintain the PNOs preserved the self-renewal of nasal-resident stem cells and the stability of the organoids during the proliferation phase. This allowed us to indefinitely expand the organoid culture while recapitulating the cell diversity of the native tissue. For the differentiation stage, the composition of the medium promoted the specialisation of cells as we confirmed by PCR and IFA. Expression of FOXJ1 and MUC5AC indicated the cilia formation and mucus production, both involved in bacterial clearance. These markers, together with ZO-1 (zonula occludens-1, a tight junction protein implicated in the maintenance of cell barrier integrity) were relevant for the analysis of the host response to both colonization by nasal commensal bacteria and the infection by the respiratory pathogen. In relation to this, the presence of mucus (Muc5A gene, secreted by goblet cells) and the tight junctions (ZO-1 gene) were more evident after 2 h of infection than after o/n incubation with the strains. This suggested that PNOs' cells were more reactive to the bacteria during the first hours and reached an equilibrium after an o/n incubation. For non-differentiated PNOs this effect was not observed, suggesting that the lack of differentiation is related to less specialization. Overall, we conclude that colonizers did not affect the integrity of PNO monolayers, whereas virulent *G. parasuis* did disrupt the tight junctions and affected the production of mucus, damaging goblet cells and probably other cellular types, which is in agreement with other studies (data not shown) (313,314).

Interactions between pathogens and members of the nasal microbiota could be essential to limit pathogen entry and their capacity to disseminate systemically (88). For instance, in humans, several studies revealed that interactions between members of the nasal microbiota, such as *Corynebacterium spp.* or *Dolosigranulum pigrum*, interfered with *Staphylococcus aureus* colonization (155,156,211,315). Nevertheless, the mechanisms involved in these host-microbiome interactions are difficult to study in a systematic way and could profit from a simplified and

convenient model like nasal organoids. Our approach with PNOs to study bacterial colonization aligns with other works that describe the *in vivo* situation. For instance, *Rothia* is prevalent but not abundant in pig nasal swab samples, while other species as *M. pluranimalium* and *G. parasuis* showed high prevalence and abundance in this type of samples (126,152). These findings were in apparent contradiction with the capacity of those bacterial species to grow in laboratory conditions, i. e., *R. nasimurium* grows abundantly in common bacterial media, while *M. pluranimalium* and *G. parasuis* are fastidious microorganisms that grow poorly. In our study, the initial inoculated amount was similar for all the strains, but we found that our PNO model may be mimicking the *in vivo* conditions of the microbial network and the nasal mucosa, where a high abundance of *Moraxella* and *Glaesserella* is typically detected in the nasal microbiota of pigs, together with a low abundance of *Rothia*.

Differentiated PNOs seemed to be less reactive to bacterial stimuli than the non-differentiated ones as they secreted less interleukins, especially IL-8, IL-12 and IL-6, the latter being only detected in non-differentiated PNOs. We hypothesized that this effect could be produced because differentiated PNOs have more specific cells associated to protection, as ciliated cells, and goblet cells, whose movement and secretion of mucus, respectively, could avoid intimate bacterial contact. Moreover, our results, confirm previous observations showing that Gram-negative bacteria induce pro-inflammatory cytokines IL-8, IL-12, IL-6 and TNFα, while Gram-positive tend to induce IL-12, TNFα and IFNγ (316), supporting the value of the PNO model. IFNγ can inhibit IL-8, TNFα and IL-6 production (317–319). In fact, IFNγ has an anti-inflammatory role when the host is infected with bacterial pathogens (316,320), in agreement with our results and results with *Rothia mucilaginosa*. *R. mucilaginosa* was negatively correlated with pro-inflammatory markers as IL-8, IL-6 and IL-1β and demonstrated an immunomodulatory activity in a three-dimensional cell culture model of the respiratory tract in the presence of pathogens as *Pseudomonas aeruginosa* (293,321,322). Similarly, *R. nasimurium* had an anti-inflammatory role in the PNOs by eliciting IFNγ production and interfered with the stimulation produced by the other members of the nasal microbiota, although the numbers of *R.*

nasimurium were lower than those of the other bacteria. Overall, our results suggest that *R. nasimurium* might be important for the maintenance of the homeostasis with potential properties as a probiotic.

We present a novel model that recreates the typical aspects of the *in vivo* nasal epithelium based on 3D PNOs (that can be indefinitely passaged and frozen for long-term expansion) and a monolayer culture derived from them, which can be convenient for microbial network and host-microbe interaction studies. It is also important to remark the breakthrough in the generation of the pig nasal organoids using a non-invasive technique (cytological brushes) as an alternative to necropsy-derived organoids, supporting the 3Rs principle of animal experimentation. Additionally, we improve our understanding of the nasal microbiota colonization and the interactions between the different members, as well as the host cellular response to both bacterial colonization and infection. All the experiments presented in this study have been performed in monolayers using 96-well plates as a "proof-of-concept". Despite monolayers recapitulated the *in vivo* structure, future improvements would include ALI cultures to simulate apical-basal compartmentalization and thus increase differentiation. Moreover, additional studies including more members of the nasal microbiota, as for example, a consortium, should be performed to fully understand the interaction network of the microbiota.

In conclusion, PNOs demonstrated to be a promising tool to expand the knowledge on the bacteria-bacteria and bacteria-host interactions occurring in piglets' noses, as well as useful to study pathogen exclusion to find new alternatives to antimicrobials and reduce the use of these drugs. Besides, PNOs can be taken into consideration for studies to predict future transmissions and pandemics, as pigs are natural reservoirs for a wide variety of zoonotic pathogens.

Materials and methods

Animal experimentation and ethics approval

For the obtention of nasal turbinates, euthanasia was performed following good veterinary practices. According to European (Directive 2010/63/EU of the European Parliament and of the Council of 22 September 2010 on the protection of animals used for scientific purposes) and Spanish (Real Decreto 53/2013) normative, this procedure did not require specific approval by an Ethical Committee (Chapter I, Article 3. 1 of 2010/63/EU).

Establishment of porcine nasal organoids (PNOs) from nasal turbinates and nasal brushes

Porcine nasal organoids were isolated from two 4-week-old male healthy piglets (*Sus scrofa domesticus*) coming from Spanish conventional farms. Piglets were transported to IRTA-CReSA facilities where they were humanly euthanized by means of an overdose of sodium pentobarbital (Dolethal). Immediately after, the complete nasal turbinates were dissected, cut longitudinally and collected in a container with Dulbecco's modified Eagle's medium (DMEM/F12) complemented with HEPES, GlutaMax, Penicillin-streptomycin (P/S) and Amphotericin B (AmphB) (complete DMEM/F12). Samples were stored on ice until processing on the lab or kept at 4ºC o/n for further processing of epithelial isolation on next day. After some washes with cold PBS 1x supplemented with P/S and AmphB, nasal turbinates were transferred onto a sterile plate using sterile tweezers and scalpel. The nasal mucosa tissue was peeled off and cut into small segments. Tissue samples were washed with cold PBS 1x supplemented with P/S and AmphB in a 50-ml centrifuge tube until the supernatant was clear, allowing mucosal segments to settle down to the bottom by gravity. Then, the pieces were incubated in collagenase IV (1 mg/mL) resuspended in 10 ml of OGM (Complete PneumaCult-Ex Plus Basal Medium [StemCell Technologies Cat #05040]) containing 1% of both AmphB and P/S) at 37°C for 1 h on a rocker (200 rpm). After digestion, collagenase IV was removed, and the airway debris was dissociated with 0.25% EDTA-Trypsin at 37°C for 30 min. Then, the debris was

harvested by centrifugation at 300 x g at 4°C for 4 min, resuspended in complete DMEM/F12 with 10% Fetal Bovine Serum (FBS), and strained through a 100-µm strainer. Once spun at 400 x g for 5 min at 4°C, airway cell pellet was washed with 10 ml of complete DMEM/F12 and 10 ml of OGM. Finally, the medium was removed, and the cell pellet was resuspended in Matrigel (Corning 356231), seeded into a 24-well plate, and incubated for 15-30 min at 37°C with 5% CO_2. After solidification, Matrigel droplets were cultured with 500 µl of OGM supplemented with P/S and AmphB and placed back into 37°C incubator with 5% CO_2. The culture medium was exchanged every other day, and the nasal organoids were passaged every 7-10 days at a 1:2 or 1:3 ratio for expansion. After 2 or 3 passages, P/S and AmphB were removed from the OGM. Additionally, PNOs were tested for *Mycoplasma* by qPCR.

PNOs were also stablished from nasal brushes using cytological brushes (Covaca). The protocol followed was the same as from nasal turbinates with some modifications. Briefly, cytological brush was inserted into the nasal cavity, softly spun and then placed into a 15-ml tube containing 10 ml of cold complete DMEM/F12. Cellular material was removed using a cut-ended pipette tip and transferred to another 15-ml tube. Both tubes were centrifuged at 300 x g for 4 min at 4ºC and the pellet was washed twice with cold PBS 1x supplemented with P/S and AmphB. TrypLE (Gibco) was added to this pellet, incubated for 10 min at 37ºC and inactivated with 5 ml of complete DMEM/F12. After that, the cellular material was passed through a 70-µm filter to obtain the epithelial cells, spun at 300 x g for 4 min at 4ºC and resuspended in Matrigel.

2D airway organoid monolayer cultures

Airway organoid monolayer cultures were prepared from 3D airway organoids as previously described (310). First, after culturing for 7 days, 3D airway organoids were washed by using ice-cold DMEM/F12 and dissociated with 0.05% trypsin-EDTA (Gibco) in a 37º water bath for 4 min. After incubation, trypsin was inactivated by adding DMEM/F12 containing 10% of FBS and the organoids were vigorously repeated pipetted up and down to dissociate into single cells. Then, the cell

suspension was filtered through a 40-µm cell strainer (352340; Corning), centrifuged and resuspended in OGM with 10 µM rock inhibitor (Y-27632). Finally, cells were seeded at $3x10^5$ airway organoid cells in each well of a 96-well plate precoated with Matrigel. After culturing for 7 days and replacing OGM every other day, the 2D airway organoid monolayers (non-differentiated PNOs) were ready for the microbiota experiments. Differentiated PNOS were prepared following the same protocol but switching the OGM to ODM; Complete PneumaCult Airway Organoid Basal Medium [StemCell Technologies Cat #05061]) at day 7 after seeding, or when monolayer is 100% confluent, replacing media every other day for one week more (11-14 days in total).

Observation of cilia oscillations

The nasal mucosa organoids, both 3D and 2D models, were observed at different cultured times for cilia movement under an optical microscope (x20 and x40) and recorded by video (**Annex 3.1**).

Fixation, paraffin-embedding, and sectioning of 3D porcine nasal organoids (PNOs)

The protocol followed is based on a previous publication (Wiley 2017). Briefly, 3D organoids were rinsed with PBS and fixed with PFA 4% for 1h at 4ºC. After several washes with PBS, organoids were centrifuged for 5 min at 1500 rpm and then were embedded in agarose 2%, cut in small, rounded pieces and introduced into the cassettes followed by dehydration in ethanol series (80%, 95% and 100%, 15 min each at RT). The 3D organoids were then subjected to paraffin embedding and sectioning. Standard haematoxylin and eosin (H&E) staining were performed to evaluate the airway structure.

Immunohistochemistry (IHC)

Paraffin-embedded nasal turbinates from piglets were used to localize and compare the expression of the different cell types. Samples were sectioned at 2’5-µm thickness, deparaffinized and rehydrated. After dH_2O washes, the endogenous peroxidase was blocked with methanol and 3% H_2O_2 for 30 min at RT. Antigen retrieval was performed at pH 6 using a sodium citrate buffer for 20 min at 98ºC.

Then, sections were washed and blocked for 1h in PBS-Tween 20-2% BSA (Bovine Serum Albumin) at RT. Primary antibodies ZO-1 dilution 1/300 (Invitrogen ZO1-1A12), acetylated α-tubulin dilution 1/10.000 (Proteintech 66200-1-Ig), Ki67 dilution 1/2000 (BD 550609) and 5 µg/ml FOXJ1 (Invitrogen 14-9965-80) were incubated o/n at 4ºC. After three washes with PBS, Envision+System-HRP labelled Polymer anti-mouse (Dako) was added at RT for 45 min. The reaction was developed by adding the DAB substrate and sections were mounted with DPX.

Immunofluorescence assays (IFA)

PNO monolayer cultures in 96-well plates were incubated for 7 days with OGM (non-differentiated PNO monolayers) or 7 days with OGM + 7 days with ODM (differentiated PNO monolayers). Then medium was removed, monolayers washed twice with PBS 1x and fixed with PFA 4% for 1h at RT. After fixation, cells were washed twice with PBS 1x, permeabilized with 0.5% Triton-X100 for 1h at RT and blocked with BSA 3% for another hour. After that, primary antibodies were added and incubated o/n at 4ºC. Next day, cells were washed 3 times with PBS and incubated with the secondary antibodies (α-mouse IgG1 antibody conjugated with ALEXA 568 or ALEXA 488 at 1/1000 dilution, mixed with phalloidin and Hoescht, for 4h at RT. After 4 h of incubation in darkness, monolayers were washed 3 times with PBS and 150 µl of PBS were finally added. The same protocol was followed for the 3D PNOs cultured 7 days with OGM (non-differentiated) or 7 days with OGM + 3 days of ODM (differentiated) but 3 washes were performed between steps for 5 min in agitation. Low-binding eppendorfs were used for the incubations. Approximately, 20 µl of 3D HIEs suspension were mounted on slides and mixed with VECTASHIELD Plus antifade mounting medium (Sigma-Aldrich). 96-well plates (monolayers) and slides (3D PNO) were observed using a fluorescence (MOTIC AE31E) and confocal microscope (Leica Stellaris 8), respectively.

RNA extraction and RT-PCRs

PNOs were disaggregated and resuspended in DNA/RNA Shield (Zymo Research R1100-50) to preserve the RNA and frozen at -20ºC until its extraction. Total RNA was

extracted using the RNeasy Mini Kit (Qiagen 74104) following the manufacturer's instructions. DNase digestion step was performed using the RNase-Free DNase Set (Qiagen 79254) as described and recommended by the manufacturer. Concentrations were measured using absorbance at 260nm (A260) with BioDrop DUO (BioDrop Ltdre). RNA was retrotranscribed to cDNA using a minimum concentration of 80 ng/ml of RNA using the PrimeScript™ RT Master Mix (Perfect Real Time) (Takara Bio #RR036B) kit following manufacturer's protocol. Finally, a conventional PCR to detect club cells (Scgb1A1), goblet cells (Muc5AC), basal cells (TP63), ciliated cells (FoxJ1) and tight junctions (ZO-1) was used. A housekeeping gene (gapdh) was included as a positive control of the extraction.

Incubation of bacteria, individually and in co-culture, with non-differentiated and differentiated 2D PNOs

Previously characterized porcine nasal isolates *R. nassimurium* UK1-9, *M. pluranimalium* LG6-2 and non-virulent *G. parasuis* F9 were used in this study (86,126). In addition, we included in the study a virulent *G. parasuis* strain that can disseminate systemically and produce Glässer's disease, a systemic inflammatory disease characterized by polyserositis (79). For the assays, the strains were grown o/n on chocolate agar at 37ºC with 5% CO_2. Next, bacterial suspensions were prepared in order to have approximately 10^3-10^5 CFU/ml of each strain. Inoculums were centrifuged at 16000 x g for 10 min and the bacterial pellet was resuspended in OGM or ODM for non-differentiated or differentiated PNO, respectively. Serial dilutions of the final inoculum were performed and plated on chocolate agar to confirm the inoculum concentration.

PNOs were prepared in 96-well plates and were inoculated with 100 µl of each individual bacterial suspension. In the case of co-cultures, 50 µl of *R. nasimurium* inoculum were mixed with 50 µl of each of the other strains in pairwise combinations (*R. nasimurium* + *M. pluranimalium*, *R. nasimurium* + non-virulent *G. parasuis* F9, and *R. nasimurium* + virulent *G. parasuis* Nagasaki) to evaluate the possible interaction between the different strains. The 96-well plates with the inoculated 2D PNOs

monolayers were incubated o/n at 37ºC with 5% CO_2 to study the colonization capacity of the strains, including stimulation capacity. Afterwards, supernatants of each well were taken for bacterial count by serial dilutions and determination of cytokine secretion by PNOs (see below). Next, 2D PNOs monolayers were washed 2 times with 150 µl of PBS and were lysed with 1 % Saponin from Quillaja Bark (Sigma S7900-25G) to assess the associated bacteria. Serial dilutions of the lysate were performed and cultured on chocolate agar. All the chocolate agar plates were incubated at 37ºC with 5% CO_2 for 48 hours. Additionally, same inoculations of the bacteria to the 2D PNOs were performed but reducing the time of incubation to 2 h to study adhesion capacity. After incubation, supernatants and PNOs monolayers were processed as indicated above.

One of the infected 96-well plates was used to RNA extraction and RT-PCR analysis for the muc5ac and zo-1 gene expression, presence of goblet cells and tight junction respectively, as described before.

As growth controls, bacterial inocula, individually and in co-culture, were incubated o/n with fresh OGM and ODM. Bacterial growth after incubation was assessed by serial dilution of the cultures and plating on chocolate agar for colony counts.

Cytokine detection in the non-differentiated and differentiated 2D PNOs

To detect cytokines, chemokines and interleukins, supernatants were taken from the 96-well plate seeded with 2D PNOs infected with the bacteria after o/n infection. Supernatants were centrifuged at 16000 x g 10 minutes to eliminate the bacterial cells and frozen at –80ºC until its use. Negative controls from non-inoculated PNOs were also included.

Cytokine & Chemokine 9-Plex Porcine ProcartaPlex™ Panel 1 assay (ThermoFisher Scientific #EPX090-60829-901) was used following manufacturer's protocol to detect FNα, IFNγ, IL-1β, IL-10, IL-12, IL-4, IL-6, IL-8 (CXCL8) and TNFα. Standards were prepared with the growth media of the PNOs.

In parallel, IL-8 secretion was assessed with an Enzyme-Linked Immunosorbent Assay (ELISA) following the manufacturer's protocol ((R&D system #DY535). The coat was made with 1:180 dilution of 360 µg/ml IL-8 capture antibody in PBS 1x. 300 µl of block buffer (1% Bovine Serum Albumin, BSA in PBS 1x) were added and incubated 1 h 50 rpm at RT. Samples were added using a 1:50 dilution in the reagent diluent (0,1%BSA, 0,05% Tween20 in PBS 1x). A 1:180 dilution in the reagent diluent of 5,4ug/ml detection antibody was used.

IFNγ secretion was also assessed with an ELISA following manufacturer's protocol (Swine IFN gamma Polyclonal Antibody, PB0157S-100; Swine IFN gamma Polyclonal Antibody Biotinylated, PBB0269S-050; Swine IFN gamma [Yeast-derived Recombinant Protein], RP0126S-005; Kingfisher Biotech, Inc). Samples were added 1:5 diluted in the same media used for the PNOs growthIL-10 and IL-17A ELISAs were tested as described for IFNγ.

Statistical analysis

Graphpad 8.3 (538) Prism software (Dotmatics, San Diego CA) was used to analyse the all the data.

Kruskal-Wallis multiple comparison with Benjamini, Krieger and Yekutieli post-hoc test was used to compare the concentrations of individual strains, as well as to assess the concentration of *R. nasimurium* co-cultured with the other strains. This test was also used to compare the differences in the levels of cytokines secreted by the PNOs in the presence or absence of the different bacteria. Welch's and Mann-Whitney t tests were used to compare the concentrations of *M. pluranimalium*, non-virulent and virulent *G. parasuis* strains after single or co-culture with *R. nasimurium*. A significance level of $P < 0.05$ was considered statistically significant.

Annexes

Annex 3.1. Cilia movement in 3D Porcine Nasal Organoids (PNOs).

Available at Zenodo repository in this link/QR code:

https://zenodo.org/records/15019822

General discussion

The nasal microbiota, together with the nasal mucosa, constitute the first line of defence against environmental pollutants, particles and respiratory pathogens. Recent human studies have shown that interactions between the commensals of the nasal microbiota are crucial to avoid pathogen colonization (323–325). Understanding the underlying mechanisms could lead to the development of new strategies to control infectious diseases. In pigs, recent research has also demonstrated the importance of such microbial interactions in pathogen infections (116,326). In the present thesis, new tools were developed to further unravel the functionality of the piglet nasal microbiota, as well as to systematically study the interactions within this community and with respiratory pathogens in the host context.

Different animal models have been used to study the microbiota of pigs. Germ-free BALB/c mice have been employed to investigate the pig gut microbiota as well as bacterial and viral infections. Although they are not the natural host, these animals offer the advantage of being much easier to handle (205,327,328). Conventional mice treated with a broad-spectrum antibiotic cocktail have been also useful to study human diseases, such as cardiovascular complications and colitis, as well as the effect of microbiota in the gut-brain axis communication, among other functions (329–331). In order to use the native host, Modrackova et al. (2024) obtained germ-free piglets by hysterectomy of pregnant miniature sows and studied the colonization of a combination of nine bacterial strains from the pig gut microbiota and the effect on a subsequent infection with *Salmonella* Thyphimurium LT2. They showed that the inoculated commensals colonized the gnotobiotic pigs, but this colonization did not confer a significant protection against the inoculated pathogen (332,333). Similarly, colostrum-deprived, caesarean derived (CDCD) piglets were proven to be useful for studying infections produced by *Glaesserella parasuis*, *Streptococcus suis*, *Bordetella bronchiseptica* and *Mycoplasma hyorhinis* (91,334–336), as well as to assess gut microbiota colonization (337,338). However, the main limitation of these models is that animal survival is compromised by the absence of maternal immunity, and

thereby, the immunodeficient state of the piglets makes their manipulation more challenging (339).

In the present thesis, to avoid the complex housing conditions of gnotobiotic animals, and following the studies done in mice, we administered an intensive antibiotic treatment with ceftiofur and tulathromycin to sows, as it is known that the sow is the main microbiota source for their piglets (52). Although the antibiotic treatment did not completely prevent the nasal microbiota transfer from the sows to the piglets, it significantly reduced it. We evaluated this model by intranasally inoculating a mixture of three common nasal commensals (*Moraxella pluranimalium*, *Rothia nasimurium* and *Streptococcus pluranimalium*) on the first day of life of the piglets (data not shown). However, none of the inoculated strains successfully colonized the animals. We hypothesize that the failure in colonizing these piglets by the three professional colonizers could be explained because they may require the interaction with other commensals to establish a stable nasal community, or alternatively, the presence of environmental bacteria could interfere in their establishment. A previous study from our group showed that inoculating the same colonizers but including *Vagococcus lutrae* and a non-virulent *G. parasuis* strain resulted in a successful colonization by *M. pluranimalium*, *R. nasimurium*, *G. parasuis* and *S. pluranimalium*. In addition, this colonization showed an amelioration of the nasal microbiota alterations produced by antibiotic treatments (126). Next steps may include the inoculation of different doses of the mentioned strains and/or the inoculation of different combinations of the members of the synthetic community defined in the present thesis, the Porcine Nasal Consortium (PNC8), to elucidate which are the minimum essential members of the pig nasal microbiota needed to establish the community. The subsequent inoculation with respiratory pathogens/pathobionts, such as *G. parasuis*, *M. hyorhinis* or *S. suis* would enable the understanding of the nasal microbiota role in pathogen exclusion. Finally, other commensals besides the ones constituting the PNC8 should be considered, such as *Coryneobacterium*, which was recently isolated from healthy piglets in our laboratory.

In accordance with the 3Rs principle, we next aimed to develop *in vitro* approaches to recapitulate the host environment and represent the nasal microbiota, such as the PNC8 consortium and the Porcine Nasal Organoids (PNOs) presented in this thesis.

In relation to the PNC8 consortium, we showed that the 8 selected species had different nutritional requirements across various *in vitro* conditions, representing the complexity of the nasal microbiota and supporting the existence of interactions. For instance, we identified a positive interaction between *G. parasuis* (non-virulent and virulent strains) and either *R. nasimurium* or *Staphylococcus aureus* in a nutrient-limiting medium. These results align with recent evidence confirming that cooperative events among microorganisms are more likely to occur when they face environmental pressures, such as antibiotics or nutrient deficiencies (Shuang Wang et al., 2024 microbial collaborations). Regarding this, Machado et al. (2021) highlighted that cooperative communities harbour complementary auxotrophies, such as for amino acid biosynthesis, while competitive communities have diverse metabolic capacities to exploit the available nutrients, which indirectly antagonize bacteria and reduce the dependence on the other species (340). More interaction experiments using different PNC8 member combinations and/or respiratory pathogens must be performed to elucidate the type of interactions present in the pig nose. This should include culture media with different richness and mimicking the scarce-nutrient environment of the nose (269). Other approaches such as the culture of the PNC8 strains in each other's spent media, or metabolomic analysis could be useful to determine the metabolic role in these interactions (150,152,153,341).

To study the nasal commensals in a more *in vivo*-like system, we used the PNO model and corroborated that PNC8 members *R. nasimurium*, *M. pluranimalium* and *G. parasuis* F9 strain and the virulent Nagasaki *G. parasuis* strain were able to colonize this model. None of the tested commensals affected the PNO monolayer integrity. In contrast, consistent with previous studies (313,314), the virulent Nagasaki strain disrupted the tight junctions and altered mucus production (data not

shown). However, here monolayer integrity was only examined through observation and RT-PCR of cell markers. Additional techniques would allow to confirm our observations, such as transmission electron microscopy or time-lapse observation of the organoids using a confocal microscope.

On the other hand, we demonstrated the existence of interactions between *R. nasimurium* and the other selected bacteria in PNOs. When *M. pluranimalium* and *G. parasuis* strains were individually incubated, PNOs responded secreting proinflammatory cytokines. In contrast, when co-cultured with *R. nasimurium*, proinflammatory cytokine levels decreased. This result evidenced the anti-inflammatory role of *R. nasimurium* in the PNO model, probably by the interference in cell signalling through INFγ production, showing its capacity to modulate host cytokine release and mitigating the pathogens' effect. In agreement, Goeteyn et al. (2023) showed that *Rothia* can synergistically interact with other commensal bacteria (*Actinomyces naeslundii*) to reduce the activation of the NF-κβ pathway of A549 cells, which is related with inflammation (293). In the present thesis, host inflammatory responses were only assessed by quantification of selected cytokines. Other strategies such as transcriptomic analysis of the PNOs would allow the comprehension of host gene expression after bacterial colonization, including the understanding of the role of *R. nasimurium* in the modulation of the host inflammatory responses (194,197,342–344).Our results are also in agreement with recent research that have highlighted the potential probiotic effect of *Rothia* in humans due to its capacity to avoid the colonization of some respiratory pathogens (e. g. *Pasteurella multocida* and *Moraxella catarrhalis*) and its anti-inflammatory role in the LRT, improving chronic respiratory disorders (153,293,312,322). Hence, we propose that *R. nasimurium* is a potential probiotic candidate for swine microbiota interventions. Additional PNO colonization experiments should be conducted with *R. nasimurium,* including testing different bacterial concentrations to determine whether its effect is dose dependent, or using other isolates to assess the reliability of its effect across different strains. Furthermore, inoculation with dead *Rothia* or its

derived components, could also be interesting to evaluate if it could act as a postbiotic, as done in a recent study (345).

Further colonization experiments should be carried out, as in the present thesis only few PNC8 members and a single pathobiont were tested in the PNO model. Individual incubation of all PNC8 strains and other respiratory pathogens in PNOs should be conducted to confirm their capacity to colonize this model. Additionally, the interactions between other PNC8 members and different respiratory pathogens should be tested. In relation with this, a recent study showed that some taxa of the pig nasal microbiota, including *Moraxella, Lactobacillus* and *Rothia*, negatively correlated with pathogens such as *M. hyorhinis*, *G. parasuis, P. multocida*, *Mannheimia varigena* and *S. suis* (326). The PNOs presented here, can be a useful model for the experimental confirmation of these and other correlations observed *in silico*. All these additional experiments would verify the robustness of the PNO approach and would evidence the capacity to reproduce *in vivo* colonization/infection. Finally, live monitoring of the bacteria during the colonization/infection could provide crucial information to understand the microbiota network and its role in pathogen exclusion. To achieve that, fluorescent-labelled strains would be useful (346,347). For example, Rapún-Araiz et al. (2023) transformed *Haemophilus influenzae* with plasmids containing genes coding for fluorescent proteins and tracked the bacteria over-time in human alveolar basal epithelial cells (346). Labelling the PNC8 strains and the relevant respiratory pathogens with different fluorescent genes would allow the simultaneous imaging of the spatial distribution and the abundance of nasal species in the PNOs or in *in vivo* experiments.

Future directions to study the pig nasal microbiota must be explored, such as using organoids in ALI conditions, which have demonstrated to better recapitulate the nasal tissue characteristics. ALI conditions would allow the exposure of cells to the air by the apical side, while only the basolateral side remains in contact with the medium, mimicking the respiratory tissue and therefore, promoting a more

advanced state of differentiation (157,202,348). Boyd et al. (2024) cultured human nasal organoids in ALI conditions and confirmed the capacity of some pathogenic and commensal nasal species to individually colonize these cultures for 48 h. They also showed how these strains modulated the secretion of relevant cytokines, such as the increase in CXCL11 when the organoids were colonized with *Streptococcus pneumoniae*, or the decrease in CXCL10 when colonized with *S. aureus* or *Dolosigranulum pigrum* (197). Following research could also consider the co-culture of organoids and immune cells, such as macrophages, adding another layer of complexity to the model (349,350). However, factors such as the absence of airflow dynamics may still limit their ability to fully mimic natural colonization conditions. For that, new tools such as the organ-on-a-chip (OoC) devices are being employed to physiologically recapitulate many human tissues. Specifically, OoC can recreate the mucosal interface to study the host-microbiota interplay, as it includes microfluidic-based flow dynamics, shear stress, the possibility of mechanical deformation and oxygen control (351,352). Recent studies have employed the OoC technology to elucidate human microbiota interactions as well as to study the pathogenicity of viral and bacterial infections in a more *in vivo*-like environment compared to other approaches, such as static primary cell cultures or non-human animal models (353–356). Lee et al. (2024) evidenced that gut OoC had a more suitable environment for microbial colonization due to the 3D structure that simulates the human intestinal structure (356). Similarly, Izadifar et al. (2024) highlighted that vaginal OoC produced a more realistic cervical mucus than other *in vitro* approaches due to the dynamic flow of this technology (354). Furthermore, the combination of organoids and OoC technologies (OrgOC) have been applied to multiple human tissues (357–360). These OrgOC models can be used to explore the human microbiota, as done by Tovaglieri et al. (2019). In this study, an OrgOC model co-culturing human colon organoids and human intestinal microvascular endothelial cells (HIMEC) was established and successfully infected with an enterohemorrhagic *Escherichia coli* strain, combined with human gut microbiota metabolites (361). They found that some of these metabolites could mediate the epithelial injury produced by this pathogenic *E. coli*.

In pigs, a recent study developed a porcine jejunum OrgOC model and used it to assess intestine drug metabolism (362). However, to the best of our knowledge, no studies have explored pig microbiota using the OrgOC technology. Hence, we believe that stablishing a pig nasal OrgOC model would be a valuable tool to elucidate the microbe-microbe and pathogen-microbe interplay using the defined PNC8 consortium in an environment that better recapitulates the *in vivo* tissue characteristics.

Overall, in the present thesis we developed a comprehensive framework for studying the nasal microbiota combining complementary approaches. This work may allow the discovery of alternatives to antibiotics through microbiota interventions directed to exclude respiratory pathogens affecting pigs, without contributing to the rise of AMR.

Conclusions

1. An intensive antibiotic treatment consisting of crystalline ceftiofur and tulathromycin applied to sows, significantly reduced the nasal microbiota transfer to the piglets. Additional interventions to avoid microbiota transference may be needed to obtain an appropriate pig model for microbiota studies.
2. The Porcine Nasal Consortium (PNC8) was defined based on the eight most prevalent and/or abundant genera found in the piglet nasal microbiota. PNC8 represents an *in-vitro* convenient tool to explore the interaction network within the piglet nasal community, as well as to elucidate pathogen exclusion strategies.
3. Porcine Nasal Organoids (PNOs) were established for the first time as a model that properly recapitulates the characteristics of the *in vivo* piglet nasal mucosa. This model can be used to study microbial interactions in the context of the host.
4. PNOs were colonized by selected strains from the PNC8 consortium and responded to the colonization by secreting relevant cytokines. *Rothia nasimurium* showed an anti-inflammatory role in the PNOs, interfering in the pro-inflammatory stimulation produced by the other bacteria.
5. PNOs support the reduction of the number of animals used in experimental studies, being in line with the 3Rs principles. This approach, in combination with the PNC8 consortium, constitute a good alternative for *in-vivo* approaches to study the piglet nasal microbiota, providing insights into microbial behaviour and host responses.

References

1. Berg G, Rybakova D, Fischer D, Cernava T, Vergès MCC, Charles T, et al. Microbiome definition re-visited: old concepts and new challenges. Microbiome. 2020 Dec;8(1):103.

2. Lederberg J, McCray AT. 'Ome Sweet 'Omics-- A Genealogical treasury of words. The scientist. 2001 Apr;15(7):8.

3. Marchesi JR, Ravel J. The vocabulary of microbiome research: a proposal. Microbiome. 2015 Dec;3(1):31, s40168-015-0094–5.

4. Pickard JM, Zeng MY, Caruso R, Núñez G. Gut microbiota: Role in pathogen colonization, immune responses, and inflammatory disease. Immunol Rev. 2017 Sep;279(1):70–89.

5. Blaser MJ. The microbiome revolution. J Clin Invest. 2014 Oct 1;124(10):4162–5.

6. Cho I, Blaser MJ. The human microbiome: at the interface of health and disease. Nat Rev Genet. 2012 Apr;13(4):260–70.

7. Thursby E, Juge N. Introduction to the human gut microbiota. Biochemical Journal. 2017 Jun 1;474(11):1823–36.

8. Abenavoli L, Maurizi V, Rinninella E, Tack J, Di Berardino A, Santori P, et al. Fecal microbiota transplantation in NAFLD treatment. Medicina. 2022 Oct 30;58(11):1559.

9. Al-Rashidi HE. Gut microbiota and immunity relevance in eubiosis and dysbiosis. Saudi Journal of Biological Sciences. 2022 Mar;29(3):1628–43.

10. Bozzetti V, Senger S. Organoid technologies for the study of intestinal microbiota–host interactions. Trends in Molecular Medicine. 2022 Apr;28(4):290–303.

11. Iebba V, Totino V, Gagliardi A, Santangelo F, Cacciotti F, Trancassini M, et al. Eubiosis and dysbiosis: the two sides of the microbiota. New Microbiol. 2016 Jan;39(1):1-12.

12. Dalile B, Van Oudenhove L, Vervliet B, Verbeke K. The role of short-chain fatty acids in microbiota–gut–brain communication. Nat Rev Gastroenterol Hepatol. 2019 Aug;16(8):461–78.

13. Gomaa EZ. Human gut microbiota/microbiome in health and diseases: a review. Antonie van Leeuwenhoek. 2020 Dec;113(12):2019–40.

14. Lynch SV, Pedersen O. The human intestinal microbiome in health and disease. Phimister EG, editor. N Engl J Med. 2016 Dec 15;375(24):2369–79.

15. Kawano Y, Edwards M, Huang Y, Bilate AM, Araujo LP, Tanoue T, et al. Microbiota imbalance induced by dietary sugar disrupts immune-mediated protection from metabolic syndrome. Cell. 2022 Sep;185(19):3501-3519.e20.

16. Ma Z, Akhtar M, Pan H, Liu Q, Chen Y, Zhou X, et al. Fecal microbiota transplantation improves chicken growth performance by balancing jejunal Th17/Treg cells. Microbiome. 2023 Jun 21;11(1):137.

17. Atarashi K, Nishimura J, Shima T, Umesaki Y, Yamamoto M, Onoue M, et al. ATP drives lamina propria TH17 cell differentiation. Nature. 2008 Oct;455(7214):808–12.

18. Van Dalen R, Elsherbini AMA, Harms M, Alber S, Stemmler R, Peschel A. Secretory IgA impacts the microbiota density in the human nose. Microbiome. 2023 Oct 21;11(1):233.

19. Hyun DW, Min HJ, Kim MS, Whon TW, Shin NR, Kim PS, et al. Dysbiosis of inferior turbinate microbiota is associated with high total IgE levels in patients with allergic rhinitis. Raffatellu M, editor. Infect Immun. 2018 Apr;86(4):e00934-17.

20. Ruokolainen L, Fyhrquist N, Laatikainen T, Auvinen P, Fortino V, Scala G, et al. Immune-microbiota interaction in Finnish and Russian Karelia young people with high and low allergy prevalence. Clin Experimental Allergy. 2020 Oct;50(10):1148–58.

21. Lim KH, Staudt LM. Toll-Like Receptor signaling. Cold Spring Harbor Perspectives in Biology. 2013 Jan 1;5(1):a011247–a011247.

22. Newton K, Dixit VM. Signaling in Innate immunity and inflammation. Cold Spring Harbor Perspectives in Biology. 2012 Mar 1;4(3):a006049–a006049.

23. Kim S, Covington A, Pamer EG. The intestinal microbiota: antibiotics, colonization resistance, and enteric pathogens. Immunological Reviews. 2017 Sep;279(1):90–105.

24. Sana TG, Lugo KA, Monack DM. T6SS: The bacterial 'fight club' in the host gut. Hogan DA, editor. PLoS Pathog. 2017 Jun 8;13(6):e1006325.

25. Lauridsen C. Effects of dietary fatty acids on gut health and function of pigs pre- and post-weaning. Journal of Animal Science. 2020 Apr 1;98(4):skaa086.

26. Chen W, Tan D, Yang Z, Tang J, Bai W, Tian L. Fermentation patterns of prebiotics fructooligosaccharides-SCFA esters inoculated with fecal microbiota from ulcerative colitis patients. Food and Chemical Toxicology. 2023 Oct;180:114009.

27. Corr SC, Li Y, Riedel CU, O'Toole PW, Hill C, Gahan CGM. Bacteriocin production as a mechanism for the antiinfective activity of *Lactobacillus salivarius* UCC118. Proc Natl Acad Sci USA. 2007 May;104(18):7617–21.

28. Sequeira RP, McDonald JAK, Marchesi JR, Clarke TB. Commensal *Bacteroidetes* protect against *Klebsiella pneumoniae* colonization and transmission through IL-36 signalling. Nat Microbiol. 2020 Jan 6;5(2):304–13.

29. Taherali F, Varum F, Basit AW. A slippery slope: On the origin, role and physiology of mucus. Advanced Drug Delivery Reviews. 2018 Jan;124:16–33.

30. Man WH, De Steenhuijsen Piters WAA, Bogaert D. The microbiota of the respiratory tract: gatekeeper to respiratory health. Nat Rev Microbiol. 2017 May;15(5):259–70.

31. Niederwerder MC. Role of the microbiome in swine respiratory disease. Veterinary Microbiology. 2017 Sep;209:97–106.

32. Pirolo M, Espinosa-Gongora C, Bogaert D, Guardabassi L. The porcine respiratory microbiome: recent insights and future challenges. Anim microbiome. 2021 Dec;3(1):9.

33. Requena T, Velasco M. The human microbiome in sickness and in health. Revista Clínica Española (English Edition). 2021 Apr;221(4):233–40.

34. Zhang J, Liu H, Yang Q, Li P, Wen Y, Han X, et al. Genomic sequencing reveals the diversity of seminal bacteria and relationships to reproductive potential in boar sperm. Front Microbiol. 2020 Aug 4;11:1873.

35. Michael J. Yaeger, William G. Van Alstine. Respiratory system. In: Diseases of Swine. 11th ed. Wiley; 2019. p. 393–407.

36. Robinson NE. Airway Physiology. Veterinary Clinics of North America: Small Animal Practice. 1992 Sep;22(5):1043–64.

37. McMullen C, Alexander TW, Léguillette R, Workentine M, Timsit E. Topography of the respiratory tract bacterial microbiota in cattle. Microbiome. 2020 Dec;8(1):91.

38. Aragon V, Correa-Fiz F. Microbiota respiratoria. In: La microbiota en el ámbito veterinario y su modulación. 1st ed. Ergon; 2023. p. 193–9.

39. Salzano FA, Marino L, Salzano G, Botta RM, Cascone G, D'Agostino Fiorenza U, et al. Microbiota composition and the integration of exogenous and endogenous signals in reactive nasal inflammation. Journal of Immunology Research. 2018 Jun 3;2018:1–17.

40. Harkema JR, Carey SA, Wagner JG. The nose revisited: A brief review of the comparative structure, function, and toxicologic pathology of the nasal epithelium. Toxicol Pathol. 2006 Apr;34(3):252–69.

41. Li Y, Yang C, Jiang Y, Wang X, Yuan C, Qi J, et al. Characteristics of the nasal mucosa of commercial pigs during normal development. Vet Res. 2023 Apr 24;54(1):37.

42. Siegel SJ, Weiser JN. Mechanisms of bacterial colonization of the respiratory tract. Annu Rev Microbiol. 2015 Oct 15;69(1):425–44.

43. Tai J, Han MS, Kwak J, Kim TH. Association between microbiota and nasal mucosal diseases in terms of immunity. IJMS. 2021 Apr 29;22(9):4744.

44. Blanco-Fuertes M, Correa-Fiz F, Fraile L, Sibila M, Aragon V. Altered nasal microbiota composition associated with development of polyserositis by *Mycoplasma hyorhinis*. Pathogens. 2021 May 14;10(5):603.

45. Correa-Fiz F, Fraile L, Aragon V. Piglet nasal microbiota at weaning may influence the development of Glässer's disease during the rearing period. BMC Genomics. 2016 Dec;17(1):404.

46. Espinosa-Gongora C, Larsen N, Schønning K, Fredholm M, Guardabassi L. Differential analysis of the nasal microbiome of pig carriers or non-carriers of *Staphylococcus aureus*. De Lencastre H, editor. PLoS ONE. 2016 Aug 10;11(8):e0160331.

47. Slifierz MJ, Friendship RM, Weese JS. Longitudinal study of the early-life fecal and nasal microbiotas of the domestic pig. BMC Microbiol. 2015 Dec;15(1):184.

48. Zeineldin M, Aldridge B, Blair B, Kancer K, Lowe J. Microbial shifts in the swine nasal microbiota in response to parenteral antimicrobial administration. Microbial Pathogenesis. 2018 Aug;121:210–7.

49. Weese J, Slifierz M, Jalali M, Friendship R. Evaluation of the nasal microbiota in slaughter-age pigs and the impact on nasal methicillin-resistant *Staphylococcus aureus* (MRSA) carriage. BMC Vet Res. 2014;10(1):69.

50. Obregon-Gutierrez P, Bonillo-Lopez L, Correa-Fiz F, Sibila M, Segalés J, Kochanowski K, et al. Gut-associated microbes are present and active in the pig nasal cavity. Sci Rep. 2024 Apr 11;14(1):8470.

51. Correa-Fiz F, Neila-Ibáñez C, López-Soria S, Napp S, Martinez B, Sobrevia L, et al. Feed additives for the control of post-weaning *Streptococcus suis* disease and the effect on the faecal and nasal microbiota. Sci Rep. 2020 Nov 23;10(1):20354.

52. Obregon-Gutierrez P, Aragon V, Correa-Fiz F. Sow contact is a major driver in the development of the nasal microbiota of piglets. Pathogens. 2021 Jun 3;10(6):697.

53. Browne HP, Shao Y, Lawley TD. Mother–infant transmission of human microbiota. Current Opinion in Microbiology. 2022 Oct;69:102173.

54. Liu B, Zhu X, Cui Y, Wang W, Liu H, Li Z, et al. Consumption of dietary fiber from different sources during pregnancy alters sow gut microbiota and improves performance and reduces inflammation in sows and piglets. Byndloss MX, editor. mSystems. 2021 Feb 23;6(1):e00591-20.

55. Nowland T, Plush K, Barton M, Kirkwood R. Development and function of the intestinal microbiome and potential implications for pig production. Animals. 2019 Feb 28;9(3):76.

56. Akkerman R, Faas MM, De Vos P. Non-digestible carbohydrates in infant formula as substitution for human milk oligosaccharide functions: effects on microbiota and gut maturation. Critical Reviews in Food Science and Nutrition. 2019 May 15;59(9):1486–97.

57. Bosch AATM, Levin E, Van Houten MA, Hasrat R, Kalkman G, Biesbroek G, et al. Development of upper respiratory tract microbiota in infancy is affected by mode of delivery. EBioMedicine. 2016 Jul;9:336–45.

58. Ríos-Covian D, Langella P, Martín R. From Short- to long-term effects of C-section delivery on microbiome establishment and host health. Microorganisms. 2021 Oct 9;9(10):2122.

59. Kim H, Sitarik AR, Woodcroft K, Johnson CC, Zoratti E. Birth mode, breastfeeding, pet exposure, and antibiotic use: associations with the gut microbiome and sensitization in children. Curr Allergy Asthma Rep. 2019 Apr;19(4):22.

60. Notarbartolo V, Giuffrè M, Montante C, Corsello G, Carta M. Composition of human breast milk microbiota and its role in children's health. Pediatr Gastroenterol Hepatol Nutr. 2022;25(3):194.

61. Morissette B, Talbot G, Beaulieu C, Lessard M. Growth performance of piglets during the first two weeks of lactation affects the development of the intestinal microbiota. Animal Physiology Nutrition. 2018 Apr;102(2):525–32.

62. Campbell JM, Crenshaw JD, Polo J. The biological stress of early weaned piglets. J Animal Sci Biotechnol. 2013 Dec;4(1):19.

63. Guevarra RB, Lee JH, Lee SH, Seok MJ, Kim DW, Kang BN, et al. Piglet gut microbial shifts early in life: causes and effects. J Animal Sci Biotechnol. 2019 Dec;10(1):1.

64. Blanco-Fuertes M, Correa-Fiz F, López-Serrano S, Sibila M, Aragon V. Sow vaccination against virulent *Glaesserella parasuis* shapes the nasal microbiota of their offspring. Sci Rep. 2022 Dec;12(1):3357.

65. Van Sambeek DM, Tran H, Fernando SC, Ciobanu DC, Miller PS, Burkey TE. Alteration of the pig intestinal microbiome when vaccinated against or inoculated with porcine circovirus 2 using a multivariate analysis model1. Journal of Animal Science. 2016 Sep 1;94(suppl_3):387–90.

66. Yuan F, Sharma J, Nanjappa SG, Gaulke CA, Fang Y. Effect of Killed PRRSV Vaccine on gut microbiota diversity in pigs. Viruses. 2022 May 18;14(5):1081.

67. Hiergeist A, Gläsner J, Reischl U, Gessner A. Analyses of intestinal microbiota: culture versus sequencing: Figure 1. ILAR J. 2015 Aug 31;56(2):228–40.

68. Wang WL, Xu SY, Ren ZG, Tao L, Jiang JW, Zheng SS. Application of metagenomics in the human gut microbiome. WJG. 2015;21(3):803.

69. Lagier JC, Dubourg G, Million M, Cadoret F, Bilen M, Fenollar F, et al. Culturing the human microbiota and culturomics. Nat Rev Microbiol. 2018 Sep;16(9):540–50.

70. Lee JY. The Principles and applications of High-Throughput Sequencing Technologies. Dev Reprod. 2023 Apr;27(1):9–24.

71. Pollock J, Glendinning L, Wisedchanwet T, Watson M. The madness of microbiome: attempting to find consensus "best practice" for 16S microbiome studies. Liu SJ, editor. Appl Environ Microbiol. 2018 Apr;84(7):e02627-17.

72. Hu T, Chitnis N, Monos D, Dinh A. Next-generation sequencing technologies: an overview. Human Immunology. 2021 Nov;82(11):801–11.

73. Sanger F, Nicklen S, Coulson AR. DNA sequencing with chain-terminating inhibitors. Proc Natl Acad Sci USA. 1977 Dec;74(12):5463–7.

74. Johnson JS, Spakowicz DJ, Hong BY, Petersen LM, Demkowicz P, Chen L, et al. Evaluation of 16S rRNA gene sequencing for species and strain-level microbiome analysis. Nat Commun. 2019 Nov 6;10(1):5029.

75. Pallares FJ. Economic impact of respiratory diseases in pig [Internet]. [accessed on 01/04/2025]. Available from: https://swinehealth.ceva.com/blog/economic-impact-of-respiratory-diseases-in-pigs

76. Truszczynski MJ. The role and importance of veterinary laboratories in the prevention and control of infectious diseases of animals. Rev Sci Tech OIE. 1998 Aug 1;17(2):405–10.

77. Yon L, Duff JP, Ågren EO, Erdélyi K, Ferroglio E, Godfroid J, et al. Recent changes in infectious diseases in european wildlife. Journal of Wildlife Diseases. 2019 Jan 1;55(1):3.

78. Aragon V, Cerdà-Cuéllar M, Fraile L, Mombarg M, Nofrarías M, Olvera A, et al. Correlation between clinico-pathological outcome and typing of *Haemophilus parasuis* field strains. Veterinary Microbiology. 2010 May;142(3–4):387–93.

79. Aragon V, Segales J, AW T. Glässer's disease. In: Diseases of Swine. 11th ed. 2019. p. 844–53.

80. Gottschalk M, Segura M. Streptococcosis. In: Diseases of Swine. 11th ed. Wiley; 2019. p. 934–50.

81. Pieters M, Maes D. Mycoplasmosis. In: Diseases of Swine. 11th ed. Wiley; 2019. p. 863–83.

82. Salogni C, Lazzaro M, Giovannini S, Vitale N, Boniotti MB, Pozzi P, et al. Causes of swine polyserositis in a high-density breeding area in Italy. J VET Diagn Invest. 2020 Jul;32(4):594–7.

83. Palzer A, Haedke K, Heinritzi K, Zoels S, Ladinig A, Ritzmann M. Associations among *Haemophilus parasuis*, *Mycoplasma hyorhinis*, and porcine reproductive and respiratory syndrome virus infections in pigs with polyserositis. Can Vet J. 2015 Mar;56(3):285-7.

84. Costa-Hurtado M, Barba-Vidal E, Maldonado J, Aragon V. Update on Glässer's disease: How to control the disease under restrictive use of antimicrobials. Veterinary Microbiology. 2020 Mar;242:108595.

85. Cerdà-Cuéllar M, Naranjo JF, Verge A, Nofrarías M, Cortey M, Olvera A, et al. Sow vaccination modulates the colonization of piglets by *Haemophilus parasuis*. Veterinary Microbiology. 2010 Oct;145(3–4):315–20.

86. Bello-Orti B, Costa-Hurtado M, Martinez-Moliner V, Segalés J, Aragon V. Time course *Haemophilus parasuis* infection reveals pathological differences between virulent and non-virulent strains in the respiratory tract. Veterinary Microbiology. 2014 Jun;170(3–4):430–7.

87. Olvera A, Calsamiglia M, Aragon V. Genotypic Diversity of *Haemophilus parasuis* Field Strains. Appl Environ Microbiol. 2006 Jun;72(6):3984–92.

88. Guo M, Yang K, Lin S, Tang J, Liu M, Zhou H, et al. Coinfection with porcine circovirus type 2 and *Glaesserella parasuis* serotype 4 enhances pathogenicity in piglets. Veterinary Microbiology. 2023 Mar;278:109663.

89. Jiang N, Liu H, Wang P, Huang J, Han H, Wang Q. Illumina MiSeq Sequencing investigation of microbiota in Bronchoalveolar Lavage Fluid and cecum of the swine infected with PRRSV. Curr Microbiol. 2019 Feb;76(2):222–30.

90. Pomorska-Mól M, Dors A, Kwit K, Czyżewska-Dors E, Pejsak Z. Coinfection modulates inflammatory responses, clinical outcome and pathogen load of H1N1 swine influenza virus and *Haemophilus parasuis* infections in pigs. BMC Vet Res. 2017 Dec;13(1):376.

91. Neila-Ibáñez C, Casal J, Hennig-Pauka I, Stockhofe-Zurwieden N, Gottschalk M, Migura-García L, et al. Stochastic assessment of the economic impact of *Streptococcus suis*-associated disease in German, Dutch and Spanish swine farms. Front Vet Sci. 2021 Aug 19;8:676002.

92. Vötsch D, Willenborg M, Weldearegay YB, Valentin-Weigand P. *Streptococcus suis* – The "two faces" of a pathobiont in the porcine respiratory tract. Front Microbiol. 2018 Mar 15;9:480.

93. Gottschalk M, Segura M, Xu J. *Streptococcus suis* infections in humans: the Chinese experience and the situation in North America. Anim Health Res Rev. 2007 Jun;8(1):29–45.

94. Tang J, Wang C, Feng Y, Yang W, Song H, Chen Z, et al. Streptococcal Toxic Shock Syndrome caused by *Streptococcus suis* serotype 2. Vincent JL, editor. PLoS Med. 2006 Apr 11;3(5):e151.

95. Lun ZR, Wang QP, Chen XG, Li AX, Zhu XQ. *Streptococcus suis*: an emerging zoonotic pathogen. The Lancet Infectious Diseases. 2007 Mar;7(3):201–9.

96. Segura M, Calzas C, Grenier D, Gottschalk M. Initial steps of the pathogenesis of the infection caused by *Streptococcus suis*: fighting against nonspecific defenses. FEBS Lett. 2016 Nov;590(21):3772–99.

97. Bleuzé M, Gottschalk M, Segura M. Neutrophils in *Streptococcus suis* infection: from host defense to pathology. Microorganisms. 2021 Nov 20;9(11):2392.

98. Li J, Wang J, Liu Y, Yang J, Guo L, Ren S, et al. Porcine reproductive and respiratory syndrome virus NADC 30-like strain accelerates *Streptococcus suis* serotype 2 infection in vivo and *in vitro*. Transbound Emerg Dis. 2019 Mar;66(2):729–42.

99. Obradovic MR, Segura M, Segalés J, Gottschalk M. Review of the speculative role of co-infections in *Streptococcus suis*-associated diseases in pigs. Vet Res. 2021 Mar 20;52(1):49.

100. Clavijo MJ, Davies P, Morrison R, Bruner L, Olson S, Rosey E, et al. Temporal patterns of colonization and infection with *Mycoplasma hyorhinis* in two swine production systems in the USA. Veterinary Microbiology. 2019 Jul;234:110–8.

101. Razin S. Peculiar properties of mycoplasmas: The smallest self-replicating prokaryotes. FEMS Microbiol Lett. 1992 Dec 15;100(1-3):423-31.

102. Bünger M, Brunthaler R, Unterweger C, Loncaric I, Dippel M, Ruczizka U, et al. *Mycoplasma hyorhinis* as a possible cause of fibrinopurulent meningitis in pigs? - a case series. Porc Health Manag. 2020 Dec;6(1):38.

103. Goiš M, Kuksa F, Skišák F. Experimental infection of gnotobiotic piglets with *Mycoplasma hyorhinis* and *Bordetella bronchiseptica*. Zentralblatt für Veterinärmedizin Reihe B. 1977 Mar;24(2):89–96.

104. Hennig-Pauka I, Sudendey C, Kleinschmidt S, Ruppitsch W, Loncaric I, Spergser J. Swine conjunctivitis associated with a novel *Mycoplasma* species closely related to *Mycoplasma hyorhinis*. Pathogens. 2020 Dec 25;10(1):13.

105. Morita T, Ohiwa S, Shimada A, Kazama S, Yagihashi T, Umemura T. Intranasally inoculated *Mycoplasma hyorhinis* causes eustachitis in pigs. Vet Pathol. 1999 Mar;36(2):174–8.

106. Clavijo MJ, Sreevatsan S, Johnson TJ, Rovira A. Molecular epidemiology of *Mycoplasma hyorhinis* porcine field isolates in the United States. Lin B, editor. PLoS ONE. 2019 Oct 21;14(10):e0223653.

107. Goiš M, Pospišil Z, Černy M, Mrva V. Production of pneumonia after intranasal inoculation of gnotobiotic piglets with three strains of *Mycoplasma hyorhinis*. Journal of Comparative Pathology. 1971 Jul;81(3):401-IN19.

108. Lin J, Chen S, Yeh K, Weng C. *Mycoplasma hyorhinis* in Taiwan: Diagnosis and isolation of swine pneumonia pathogen. Veterinary Microbiology. 2006 Jun 15;115(1–3):111–6.

109. Fourour S, Tocqueville V, Paboeuf F, Lediguerher G, Morin N, Kempf I, et al. Pathogenicity study of *Mycoplasma hyorhinis* and *M. flocculare* in specific-pathogen-free pigs pre-infected with *M. hyopneumoniae*. Veterinary Microbiology. 2019 May;232:50–7.

110. Gagnon CA, Tremblay D, Tijssen P, Venne MH, Houde A, Elahi SM. The emergence of porcine circovirus 2b genotype (PCV-2b) in swine in Canada. 48.

111. Lee JA, Oh YR, Hwang MA, Lee JB, Park SY, Song CS, et al. Mycoplasma hyorhinis is a potential pathogen of porcine respiratory disease complex that aggravates pneumonia caused by porcine reproductive and respiratory syndrome virus. Veterinary Immunology and Immunopathology. 2016 Sep;177:48–51.

112. Fredriksen S, Neila-Ibáñez C, Hennig-Pauka I, Guan X, Dunkelberger J, De Oliveira IF, et al. *Streptococcus suis* infection on European farms is associated with an altered tonsil microbiome and resistome. Microb Genom. 2024 Dec;10(12):001334.

113. Frana TS., Hau SJ. Staphylococcosis. In: Diseases of Swine. 11th ed. Wiley; 2019. p. 926–50.

114. Patel S, Vlasblom AA, Verstappen KM, Zomer AL, Fluit AC, Rogers MRC, et al. Differential analysis of longitudinal methicillin-resistant *Staphylococcus aureus* colonization in

relation to microbial shifts in the nasal microbiome of neonatal piglets. Sharpton TJ, editor. mSystems. 2021 Aug 31;6(4):10.1128/msystems.00152-21.

115. Obregon-Gutierrez P, Cortey M, Martín-Valls GE, Clilverd H, Correa-Fiz F, Aragón V, et al. Nasal microbial diversity is associated with survival in piglets infected by a highly virulent PRRSV-1 strain. Anim microbiome. 2025 Jan 17;7(1):9.

116. Yuan F, Yang L, Hsiao SH, Herndon NL, Gaulke CA, Fang Y. A neonatal piglet model reveals interactions between nasal microbiota and influenza A virus pathogenesis. Virology. 2024 Apr;592:109996.

117. Patel J, Harant A, Fernandes G, Mwamelo AJ, Hein W, Dekker D, et al. Measuring the global response to antimicrobial resistance, 2020–21: a systematic governance analysis of 114 countries. The Lancet Infectious Diseases. 2023 Jun;23(6):706–18.

118. Evans NA. Tulathromycin: an overview of a new triamilide antibiotic for livestock respiratory disease. Vet Ther. 2005;6(2):83–95.

119. Mark G. Papich JLD. Antimicrobial Therapy. In: Papich Handbook of Veterinary Drugs. Fifth Edition. 2021. p. 571-584.e5.

120. Abushaheen MA, Muzaheed, Fatani AJ, Alosaimi M, Mansy W, George M, et al. Antimicrobial resistance, mechanisms and its clinical significance. Disease-a-Month. 2020 Jun;66(6):100971.

121. Guidelines for the Prudent Use of Antimicrobials in Veterinary Medicine. Official Journal of the European Union (2015/C 299/04). [Internet]. [accessed on 01/04/2025]. Available from: https://ec.europa.eu/health/sites/health/files/antimicrobial_resistance/docs/2015_prudent_use_guidelines_en.pdf [Ref list]

122. Plan Nacional Resistencia Antibióticos [Internet]. [accessed on 01/04/2025]. Available from: https://www.resistenciaantibioticos.es/es

123. World Health Organization [Internet]. [accessed on 01/04/2025]. Available from: https://www.who.int/news-room/fact-sheets/detail/antimicrobial-resistance

124. Tang KWK, Millar BC, Moore JE. Antimicrobial Resistance (AMR). Br J Biomed Sci. 2023 Jun 28;80:11387.

125. Karriker LA, Coetzee JF, Friendship R, Apley, Michael D. Drug pharmacology, therapy, and prophylaxis. In: Diseases of Swine. 11th ed. Wiley; 2019. p. 158–70.

126. Blanco-Fuertes M, Sibila M, Franzo G, Obregon-Gutierrez P, Illas F, Correa-Fiz F, et al. Ceftiofur treatment of sows results in long-term alterations in the nasal microbiota of

the fffspring that can be ameliorated by inoculation of nasal colonizers. Anim Microbiome. 2023 Oct 20;5(1):53.

127. Correa-Fiz F, Gonçalves dos Santos JM, Illas F, Aragon V. Antimicrobial removal on piglets promotes health and higher bacterial diversity in the nasal microbiota. Sci Rep. 2019 Dec;9(1):6545.

128. Mou KT, Allen HK, Alt DP, Trachsel J, Hau SJ, Coetzee JF, et al. Shifts in the nasal microbiota of swine in response to different dosing regimens of oxytetracycline administration. Veterinary Microbiology. 2019 Oct;237:108386.

129. Liu H, Xue Q, Zeng Q, Zhao Z. *Haemophilus parasuis* vaccines. Veterinary Immunology and Immunopathology. 2016 Nov;180:53–8.

130. Mayer L, Liedel C, Klose K, De Greeff A, Rieckmann K, Baums CG. Immunogenicities of vaccines including the immunoglobulin M-degrading enzyme of Streptococcus suis, rIde, and protective efficacy against serotype 14 in piglets. Vaccine: X. 2024 Dec;21:100590.

131. Porcilis streptsuis 1488 ESP [package insert]. Ministerio de Sanidad, Servicios sociales e Igualdad. Agencia Española de Medicamentos y Productos Sanitarios, España. Merck Sharp & Dohme Animal Health S.L.; 2022

132. Corsaut L, Martelet L, Goyette-Desjardins G, Beauchamp G, Denicourt M, Gottschalk M, et al. Immunogenicity study of a *Streptococcus suis* autogenous vaccine in preparturient sows and evaluation of passive maternal immunity in piglets. BMC Vet Res. 2021 Dec;17(1):72.

133. Dellagostin D, Klein RL, Giacobbo I, Guizzo JA, Dazzi CC, Prigol SR, et al. TbpBY167A-based vaccine is safe in pregnant sows and induces high titers of maternal derived antibodies that reduce *Glaesserella parasuis* colonization in piglets. Veterinary Microbiology. 2023 Jan;276:109630.

134. Jeffery A, Gilbert M, Corsaut L, Gaudreau A, Obradovic MR, Cloutier S, et al. Immune response induced by a *Streptococcus suis* multi-serotype autogenous vaccine used in sows to protect post-weaned piglets. Vet Res. 2024 May 7;55(1):57.

135. Kralova N, Stepanova H, Gebauer J, Norek A, Matiaskova K, Zouharova M, et al. Vaccine against *Streptococcus suis* Infection in Pig Based on Alternative Carrier Protein Conjugate. Vaccines. 2022 Sep 27;10(10):1620.

136. López-Serrano S, Mahmmod YS, Christensen D, Ebensen T, Guzmán CA, Rodríguez F, et al. Immune responses following neonatal vaccination with conserved F4 fragment of

VtaA proteins from virulent *Glaesserella parasuis* adjuvanted with CAF®01 or CDA. Vaccine: X. 2023 Aug;14:100330.

137. Ramos Prigol S, Klein R, Chaudhuri S, Paraboni Frandoloso G, Guizzo JA, Gutiérrez Martín CB, et al. TbpBY167A-Based Vaccine Can Protect Pigs against Glässer's Disease Triggered by *Glaesserella parasuis* SV7 Expressing TbpB Cluster I. Pathogens. 2022 Jul 4;11(7):766.

138. Wei YW, Zhu HZ, Huang LP, Xia DL, Wu HL, Bian HQ, et al. Efficacy in pigs of a new inactivated vaccine combining porcine circovirus type 2 and *Mycoplasma hyorhinis*. Veterinary Microbiology. 2020 Mar;242:108588.

139. Zubair M, Wang J, Yu Y, Rasheed MA, Faisal M, Dawood AS, et al. Conserved Domains in Variable Surface Lipoproteins A-G of *Mycoplasma hyorhinis* May Serve as Probable Multi-Epitope Candidate Vaccine: Computational Reverse Vaccinology Approach. Veterinary Sciences. 2023 Sep 5;10(9):557.

140. Łojewska E, Sakowicz T. An Alternative to Antibiotics: Selected Methods to Combat Zoonotic Foodborne Bacterial Infections. Curr Microbiol. 2021 Dec;78(12):4037–49.

141. Yadav MK, Kumari I, Singh B, Sharma KK, Tiwari SK. Probiotics, prebiotics and synbiotics: safe options for next-generation therapeutics. Appl Microbiol Biotechnol. 2022 Jan;106(2):505–21.

142. Mosca F, Gianni ML, Rescigno M. Can postbiotics represent a new strategy for NEC? In: Guandalini S, Indrio F, editors. Probiotics and Child Gastrointestinal Health. Adv Exp Med Biol. 2019;1125:37-45.

143. Tsilingiri K, Rescigno M. Postbiotics: what else? BM. 2013 Mar 1;4(1):101–7.

144. Rattigan R, Wajda L, Vlasblom AA, Wolfe A, Zomer AL, Duim B, et al. Safety Evaluation of an intranasally applied cocktail of *Lactococcus lactis* strains in pigs. Animals. 2023 Nov 8;13(22):3442.

145. Yang Y, Jing Y, Yang J, Yang Q. Effects of intranasal administration with *Bacillus subtilis* on immune cells in the nasal mucosa and tonsils of piglets. Exp Ther Med. 2018 Jun;15(6):5189-5198.

146. Jennings SAV, Clavel T. Synthetic communities of gut microbes for basic research and translational approaches in animal health and nutrition. Annu Rev Anim Biosci. 2024 Feb 15;12(1):283–300.

147. Brugiroux S, Beutler M, Pfann C, Garzetti D, Ruscheweyh HJ, Ring D, et al. Genome-guided design of a defined mouse microbiota that confers colonization resistance

against *Salmonella enterica* serovar Typhimurium. Nat Microbiol. 2016 Nov 21;2(2):16215.

148. Medlock GL, Carey MA, McDuffie DG, Mundy MB, Giallourou N, Swann JR, et al. Inferring metabolic mechanisms of interaction within a defined gut microbiota. Cell Systems. 2018 Sep;7(3):245-257.e7.

149. Pérez Escriva P, Fuhrer T, Sauer U. Distinct N and cross-feeding networks in a synthetic mouse gut vonsortium. Sharpton TJ, editor. mSystems. 2022 Apr 26;7(2):e01484-21.

150. Weiss AS, Burrichter AG, Durai Raj AC, Von Strempel A, Meng C, Kleigrewe K, et al. *In vitro* interaction network of a synthetic gut bacterial community. The ISME Journal. 2022 Apr 1;16(4):1095–109.

151. Weiss AS, Niedermeier LS, Von Strempel A, Burrichter AG, Ring D, Meng C, et al. Nutritional and host environments determine community ecology and keystone species in a synthetic gut bacterial community. Nat Commun. 2023 Aug 8;14(1):4780.

152. Brugger SD, Eslami SM, Pettigrew MM, Escapa IF, Henke MT, Kong Y, et al. *Dolosigranulum pigrum* cooperation and competition in human nasal microbiota. D'Orazio SEF, editor. mSphere. 2020 Oct 28;5(5):e00852-20.

153. Stubbendieck RM, Dissanayake E, Burnham PM, Zelasko SE, Temkin MI, Wisdorf SS, et al. *Rothia* from the human nose inhibit *Moraxella catarrhalis* colonization with a secreted peptidoglycan endopeptidase. Graf J, editor. mBio. 2023 Apr 25;14(2):e00464-23.

154. Cisneros M, Blanco-Fuertes M, Lluansí A, Brotons P, Henares D, Pérez-Argüello A, et al. Inhibitory effect of *Dolosigranulum pigrum* and *Corynebacterium pseudodiphtheriticum* on pneumococcal *in vitro* growth. BioRxiv [Preprint]. 2025.

155. Laux C, Peschel A, Krismer B. *Staphylococcus aureus* Colonization of the human nose and interaction with other microbiome members. Fischetti VA, Novick RP, Ferretti JJ, Portnoy DA, Braunstein M, Rood JI, editors. Microbiol Spectr. 2019 Apr 12;7(2):7.2.34.

156. Liu CM, Price LB, Hungate BA, Abraham AG, Larsen LA, Christensen K, et al. *Staphylococcus aureus* and the ecology of the nasal microbiome. Sci Adv. 2015 Jun 5;1(5):e1400216.

157. Aguilar C, Alves Da Silva M, Saraiva M, Neyazi M, Olsson IAS, Bartfeld S. Organoids as host models for infection biology – a review of methods. Exp Mol Med. 2021 Oct;53(10):1471–82.

158. Guo D, Zhang L, Wang X, Zheng J, Lin S. Establishment methods and research progress of livestock and poultry immortalized cell lines: A review. Front Vet Sci. 2022 Sep 2;9:956357.

159. Stacey G, MacDonald C. Immortalisation of Primary Cells. In: Stacey GN, Doyle A, Ferro M, editors. Cell Biol Toxicol. 2001;17(4-5):231-46.

160. Ma B, Hua K, Zhou S, Zhou H, Chen Y, Luo R, et al. *Haemophilus parasuis* infection activates NOD1/2-RIP2 signaling pathway in PK-15 cells. Developmental & Comparative Immunology. 2018 Feb;79:158–65.

161. Xiong Q, Wang J, Ji Y, Ni B, Zhang B, Ma Q, et al. The functions of the variable lipoprotein family of *Mycoplasma hyorhinis* in adherence to host cells. Veterinary Microbiology. 2016 Apr;186:82–9.

162. Zhang Y, Li Y, Yuan W, Xia Y, Shen Y. Autophagy is associated with pathogenesis of *Haemophilus parasuis*. Front Microbiol. 2016 Sep; 7:1423.

163. López-Serrano S, Galofré-Milà N, Costa-Hurtado M, Pérez-de-Rozas AM, Aragon V. Heterogeneity of *Moraxella* isolates found in the nasal cavities of piglets. BMC Vet Res. 2020 Dec;16(1):28.

164. Lorenzo De Arriba M, Lopez-Serrano S, Galofre-Mila N, Aragon V. Characterisation of *Bergeyella* spp. isolated from the nasal cavities of piglets. The Veterinary Journal. 2018 Apr;234:1–6.

165. Auger E, Deslandes V, Ramjeet M, Contreras I, Nash JHE, Harel J, et al. Host-pathogen interactions of *Actinobacillus pleuropneumoniae* with Porcine Lung and Tracheal Epithelial Cells. Infect Immun. 2009 Apr;77(4):1426–41.

166. Dang Y, Lachance C, Wang Y, Gagnon CA, Savard C, Segura M, et al. Transcriptional approach to study porcine tracheal epithelial cells individually or dually infected with swine influenza virus and *Streptococcus suis*. BMC Vet Res. 2014 Dec;10(1):86.

167. Ferrari M, Scalvini A, Losio MN, Corradi A, Soncini M, Bignotti E, et al. Establishment and characterization of two new pig cell lines for use in virological diagnostic laboratories. Journal of Virological Methods. 2003 Feb;107(2):205–12.

168. Li Y, Guo M, Wang Q, Zhou H, Wu W, Lin H, et al. *Glaesserella parasuis* serotype 5 induces pyroptosis via the RIG-I/MAVS/NLRP3 pathway in swine tracheal epithelial cells. Veterinary Microbiology. 2024 Jul;294:110127.

169. Mathieu-Denoncourt A, Letendre C, Auger JP, Segura M, Aragon V, Lacouture S, et al. Limited interactions between *Streptococcus suis* and *Haemophilus parasuis* in *in vitro* co-infection studies. Pathogens. 2018 Jan 6;7(1):7.

170. Wang X, Wang F, Lin L, Liang W, Liu S, Hua L, et al. Transcriptome Differences in pig tracheal epithelial cells in response to *Pasteurella multocida* infection. Front Vet Sci. 2021 Aug 19;8:682514.

171. Boekema BKHL, Stockhofe-Zurwieden N, Smith HE, Kamp EM, Van Putten JP, Verheijden JH. Adherence of *Actinobacillus pleuropneumoniae* to primary cultures of porcine lung epithelial cells. Veterinary Microbiology. 2003 May;93(2):133–44.

172. Elvert M, Sauerhering L, Heiner A, Maisner A. Isolation of Primary Porcine Bronchial Epithelial Cells for Nipah Virus Infections. Methods Mol Biol. 2023;2682:103-120.

173. Meliopoulos V, Cherry S, Wohlgemuth N, Honce R, Barnard K, Gauger P, et al. Primary Swine Respiratory Epithelial Cell Lines for the efficient isolation and propagation of Influenza A Viruses. Dutch RE, editor. J Virol. 2020 Nov 23;94(24):e01091-20.

174. Sreenivasan CC, Thomas M, Antony L, Wormstadt T, Hildreth MB, Wang D, et al. Development and characterization of swine primary respiratory epithelial cells and their susceptibility to infection by four influenza virus types. Virology. 2019 Feb;528:152–63.

175. Caswell Jeff L., Williams Kurt J. Respiratory system. In: Jubb, Kennedy, and Palmer's pathology of domestic animals. 6th ed. Elsevier; 2016.

176. Davis JD, Wypych TP. Cellular and functional heterogeneity of the airway epithelium. Mucosal Immunology. 2021 Sep;14(5):978–90.

177. Garrod DR, Collins JE. Intercellular junctions and cell adhesion in epithelial cells. In: Fleming TP, editor. Epithelial Organization and Development Dordrecht: Springer Netherlands; 1992. p. 1–52.

178. Glorieux S, Van Den Broeck W, Van Der Meulen KM, Van Reeth K, Favoreel HW, Nauwynck HJ. *In vitro* culture of porcine respiratory nasal mucosa explants for studying the interaction of porcine viruses with the respiratory tract. Journal of Virological Methods. 2007 Jun;142(1–2):105–12.

179. Liu H, Plancarte M, Ball EE, Weiss CM, Gonzales-Viera O, Holcomb K, et al. Respiratory tract explant infection dynamics of Influenza A Virus in California sea lions, northern elephant Seals, and Rhesus Macaques. Parrish CR, editor. J Virol. 2021 Jul 26;95(16):e00403-21.

180. Löndt BZ, Brookes SM, Nash BJ, Núñez A, Stagg DA, Brown IH. The infectivity of pandemic 2009 H1N1 and avian influenza viruses for pigs: an assessment by *ex vivo* respiratory tract organ culture*: *Ex vivo* assessment of infectivity of pandemic H1N1 and HPAI viruses. Influenza and Other Respiratory Viruses. 2013 May;7(3):393–402.

181. Nunes SF, Murcia PR, Tiley LS, Brown IH, Tucker AW, Maskell DJ, et al. An *ex vivo* swine tracheal organ culture for the study of influenza infection. Influenza Resp Viruses. 2010 Jan;4(1):7–15.

182. Oh D, Han S, Tignon M, Balmelle N, Cay AB, Griffioen F, et al. Differential infection behavior of African swine fever virus (ASFV) genotype I and II in the upper respiratory tract. Vet Res. 2023 Dec 15;54(1):121.

183. Punyadarsaniya D, Liang CH, Winter C, Petersen H, Rautenschlein S, Hennig-Pauka I, et al. Infection of differentiated Porcine Airway Epithelial Cells by Influenza Virus: differential susceptibility to infection by porcine and avian viruses. Poon LLM, editor. PLoS ONE. 2011 Dec 9;6(12):e28429.

184. Meng F, Wu NH, Nerlich A, Herrler G, Valentin-Weigand P, Seitz M. Dynamic Virus-Bacterium interactions in a Porcine Precision-Cut Lung Slice coinfection model: Swine Influenza Virus paves the way for *Streptococcus suis* infection in a two-step process. Camilli A, editor. Infect Immun. 2015 Jul;83(7):2806–15.

185. Vötsch D, Willenborg M, Baumgärtner W, Rohde M, Valentin-Weigand P. Bordetella bronchiseptica promotes adherence, colonization, and cytotoxicity of *Streptococcus suis* in a porcine precision-cut lung slice model. Virulence. 2021 Dec 31;12(1):84–95.

186. Dumigan A, Fitzgerald M, Santos JSPG, Hamid U, O'Kane CM, McAuley DF, et al. A Porcine *Ex Vivo* Lung Perfusion Model To Investigate Bacterial Pathogenesis. Allen IC, Goldberg JB, editors. mBio. 2019 Dec 24;10(6):e02802-19.

187. Lee-Ferris RE, Okuda K, Galiger JR, Schworer SA, Rogers TD, Dang H, et al. Prolonged airway explant culture enables study of health, disease, and viral pathogenesis. bioRxiv [Preprint] 2024.

188. Sato T, Vries RG, Snippert HJ, Van De Wetering M, Barker N, Stange DE, et al. Single Lgr5 stem cells build crypt-villus structures *in vitro* without a mesenchymal niche. Nature. 2009 May;459(7244):262–5.

189. Dutta D, Heo I, Clevers H. Disease modeling in stem cell-derived 3D organoid systems. Trends in Molecular Medicine. 2017 May;23(5):393–410.

190. Zhou J, Li C, Sachs N, Chiu MC, Wong BHY, Chu H, et al. Differentiated human airway organoids to assess infectivity of emerging influenza virus. Proc Natl Acad Sci USA. 2018 Jun 26;115(26):6822–7.

191. Aguirre Garcia M, Hillion K, Cappelier JM, Neunlist M, Mahe MM, Haddad N. Intestinal organoids: new tools to comprehend the virulence of bacterial foodborne pathogens. Foods. 2022 Jan 1;11(1):108.

192. Kim MB, Hwangbo S, Jang S, Jo YK. Bioengineered Co-culture of organoids to recapitulate host-microbe interactions. Materials Today Bio. 2022 Dec;16:100345.

193. Chiu MC, Li C, Liu X, Song W, Wan Z, Yu Y, et al. Human Nasal Organoids Model SARS-CoV-2 Upper respiratory infection and recapitulate the differential infectivity of emerging variants. Klein S, editor. mBio. 2022 Aug 30;13(4):e01944-22.

194. Li C, Yu Y, Wan Z, Chiu MC, Huang J, Zhang S, et al. Human respiratory organoids sustained reproducible propagation of human rhinovirus C and elucidation of virus-host interaction. Nat Commun. 2024 Dec 30;15(1):10772.

195. Rajan A, Weaver AM, Aloisio GM, Jelinski J, Johnson HL, Venable SF, et al. The human nose organoid respiratory virus model: an *ex vivo* human challenge model to study respiratory syncytial virus (RSV) and severe acute respiratory syndrome coronavirus 2 (SARS-CoV-2) pathogenesis and evaluate therapeutics. Ackerman ME, editor. mBio. 2022 Feb 22;13(1):e03511-21.

196. Vazquez-Armendariz AI, Tata PR. Recent advances in lung organoid development and applications in disease modeling. Journal of Clinical Investigation. 2023 Nov 15;133(22):e170500.

197. Boyd AI, Kafer LA, Escapa IF, Kambal A, Tariq H, Hilsenbeck SG, et al. Nasal microbionts differentially colonize and elicit cytokines in human nasal epithelial organoids. bioRxiv (Preprint). 2024.

198. Baquerre C, Montillet G, Pain B. Liver organoids in domestic animals: an expected promise for metabolic studies. Vet Res. 2021 Dec;52(1):47.

199. Beaumont M, Blanc F, Cherbuy C, Egidy G, Giuffra E, Lacroix-Lamandé S, et al. Intestinal organoids in farm animals. Vet Res. 2021 Dec;52(1):33.

200. Li M, Guo X, Cheng L, Zhang H, Zhou M, Zhang M, et al. Porcine kidney organoids derived from naïve-like embryonic stem cells. IJMS. 2024 Jan 4;25(1):682.

201. Liu Y, Yang N, Tan C, Zhang Y, Gao S, Cai Y, et al. Wuzhishan miniature pig-derived intestinal 2D monolayer organoids to investigate the enteric coronavirus infection. Front Vet Sci. 2024 Sep 25;11:1457719.

202. Gerhards NM, Vrieling M, Dresken R, Nguyen-van Oort S, Bordes L, Wells JM, et al. Porcine Airway Organoid-derived well-differentiated epithelial cultures as a tool for the characterization of swine influenza a virus strains. Viruses. 2024 Nov 15;16(11):1777.

203. Jiang C, Li L, Xue M, Zhao L, Liu X, Wang W, et al. Long-term expanding Porcine Airway Organoids provide insights into the pathogenesis and innate immunity of porcine

respiratory coronavirus infection. Gallagher T, editor. J Virol. 2022 Jul 27;96(14):e00738-22.

204. Ma P, Fang P, Ren T, Fang L, Xiao S. Porcine Intestinal Organoids: overview of the state of the art. Viruses. 2022 May 21;14(5):1110.

205. Yang J, Wei H, Zhou Y, Szeto CH, Li C, Lin Y, et al. High-fat diet promotes colorectal tumorigenesis through modulating gut microbiota and metabolites. Gastroenterology. 2022 Jan;162(1):135-149.e2.

206. Ethical use of animals in medicine testing. European Medicines Agency (EMA) [Internet]. [accessed on 01/04/2025]. Available from: https://www.ema.europa.eu/en/human-regulatory-overview/research-development/ethical-use-animals-medicine-testing

207. National Centre for the Replacement, Refinement & Reduction of Animals in Research (NC3Rs) [Internet]. [accessed on 01/04/2025]. Available from: https://nc3rs.org.uk/who-we-are/3rs#what-are-the-3rs?

208. Guimarães AI. Are animal models necessary? Exploring (dis)advantages and alternatives. Eur J of Neuroscience. 2025 Jan;61(1):e16651.

209. Hartung T. Thoughts on limitations of animal models. Parkinsonism & Related Disorders. 2008 Jul;14:S81–3.

210. Zhao J, Murray S, LiPuma JJ. Modeling the impact of antibiotic exposure on human microbiota. Sci Rep. 2015 May;4(1):4345.

211. Di Stadio A, Costantini C, Renga G, Pariano M, Ricci G, Romani L. The microbiota/host immune system interaction in the nose to protect from COVID-19. Life. 2020 Dec 11;10(12):345.

212. Cho HJ, Ha JG, Lee SN, Kim CH, Wang DY, Yoon JH. Differences and similarities between the upper and lower airway: focusing on innate immunity. Rhin. 2021 Aug 1;0(0):0–0.

213. Gierse LC, Meene A, Schultz D, Schwaiger T, Schröder C, Mücke P, et al. Influenza A H1N1 induced disturbance of the respiratory and fecal microbiome of German Landrace Pigs – a Multi-Omics characterization. Auchtung JM, editor. Microbiol Spectr. 2021 Oct 31;9(2):e00182-21.

214. Jansman AJM, Zhang J, Koopmans SJ, Dekker RA, Smidt H. Effects of a simple or a complex starter microbiota on intestinal microbiota composition in caesarean derived piglets. Journal of Animal Science. 2012 Dec 1;90(suppl_4):433–5.

215. Faccin JEG, Tokach MD, Allerson MW, Woodworth JC, DeRouchey JM, Dritz SS, et al. Relationship between weaning age and antibiotic usage on pig growth performance and mortality. Journal of Animal Science. 2020 Dec 1;98(12):skaa363.

216. Pearson T, Krantz S, Galina-Pantoja L. The effects of tulathromycin injectable solution on reducing the transmission of swine respiratory pathogens from sows to wean pigs. American Association of Swine Veterinarians. 2016;2016:71–4.

217. Foster DM, Jacob ME, Farmer KA, Callahan BJ, Theriot CM, Kathariou S, et al. Ceftiofur formulation differentially affects the intestinal drug concentration, resistance of fecal *Escherichia coli*, and the microbiome of steers. Mühldorfer K, editor. PLoS ONE. 2019 Oct 4;14(10):e0223378.

218. Pomorska-Mól M, Kwit K, Czyżewska-Dors E, Pejsak Z. Tulathromycin enhances humoral but not cellular immune response in pigs vaccinated against swine influenza. J vet Pharmacol Therap. 2019 May;42(3):318–23.

219. Barko PC, McMichael MA, Swanson KS, Williams DA. The Gastrointestinal microbiome: A review. J Vet Intern Med. 2018 Jan;32(1):9–25.

220. Rutjens S, Vereecke N, De Spiegelaere W, Croubels S, Devreese M. Intestinal exposure to ceftiofur and cefquinome after intramuscular treatment and the impact of ceftiofur on the pig fecal microbiome and resistome. Antibiotics. 2022 Mar 4;11(3):342.

221. Li X, Zheng W, Machesky ML, Yates SR, Katterhenry M. Degradation kinetics and mechanism of antibiotic ceftiofur in recycled water derived from a beef farm. J Agric Food Chem. 2011 Sep 28;59(18):10176–81.

222. Alvarado AC, Chekabab SM, Predicala BZ, Korber DR. Impact of raised without antibiotics measures on antimicrobial resistance and prevalence of pathogens in sow barns. Antibiotics. 2022 Sep 8;11(9):1221.

223. Offre P, Pivato B, Mazurier S, Siblot S, Berta G, Lemanceau P, et al. Microdiversity of *Burkholderiales* associated with mycorrhizal and nonmycorrhizal roots of *Medicago truncatula*: bacterial diversity associated with mycorrhizal roots. FEMS Microbiology Ecology. 2008 Aug;65(2):180–92.

224. Russell JA, Hu Y, Chau L, Pauliushchyk M, Anastopoulos I, Anandan S, et al. Indoor-biofilter growth and exposure to airborne chemicals drive similar changes in plant root bacterial communities. Yates MV, editor. Appl Environ Microbiol. 2014 Aug 15;80(16):4805–13.

225. Stinson LF, Keelan JA, Payne MS. Identification and removal of contaminating microbial DNA from PCR reagents: impact on low-biomass microbiome analyses. Letters in Applied Microbiology. 2019 Jan 1;68(1):2–8.

226. Kennedy KM, De Goffau MC, Perez-Muñoz ME, Arrieta MC, Bäckhed F, Bork P, et al. Questioning the fetal microbiome illustrates pitfalls of low-biomass microbial studies. Nature. 2023 Jan 26;613(7945):639–49.

227. Pena Cortes LC, LeVeque RM, Funk J, Marsh TL, Mulks MH. Development of the tonsillar microbiome in pigs from newborn through weaning. BMC Microbiol. 2018 Dec;18(1):35.

228. Wang Q, Cai R, Huang A, Wang X, Qu W, Shi L, et al. Comparison of oropharyngeal microbiota in healthy piglets and piglets with respiratory disease. Front Microbiol. 2018 Dec 21;9:3218.

229. Lowe BA, Marsh TL, Isaacs-Cosgrove N, Kirkwood RN, Kiupel M, Mulks MH. Defining the 'core microbiome' of the microbial communities in the tonsils of healthy pigs. BMC Microbiol. 2012 Dec;12(1):20.

230. De Greeff A, Schokker D, Roubos-van Den Hil P, Ramaekers P, Vastenhouw SA, Harders F, et al. The effect of maternal antibiotic use in sows on intestinal development in offspring. J Anim Sci. 2020 Jun 1;98(6):skaa181.

231. Moleres J, Santos-López A, Lázaro I, Labairu J, Prat C, Ardanuy C, et al. Novel *bla* $_{ROB-1}$ -Bbearing plasmid conferring resistance to β-lactams in *Haemophilus parasuis* isolates from Healthy weaning pigs. Elliot MA, editor. Appl Environ Microbiol. 2015 May;81(9):3255–67.

232. Gao FZ, Zou HY, Wu DL, Chen S, He LY, Zhang M, et al. Swine farming elevated the proliferation of *Acinetobacter* with the prevalence of antibiotic resistance genes in the groundwater. Environment International. 2020 Mar;136:105484.

233. Mateo-Estrada V, Vali L, Hamouda A, Evans BA, Castillo-Ramírez S. *Acinetobacter baumannii* sampled from cattle and pigs represent novel clones. Visca P, editor. Microbiol Spectr. 2022 Aug 31;10(4):e01289-22.

234. Posthaus H, Kittl S, Tarek B, Bruggisser J. *Clostridium perfringens* type C necrotic enteritis in pigs: diagnosis, pathogenesis, and prevention. J VET Diagn Invest. 2020 Mar;32(2):203–12.

235. Svartström O, Karlsson F, Fellström C, Pringle M. Characterization of *Treponema* spp. isolates from pigs with ear necrosis and shoulder ulcers. Veterinary Microbiology. 2013 Oct;166(3–4):617–23.

236. Nino G, Rodriguez-Martinez CE, Gutierrez MJ. Early microbial–immune interactions and innate immune training of the respiratory system during health and disease. Children. 2021 May 19;8(5):413.

237. Wilcoxon F. Individual comparisons by ranking methods. Biometrics Bulletin. 1945 Dec;1(6):80.

238. Kruskal WH, Wallis WA. Use of ranks in one-criterion variance analysis. Journal of the American Statistical Association. 1952 Dec;47(260):583–621.

239. Benjamini Y, Krieger AM, Yekutieli D. Adaptive linear step-up procedures that control the false discovery rate. Biometrika. 2006 Sep 1;93(3):491–507.

240. Galofré-Milà N, Correa-Fiz F, Lacouture S, Gottschalk M, Strutzberg-Minder K, Bensaid A, et al. A robust PCR for the differentiation of potential virulent strains of *Haemophilus parasuis*. BMC Vet Res. 2017 Dec;13(1):124.

241. Clavijo MJ, Oliveira S, Zimmerman J, Rendahl A, Rovira A. Field evaluation of a quantitative polymerase chain reaction assay for *Mycoplasma hyorhinis*. J VET Diagn Invest. 2014 Nov;26(6):755–60.

242. Bolyen E, Rideout JR, Dillon MR, Bokulich NA, Abnet CC, Al-Ghalith GA, et al. Reproducible, interactive, scalable and extensible microbiome data science using QIIME 2. Nat Biotechnol. 2019 Aug;37(8):852–7.

243. Callahan BJ, McMurdie PJ, Rosen MJ, Han AW, Johnson AJA, Holmes SP. DADA2: High-resolution sample inference from Illumina amplicon data. Nat Methods. 2016 Jul;13(7):581–3.

244. McDonald D, Price MN, Goodrich J, Nawrocki EP, DeSantis TZ, Probst A, et al. An improved Greengenes taxonomy with explicit ranks for ecological and evolutionary analyses of bacteria and archaea. ISME J. 2012 Mar;6(3):610–8.

245. Greengenes data base Vs. 13.8. [Internet]. [accessed on 01/04/2025]. Available from: http://greengenes.microbio.me/greengenes_release/gg_13_8_otus/.

246. Rognes T, Flouri T, Nichols B, Quince C, Mahé F. VSEARCH: a versatile open source tool for metagenomics. PeerJ. 2016 Oct 18;4:e2584.

247. Camacho C, Coulouris G, Avagyan V, Ma N, Papadopoulos J, Bealer K, et al. BLAST+: architecture and applications. BMC Bioinformatics. 2009 Dec;10(1):421.

248. Katoh K, Standley DM. MAFFT Multiple Sequence Alignment Software Version 7: Improvements in performance and usability. Molecular Biology and Evolution. 2013 Apr 1;30(4):772–80.

249. Lane D.J. 6s/23s rRna Sequencing. Nucleic Acid Techniques in Bacterial Systematics. John Wiley and Sons; New York, NY, USA. 1991.:115–75.

250. Price MN, Dehal PS, Arkin AP. FastTree 2 – Approximately maximum-likelihood trees for large alignments. Poon AFY, editor. PLoS ONE. 2010 Mar 10;5(3):e9490.

251. Weiss S, Xu ZZ, Peddada S, Amir A, Bittinger K, Gonzalez A, et al. Normalization and microbial differential abundance strategies depend upon data characteristics. Microbiome. 2017 Dec;5(1):27.

252. Halko N, Martinsson PG, Shkolnisky Y, Tygert M. An Algorithm for the Principal Component Analysis of large data sets. SIAM Journal on Scientific Computing. 2011;33(5):2580–94.

253. Legendre L LP. Numerical Ecology. 3rd ed. Elsevier; 2012.

254. Jaccard P. Nouvelles recherches sur la distribution florale. Bull Société Vaud Des Sci Nat. 1908;44:223–70.

255. Sørensen T.J. A Method of establishing groups of equal amplitude in plant sociology based on similarity of species content and its application to analyses of the vegetation on Danish commons. I kommission hos E Munksgaard. 1948;

256. Vázquez-Baeza Y, Pirrung M, Gonzalez A, Knight R. EMPeror: a tool for visualizing high-throughput microbial community data. GigaSci. 2013 Dec;2(1):16.

257. Oksanen J, Simpson GL, Blanchet FG, Kindt R, Legendre P, Minchin PR, et al. Vegan: Community Ecology Package. R Package Version 2.5-7. [Internet]. 2020. Available from: https://CRAN.R-project.org/package=vegan

258. Anderson MJ. A new method for non-parametric multivariate analysis of variance: non-parametric manova for ecology. Austral Ecology. 2001 Feb;26(1):32–46.

259. Werner JJ, Koren O, Hugenholtz P, DeSantis TZ, Walters WA, Caporaso JG, et al. Impact of training sets on classification of high-throughput bacterial 16s rRNA gene surveys. ISME J. 2012 Jan;6(1):94–103.

260. Jiang L, Amir A, Morton JT, Heller R, Arias-Castro E, Knight R. Discrete False-Discovery Rate improves identification of differentially abundant microbes. Neufeld JD, editor. mSystems. 2017 Dec 26;2(6):e00092-17.

261. Lin H, Peddada SD. Analysis of compositions of microbiomes with bias correction. Nat Commun. 2020 Jul 14;11(1):3514.

262. Osbelt L, Wende M, Almási É, Derksen E, Muthukumarasamy U, Lesker TR, et al. *Klebsiella oxytoca* causes colonization resistance against multidrug-resistant K. pneumoniae in the gut via cooperative carbohydrate competition. Cell Host & Microbe. 2021 Nov;29(11):1663-1679.e7.

263. Eberl C, Weiss AS, Jochum LM, Durai Raj AC, Ring D, Hussain S, et al. *E. coli* enhance colonization resistance against *Salmonella* Typhimurium by competing for galactitol, a context-dependent limiting carbon source. Cell Host & Microbe. 2021 Nov;29(11):1680-1692.e7.

264. Spragge F, Bakkeren E, Jahn MT, B. N. Araujo E, Pearson CF, Wang X, et al. Microbiome diversity protects against pathogens by nutrient blocking. Science. 2023 Dec 15;382(6676):eadj3502.

265. Isaac S, Flor-Duro A, Carruana G, Puchades-Carrasco L, Quirant A, Lopez-Nogueroles M, et al. Microbiome-mediated fructose depletion restricts murine gut colonization by vancomycin-resistant *Enterococcus*. Nat Commun. 2022 Dec 13;13(1):7718.

266. Biggs MB, Medlock GL, Moutinho TJ, Lees HJ, Swann JR, Kolling GL, et al. Systems-level metabolism of the altered Schaedler flora, a complete gut microbiota. The ISME Journal. 2017 Feb 1;11(2):426–38.

267. Hromada S, Qian Y, Jacobson TB, Clark RL, Watson L, Safdar N, et al. Negative interactions determine *Clostridioides difficile* growth in synthetic human gut communities. Molecular Systems Biology. 2021 Oct;17(10):e10355.

268. Venturelli OS, Carr AV, Fisher G, Hsu RH, Lau R, Bowen BP, et al. Deciphering microbial interactions in synthetic human gut microbiome communities. Molecular Systems Biology. 2018 Jun;14(6):e8157.

269. Adolf LA, Heilbronner S. Nutritional Interactions between Bacterial Species Colonising the Human Nasal Cavity: Current Knowledge and Future Prospects. Metabolites. 2022 May 27;12(6):489.

270. Dedrick S, Warrier V, Lemon KP, Momeni B. When does a Lotka-Volterra model represent microbial interactions? Insights from *in vitro* nasal bacterial communities. Lurgi M, editor. mSystems. 2023 Jun 29;8(3):e00757-22.

271. Lopes W, Amor DR, Gore J. Cooperative growth in microbial communities is a driver of multistability. Nat Commun. 2024 Jun 3;15(1):4709.

272. Lorenzo de Arriba, Montserrat. Characterization of *Bergeyella* and other bacteria isolated from the nasal cavities of piglets. 2016.

273. Goyette-Desjardins G, Auger JP, Xu J, Segura M, Gottschalk M. *Streptococcus suis*, an important pig pathogen and emerging zoonotic agent—an update on the worldwide distribution based on serotyping and sequence typing. Emerging Microbes & Infections. 2014 Jan;3(1):1–20.

274. Moreno LZ, Matajira CEC, Gomes VTM, Silva APS, Mesquita RE, Christ APG, et al. Molecular and antimicrobial susceptibility profiling of atypical *Streptococcus* species from porcine clinical specimens. Infection, Genetics and Evolution. 2016 Oct;44:376–81.

275. Olvera A, Ballester M, Nofrarias M, Sibila M, Aragon V. Differences in phagocytosis susceptibility in *Haemophilus parasuis* strains. Vet Res. 2009 May;40(3):24.

276. Costa-Hurtado M, Olvera A, Martinez-Moliner V, Galofré-Milà N, Martínez P, Dominguez J, et al. Changes in macrophage phenotype after infection of pigs with *Haemophilus parasuis* strains with different levels of virulence. Blanke SR, editor. Infect Immun. 2013 Jul;81(7):2327–33.

277. Zaslaver A, Bren A, Ronen M, Itzkovitz S, Kikoin I, Shavit S, et al. A comprehensive library of fluorescent transcriptional reporters for *Escherichia coli*. Nat Methods. 2006 Aug;3(8):623–8.

278. Aidelberg G, Towbin BD, Rothschild D, Dekel E, Bren A, Alon U. Hierarchy of non-glucose sugars in *Escherichia coli*. BMC Syst Biol. 2014 Dec;8(1):133.

279. Nicholson TL, Waack U, Anderson TK, Bayles DO, Zaia SR, Goertz I, et al. Comparative virulence and genomic analysis of *Streptococcus suis* isolates. Front Microbiol. 2021 Jan 26;11:620843.

280. Nielsen DW, Hau SJ, Mou KT, Alt DP, Brockmeier SL. Shifts in the swine nasal microbiota following *Bordetella bronchiseptica* challenge in a longitudinal study. Front Microbiol. 2023 Sep 29;14:1260465.

281. Chrun T, Leng J, La Ragione RM, Graham SP, Tchilian E. Changes in the nasal microbiota of pigs following single or co-infection with porcine reproductive and respiratory syndrome and Swine Influenza A Viruses. Pathogens. 2021 Sep 22;10(10):1225.

282. Strube ML, Hansen JE, Rasmussen S, Pedersen K. A detailed investigation of the porcine skin and nose microbiome using universal and *Staphylococcus* specific primers. Sci Rep. 2018 Aug 24;8(1):12751.

283. Bonillo-Lopez L, Obregon-Gutierrez P, Huerta E, Correa-Fiz F, Sibila M, Aragon V. Intensive antibiotic treatment of sows with parenteral crystalline ceftiofur and

tulathromycin alters the composition of the nasal microbiota of their offspring. Vet Res. 2023 Nov 24;54(1):112.

284. Lemon KP. Human nasal microbiota. Current Biology. 2020 Oct;30(19):R1118–9.

285. Escapa IF, Chen T, Huang Y, Gajare P, Dewhirst FE, Lemon KP. New insights into human nostril microbiome from the expanded human oral microbiome database (eHOMD): a resource for the microbiome of the human aerodigestive tract. Xu J, editor. mSystems. 2018 Oct 30;3(6):10.1128/msystems.00187-18.

286. Palmer JD, Foster KR. Bacterial species rarely work together. Science. 2022 May 6;376(6593):581–2.

287. Brugger SD, Bomar L, Lemon KP. Commensal–pathogen interactions along the human nasal passages. Hogan DA, editor. PLoS Pathog. 2016 Jul 7;12(7):e1005633.

288. Uehara Y, Nakama H, Agematsu K, Uchida M, Kawakami Y, Abdul Fattah ASM, et al. Bacterial interference among nasal inhabitants: eradication of *Staphylococcus aureus* from nasal cavities by artificial implantation of *Corynebacterium* sp. Journal of Hospital Infection. 2000 Feb;44(2):127–33.

289. Sultana KN, Kuldeep J, Siddiqi MI, Srivastava SK. Crystallographic and molecular dynamics simulation analysis of NAD synthetase from methicillin resistant *Staphylococcus aureus* (MRSA). International Journal of Biological Macromolecules. 2020 Dec;165:2349–62.

290. Sultana KN, Srivastava SK. Structural and molecular dynamics of ammonia transport in *Staphylococcus aureus* NH_3-dependent NAD synthetase. International Journal of Biological Macromolecules. 2022 Apr;203:593–600.

291. Oliveira S. *Haemophilus parasuis* diagnostics. JSHAP. 2007 Mar 1;15(2):99–103.

292. Hardy BL, Merrell DS. Friend or foe: interbacterial competition in the nasal cavity. Margolin W, editor. J Bacteriol. 2021 Feb 8;203(5):e00480-20.

293. Goeteyn E, Grassi L, Van Den Bossche S, Rigauts C, Vande Weygaerde Y, Van Braeckel E, et al. Commensal bacteria of the lung microbiota synergistically inhibit inflammation in a three-dimensional epithelial cell model. Front Immunol. 2023 Apr 21;14:1176044.

294. Aranda-Díaz A, Ng KM, Thomsen T, Real-Ramírez I, Dahan D, Dittmar S, et al. Establishment and characterization of stable, diverse, fecal-derived *in vitro* microbial communities that model the intestinal microbiota. Cell Host & Microbe. 2022 Feb;30(2):260-272.e5.

295. Gottschalk Marcelo, Broes André. Actinobacillosis. In: Diseases of Swine. 11th ed. Wiley; 2019. p. 749–65.

296. Farne H, Groves HT, Gill SK, Stokes I, McCulloch S, Karoly E, et al. Comparative metabolomic sampling of upper and lower airways by four different methods to identify biochemicals that may support bacterial growth. Front Cell Infect Microbiol. 2018 Dec 18;8:432.

297. Krismer B, Liebeke M, Janek D, Nega M, Rautenberg M, Hornig G, et al. Nutrient limitation governs *Staphylococcus aureus* metabolism and niche adaptation in the human nose. Gilmore MS, editor. PLoS Pathog. 2014 Jan 16;10(1):e1003862.

298. Gudis DA, Cohen NA. Cilia Dysfunction. Otolaryngologic clinics of North America. 2010 Jun;43(3):461–72.

299. Zhang N, Van Crombruggen K, Gevaert E, Bachert C. Barrier function of the nasal mucosa in health and type-2 biased airway diseases. Allergy. 2016 Mar;71(3):295–307.

300. Clark SE. Commensal bacteria in the upper respiratory tract regulate susceptibility to infection. Current Opinion in Immunology. 2020 Oct;66:42–9.

301. Ritchie ND, Ijaz UZ, Evans TJ. IL-17 signalling restructures the nasal microbiome and drives dynamic changes following *Streptococcus pneumoniae* colonization. BMC Genomics. 2017 Dec;18(1):807.

302. Lee JT, Kim CM, Ramakrishnan V. Microbiome and disease in the upper airway. Current Opinion in Allergy & Clinical Immunology. 2019 Feb;19(1):1–6.

303. Krunkosky M, Krunkosky TM, Meliopoulos V, Kyriakis CS, Schultz-Cherry S, Tompkins SM. Establishment of swine primary nasal, tracheal, and bronchial epithelial cell culture models for the study of Influenza Virus Infection. Journal of Virological Methods. 2024 Jun;327:114943.

304. Barclay AM, Ninaber DK, Van Veen S, Hiemstra PS, Ottenhoff THM, Van Der Does AM, et al. Airway epithelial cells mount an early response to mycobacterial infection. Front Cell Infect Microbiol. 2023 Sep 26;13:1253037.

305. Ordovas-Montanes J, Dwyer DF, Nyquist SK, Buchheit KM, Vukovic M, Deb C, et al. Allergic inflammatory memory in human respiratory epithelial progenitor cells. Nature. 2018 Aug;560(7720):649–54.

306. Ong HX, Jackson CL, Cole JL, Lackie PM, Traini D, Young PM, et al. Primary Air–Liquid Interface culture of nasal epithelium for nasal drug delivery. Mol Pharmaceutics. 2016 Jul 5;13(7):2242–52.

307. Delgado-Ortega M, Olivier M, Sizaret PY, Simon G, Meurens F. Newborn pig trachea cell line cultured in air-liquid interface conditions allows a partial *in vitro* representation of the porcine upper airway tissue. BMC Cell Biol. 2014 Dec;15(1):14.

308. Gentemann L, Donath S, Seidler AE, Patyk L, Buettner M, Heisterkamp A, et al. Mimicking acute airway tissue damage using femtosecond laser nanosurgery in airway organoids. Front Cell Dev Biol. 2023 Sep 8;11:1268621.

309. Su A, Yan M, Pavasutthipaisit S, Wicke KD, Grassl GA, Beineke A, et al. Infection studies with Airway Organoids from *Carollia perspicillata* indicate that the respiratory epithelium is not a barrier for interspecies transmission of Influenza Viruses. Kibenge FSB, editor. Microbiol Spectr. 2023 Apr 13;11(2):e03098-22.

310. Ettayebi K, Crawford SE, Murakami K, Broughman JR, Karandikar U, Tenge VR, et al. Replication of human noroviruses in stem cell–derived human enteroids. Science. 2016 Sep 23;353(6306):1387–93.

311. Bonillo-Lopez L, Rouam-el Khatab O, Obregon-Gutierrez P, Florez-Sarasa I, Correa-Fiz F, Sibila M, et al. *In vitro* metabolic interaction network of a rationally designed nasal microbiota community. bioRxiv [Preprint]. 2024.

312. West SR, Suddaby AB, Lewin GR, Ibberson CB. *Rothia*. Trends in Microbiology. 2024 Jul;32(7):720–1.

313. Wang Q, Chang X, Liu M, Lu Q, Zhu M, Lin H, et al. *Glaesserella parasuis* serotype 4 HPS4-YC disrupts the integrity of the swine tracheal epithelial barrier and facilitates bacterial translocation. Vet Res. 2021 Dec;52(1):135.

314. Hua K, Li T, He Y, Guan A, Chen L, Gao Y, et al. Resistin secreted by porcine alveolar macrophages leads to endothelial cell dysfunction during *Haemophilus parasuis* infection. Virulence. 2023 Dec 31;14(1):2171636.

315. Stubbendieck RM, May DS, Chevrette MG, Temkin MI, Wendt-Pienkowski E, Cagnazzo J, et al. Competition among nasal bacteria suggests a role for siderophore-mediated interactions in shaping the human nasal microbiota. Stabb EV, editor. Appl Environ Microbiol. 2019 May 15;85(10):e02406-18.

316. Skovbjerg S, Martner A, Hynsjö L, Hessle C, Olsen I, Dewhirst FE, et al. Gram-positive and Gram-negative bacteria induce different patterns of cytokine production in Human Mononuclear Cells irrespective of taxonomic relatedness. Journal of Interferon & Cytokine Research. 2010 Jan;30(1):23–32.

317. Mühl H, Pfeilschifter J. Anti-inflammatory properties of pro-inflammatory interferon-γ. International Immunopharmacology. 2003 Sep;3(9):1247–55.

318. Zhang M, Huang L, Ding G, Huang H, Cao G, Sun X, et al. Interferon gamma inhibits CXCL8–CXCR2 axis mediated tumor-associated macrophages tumor trafficking and enhances anti-PD1 efficacy in pancreatic cancer. J Immunother Cancer. 2020 Feb;8(1):e000308.

319. Gatto L, Berlato C, Poli V, Tininini S, Kinjyo I, Yoshimura A, et al. Analysis of SOCS-3 Promoter responses to interferon γ. Journal of Biological Chemistry. 2004 Apr;279(14):13746–54.

320. Pereiro P, Forn-Cuni G, Figueras A, Novoa B. Pathogen-dependent role of turbot (*Scophthalmus maximus*) interferon-gamma. Fish & Shellfish Immunology. 2016 Dec;59:25–35.

321. Lee S, Ro H, In HJ, Choi JH, Kim MO, Lee J, et al. Fisetin inhibits TNF-α/NF-κB-induced IL-8 expression by targeting PKCδ in human airway epithelial cells. Cytokine. 2018 Aug;108:247–54.

322. Rigauts C, Aizawa J, Taylor SL, Rogers GB, Govaerts M, Cos P, et al. *Rothia mucilaginosa* is an anti-inflammatory bacterium in the respiratory tract of patients with chronic lung disease. Eur Respir J. 2022 May;59(5):2101293.

323. Zhao Y, Bitzer A, Power JJ, Belikova D, Torres Salazar BO, Adolf LA, et al. Nasal commensals reduce *Staphylococcus aureus* proliferation by restricting siderophore availability. The ISME Journal. 2024 Jan 8;18(1):wrae123.

324. Zani K, Hobeika J, Sun Y, Kohler C, Cherian A, Fields T, et al. Nasal microbiota predictors for methicillin resistant *Staphylococcus* colonization in critically ill children. Zhang K, editor. PLoS ONE. 2025 Jan 15;20(1):e0316460.

325. Rosenstein R, Torres Salazar BO, Sauer C, Heilbronner S, Krismer B, Peschel A. The *Staphylococcus aureus*-antagonizing human nasal commensal *Staphylococcus lugdunensis* depends on siderophore piracy. Microbiome. 2024 Oct 22;12(1):213.

326. Vlasblom AA, Duim B, Patel S, Luiken REC, Crespo-Piazuelo D, Eckenberger J, et al. The developing pig respiratory microbiome harbors strains antagonistic to common respiratory pathogens. Van Laar TA, editor. mSystems. 2024 Oct 22;9(10):e00626-24.

327. Diao H, Yan HL, Xiao Y, Yu B, Yu J, He J, et al. Intestinal microbiota could transfer host gut characteristics from pigs to mice. BMC Microbiol. 2016 Dec;16(1):238.

328. Kiupel M, Stevenson GW, Choi J, Latimer KS, Kanitz CL, Mittal SK. Viral replication and lesions in BALB/c mice experimentally inoculated with porcine circovirus isolated from a pig with postweaning multisystemic wasting disease. Vet Pathol. 2001 Jan;38(1):74–82.

329. Hernández-Chirlaque C, Aranda CJ, Ocón B, Capitán-Cañadas F, Ortega-González M, Carrero JJ, et al. Germ-free and antibiotic-treated mice are highly susceptible to epithelial injury in DSS colitis. ECCOJC. 2016 Nov;10(11):1324–35.

330. Bayer F, Ascher S, Pontarollo G, Reinhardt C. Antibiotic treatment protocols and germ-free mouse models in vascular research. Front Immunol. 2019 Sep 12;10:2174.

331. Fröhlich EE, Farzi A, Mayerhofer R, Reichmann F, Jačan A, Wagner B, et al. Cognitive impairment by antibiotic-induced gut dysbiosis: Analysis of gut microbiota-brain communication. Brain, Behavior, and Immunity. 2016 Aug;56:140–55.

332. Modrackova N, Horvathova K, Mekadim C, Splichal I, Splichalova A, Amin A, et al. Defined pig microbiota mixture as promising strategy against *Salmonellosis* in gnotobiotic piglets. Animals. 2024 Jun 13;14(12):1779.

333. Horvathova K, Modrackova N, Splichal I, Splichalova A, Amin A, Ingribelli E, et al. Defined pig microbiota with a potential protective effect against infection with *Salmonella Typhimurium*. Microorganisms. 2023 Apr 12;11(4):1007.

334. Wang J, Hua L, Gan Y, Yuan T, Li L, Yu Y, et al. Virulence and inoculation route influence the consequences of *Mycoplasma hyorhinis* infection in Bama miniature pigs. Ferran AA, editor. Microbiol Spectr. 2022 Jun 29;10(3):e02493-21.

335. Vahle JL, Haynes JS, Andrews JJ. Experimental reproduction of *Haemophilus parasuis* infection in swine: Clinical, Bacteriologic, and Morphologic Findings. J VET Diagn Invest. 1995 Oct;7(4):476–80.

336. Hau SJ, Nielsen DW, Brockmeier SL. Prior infection with *Bordetella bronchiseptica* enhanced colonization but not disease with *Streptococcus suis*. Veterinary Microbiology. 2023 Sep;284:109841.

337. Laycock G, Sait L, Inman C, Lewis M, Smidt H, Van Diemen P, et al. A defined intestinal colonization microbiota for gnotobiotic pigs. Veterinary Immunology and Immunopathology. 2012 Oct;149(3–4):216–24.

338. Widmer KM, Rahic-Seggerman F, Forster A, Ahrens-Kress A, Sauer M, Mooyottu S, et al. Effect of genotype and age on a defined microbiota in gnotobiotic SCID piglets. bioRxiv [Preprint]. 2024.

339. Vodolazska D, Feyera T, Lauridsen C. The impact of birth weight, birth order, birth asphyxia, and colostrum intake per se on growth and immunity of the suckling piglets. Sci Rep. 2023 May 17;13(1):8057.

340. Machado D, Maistrenko OM, Andrejev S, Kim Y, Bork P, Patil KR, et al. Polarization of microbial communities between competitive and cooperative metabolism. Nat Ecol Evol. 2021 Jan 4;5(2):195–203.

341. Ho PY, Nguyen TH, Sanchez JM, DeFelice BC, Huang KC. Resource competition predicts assembly of gut bacterial communities *in vitro*. Nat Microbiol. 2024 Mar 14;9(4):1036–48.

342. Xie LW, Cai S, Lu HY, Tang FL, Zhu RQ, Tian Y, et al. Microbiota-derived I3A protects the intestine against radiation injury by activating AhR/IL-10/Wnt signaling and enhancing the abundance of probiotics. Gut Microbes. 2024 Dec 31;16(1):2347722.

343. Arnauts K, Sudhakar P, Verstockt S, Lapierre C, Potche S, Caenepeel C, et al. Microbiota, not host origin drives *ex vivo* intestinal epithelial responses. Gut Microbes. 2022 Dec 31;14(1):2089003.

344. Triana S, Metz-Zumaran C, Ramirez C, Kee C, Doldan P, Shahraz M, et al. Single-cell analyses reveal SARS-CoV-2 interference with intrinsic immune response in the human gut. Molecular Systems Biology. 2021 Apr;17(4):e10232.

345. Tort-Miró A, Alonso U, Martín-Mur B, Muñoz-Basagoiti J, Zeng Y, Ezcurra E, et al. 1 Inactivated *Rothia nasimurium* promotes a persistent antiviral immune 2 status in porcine alveolar macrophages.

346. Rapún-Araiz B, Sorzabal-Bellido I, Asensio-López J, Lázaro-Díez M, Ariz M, Sobejano De La Merced C, et al. *In vitro* modeling of polyclonal infection dynamics within the human airways by *Haemophilus influenzae* differential fluorescent labeling. Atack JM, editor. Microbiol Spectr. 2023 Dec 12;11(6):e00993-23.

347. Dai F, Zhuang Q, Zhao X, Shao Y, Guo M, Lv Z, et al. Green fluorescent protein-tagged *Vibrio splendidus* for monitoring bacterial infection in the sea cucumber *Apostichopus japonicus*. Aquaculture. 2020 Jun;523:735169.

348. Rodenburg LW, Van Der Windt IS, Dreyer HHM, Smits SMA, Den Hertog - Oosterhoff LA, Aarts EM, et al. Protocol for generating airway organoids from 2D air liquid interface-differentiated nasal epithelia for use in a functional CFTR assay. STAR Protocols. 2023 Sep;4(3):102337.

349. Zhu J, Zhou J, Feng B, Pan Q, Yang J, Lang G, et al. MSCs alleviate LPS-induced acute lung injury by inhibiting the proinflammatory function of macrophages in mouse lung organoid–macrophage model. Cell Mol Life Sci. 2024 Dec;81(1):124.

350. Bogoslowski A, An M, Penninger JM. Incorporating Immune cells into organoid models: essential for studying human disease. Organoids. 2023 Aug 12;2(3):140–55.

351. Sidhaye VK, Schweitzer KS, Caterina MJ, Shimoda L, King LS. Shear stress regulates aquaporin-5 and airway epithelial barrier function. Proc Natl Acad Sci USA. 2008 Mar 4;105(9):3345–50.

352. Shin YC, Than N, Min S, Shin W, Kim HJ. Modelling host–microbiome interactions in organ-on-a-chip platforms. Nat Rev Bioeng. 2023 Nov 17;2(2):175–91.

353. Mahajan G, Doherty E, To T, Sutherland A, Grant J, Junaid A, et al. Vaginal microbiome-host interactions modeled in a human vagina-on-a-chip. Microbiome. 2022 Nov 26;10(1):201.

354. Izadifar Z, Cotton J, Chen S, Horvath V, Stejskalova A, Gulati A, et al. Mucus production, host-microbiome interactions, hormone sensitivity, and innate immune responses modeled in human cervix chips. Nat Commun. 2024 May 29;15(1):4578.

355. Hayes JA, Lunger AW, Sharma AS, Fernez MT, Carrier RL, Koppes AN, et al. Engineered bacteria titrate hydrogen sulfide and induce concentration-dependent effects on the host in a gut microphysiological system. Cell Reports. 2023 Dec;42(12):113481.

356. Lee J, Menon N, Lim CT. Dissecting Gut-Microbial Community Interactions using a Gut Microbiome-on-a-Chip. Advanced Science. 2024 May;11(20):2302113.

357. Tan SY, Feng X, Cheng LKW, Wu AR. Vascularized human brain organoid on-chip. Lab Chip. 2023;23(12):2693–709.

358. Hu Y, Zhang H, Wang S, Cao L, Zhou F, Jing Y, et al. Bone/cartilage organoid on-chip: Construction strategy and application. Bioactive Materials. 2023 Jul;25:29–41.

359. Kim HJ, Park S, Jeong S, Kim J, Cho YJ. Lung Organoid on a Chip: A New Ensemble Model for Preclinical Studies. Int J Stem Cells. 2024 Feb 28;17(1):30–7.

360. Yu T, Yang Q, Peng B, Gu Z, Zhu D. Vascularized organoid-on-a-chip: design, imaging, and analysis. Angiogenesis. 2024 May;27(2):147–72.

361. Tovaglieri A, Sontheimer-Phelps A, Geirnaert A, Prantil-Baun R, Camacho DM, Chou DB, et al. Species-specific enhancement of enterohemorrhagic *E. coli* pathogenesis mediated by microbiome metabolites. Microbiome. 2019 Dec;7(1):43.

362. Bacon J, Kitchel H, Stutz J, Chen JH, Smith A, Van Horn RD, et al. Porcine Intestinal Organoids cultured in an Organ-on-A-Chip microphysiological system. SSRN [Preprint]. 2025.